Curriculum Vitae

Gillian Mbambo
PhD Candidate, Program in Molecular Microbiology, and Immunology
University of Maryland, School of Medicine

Contact Information

Institute for Genome Sciences
675 West Baltimore Street
Baltimore, MD 21201
gmbambo1@gmail.com

Education

2023	Ph.D., Molecular Microbiology and Immunology, University of Maryland, Baltimore
2013	B.S., Cell Biology and Genetics, University of Maryland, College Park

Research Experience

2018-present	Ph.D. Candidate, co-PI: Dr. Joana C. Silva and Dr. Kirsten E. Lyke, Host immunotranscriptomics during malaria infection and malaria-schistosomiasis co-infection
2018	Rotation Student, PI: Dr. Nevil Singh, Dept. Microbiology and Immunology, UMSOM
2018	Rotation Student, PI: Dr. Mary Ann Rizk, Research and Diagnostics, UMSOD
2014-2017	Research Assistant, co-PI: Dr. Christopher Plowe and Dr. Miriam Laufer

Teaching Experience and Student Service

2022	Lecturer - Molecular Epidemiology (PREV780) Department of Epidemiology and Public Health University of Maryland, Baltimore
2020-2021	Workshop Instructor - Basic Immunology (GPLS702) Department of Microbiology and Immunology University of Maryland, Baltimore
2020-2021	Discussion Leader - Host Defenses and Infectious Diseases (MSPR520) Department of Microbiology and Immunology University of Maryland, School of Medicine
2018-2020	Tutor - Mechanisms in Biomedical Sciences at UMB (GPILS601) Graduate Program in Life Sciences University of Maryland, School of Medicine

Extracurricular University Service

2020 – 2022	**Treasurer**, Graduate Student Association
2019	**Committee Member**, Graduate Program in Life Sciences/Office of Postdoctoral Studies Award Selection Committee, UMSOM
2019 - 2021	**Committee Member**, University Student Government Association Pennington Volunteer Committee
2019 - 2020	**Committee Member**, Graduate Student Association GRC Planning Committee
2019 - 2021	**Committee Member**, Graduate Student Association Volunteer Committee
2019 - 2020	**Co-organizer**, Immunology Journal Club
2019 - 2020	**Graduate School Senator**, University Student Government Association
2018 - 2020	**Program in Molecular Microbiology and Immunology representative**, Graduate Student Association
2018 - 2020	**Committee Member**, Graduate Student Association Finance Committee
2018 - 2020	**Program in Molecular Microbiology and Immunology representative**, Graduate Program in Life Science Student Advisory Council

Awards and Honors

Presentation & Research Awards
Outstanding Poster Presentation, UMB Graduate Research Conference

Academic Recognition
Stimulating Participation in Academically Rigorous Kinship (SPARK) Award, UMB

Professional Membership

American Society of Tropical Medicine and Hygiene

Publications

1. **Mbambo G**, Dwivedi A, Ifeonu OO, Munro JB, Shrestha B, Bromley RE, Hodges T, Adkins RS, Kouriba B, Diarra I, Niangaly A, Kone AK, Coulibaly D, Traore K, Dolo A, Thera MA, Laurens MB, Doumbo OK, Plowe CV, Berry AA, Travassos M, Lyke KE, Silva JC. Immunogenomic profile at baseline predicts host susceptibility to clinical malaria. Front Immunol. 2023 Jul 3;14:1179314. doi: 10.3389/fimmu.2023.1179314. PMID: 37465667; PMCID: PMC10351378.
2. Yaqoob A, Khattak AA, Nadeem MF, Fatima H, **Mbambo G**, Ouattara A, Adams M, Zeeshan N, Takala-Harrison S. Prevalence of molecular markers of sulfadoxine-pyrimethamine and artemisinin resistance in Plasmodium falciparum from Pakistan. Malar J. 2018 Dec 17;17(1):471. doi: 10.1186/s12936-018-2620-y. PMID: 30558587; PMCID: PMC6296135
3. Adams M, Joshi SN, **Mbambo G**, Mu AZ, Roemmich SM, Shrestha B, Strauss KA, Johnson NE, Oo KZ, Hlaing TM, Han ZY, Han KT, Thura S, Richards AK,

Huang F, Nyunt MM, Plowe CV. An ultrasensitive reverse transcription polymerase chain reaction assay to detect asymptomatic low-density *Plasmodium falciparum* and *Plasmodium vivax* infections in small volume blood samples. Malar J. 2015 Dec 23;14:520. PubMed PMID: 26701778; PubMed Central PMCID: PMC4690410.

4. Huang F, Takala-Harrison S, Liu H, Xu JW, Yang HL, Adams M, Shrestha B, **Mbambo G**, Rybock D, Zhou SS, Xia ZG, Zhou XN, Plowe CV, Nyunt MM. Prevalence of Clinical and Subclinical *Plasmodium falciparum* and *Plasmodium vivax* Malaria in Two Remote Rural Communities on the Myanmar-China Border. Am J Trop Med Hyg. 2017 Nov;97(5):1524-1531. PubMed PMID: 29016341; PubMed Central PMCID: PMC5817756.
5. Nyangulu WJ, Mwinjiwa E, Divala TH, Mungwira RG, Nyirenda O, Kanjala M, **Mbambo G**, Mallewa J, Taylor TE, Laurens MB, Laufer MK, van Oosterhout JJ. Frequent malaria illness episodes in two Malawian patients on antiretroviral therapy soon after stopping cotrimoxazole preventive therapy. Malawi Med J. 2017 Mar;29(1):57-60. PubMed PMID: 28567199; PubMed Central PMCID: PMC5442494.

Presentations

1. **Gillian Mbambo**, Ankit Dwivedi, Holly Bowen, Yang Song, Drissa Coulibaly, Abdoulaye Kassoum Kone, Bourema Kouriba, Charles Arama. Abdoulaye Dabo, Kirsten Lyke, Joana Carneiro da Silva. (2022). Altered gene expression in gamma delta T cells in children with malaria and schistosomiasis co-infection relative to children infected with malaria alone. (**Poster Presentation**). 51th Annual meeting of American Society of Tropical Medicine and Hygiene
2. **Gillian Mbambo**, Ankit Dwivedi, Amol Shetty, Kemi Ifeonu, Theresa Hodges, Ricky S. Adkins, Anup Mahurkar, Drissa Coulibaly, Abdoulaye Kassoum Kone, Ando B. Guindo, Mahamadou A. Thera, Kirsten Lyke, Joana Carneiro da Silva. (2020). Differential gene expression analysis of PBMCs from Malian children reveals molecular mechanisms associated with varying susceptibility to clinical malaria disease. (**Poster Presentation**). 49th Annual meeting of American Society of Tropical Medicine and Hygiene
3. **Gillian Mbambo**, Ankit Dwivedi, Amol Shetty, Kemi Ifeonu, Kirsten Lyke, Joana Carneiro da Silva. (2020). Differential gene expression analysis of PBMCs from Malian children reveals molecular mechanisms associated with varying susceptibility to clinical malaria disease. (**Oral Presentation**). GCID Virtual Meeting
4. **Gillian Mbambo**, Ankit Dwivedi, Kirsten Lyke, Joana Carneiro da Silva. (2020). Differential gene expression analysis of PBMCs from Malian children reveals molecular mechanisms associated with varying susceptibility to clinical malaria disease. (**Oral Presentation**). Program in Molecular Microbiology and Immunology Annual Graduate Student Symposium, Baltimore MD
5. **Gillian Mbambo**, Ankit Dwivedi, Theresa Hodges, Anup Mahurkar, Shaun Adkins, Kirsten Lyke, Joana C. Silva. (2019). Characterization of host immune gene expression profiles in malaria-protected and malaria-susceptible individuals.

(**Poster Presentation**). 48th Annual meeting of American Society of Tropical Medicine and Hygiene, National Harbor, MD

6. **Gillian Mbambo**, Zalak Shah, Kara Moser, Anup Mahurkar, Kemi Ifeonu, Mark Travassos, Andrea Berry, Shannon Takala, Amed Ouattara, Kirsten Lyke, Joana C. Silva. (2018). Utilizing in silico tools to perform B cell epitope prediction in *Plasmodium falciparum*. (**Poster Presentation**). 47th Annual meeting of American Society of Tropical Medicine and Hygiene, New Orleans LA
7. **Gillian Mbambo**, Ankit Dwivedi, Kirsten Lyke, Joana Carneiro da Silva. (2019). Characterization of host immune gene expression profiles in malaria-susceptible and -protected Malian children. (**Oral Presentation**). Program in Molecular Microbiology and Immunology Annual Graduate Student Symposium, Baltimore MD
8. **Gillian Mbambo**, Kara Moser, Kirsten Lyke, Joana Carneiro da Silva. (2018). B cell epitope prediction in *Plasmodium falciparum*. (**Oral Presentation**). Program in Molecular Microbiology and Immunology Annual Graduate Student Symposium, Baltimore MD

Abstract

Title of dissertation: Host immunotranscriptomics during malaria infection and malaria-schistosomiasis co-infection in Malian pediatric cohorts

Gillian Mbambo, Doctor of Philosophy, 2023

Dissertation Directed by: Joana C Silva, Ph.D, Professor, and Department of Microbiology and Immunology and Kirsten E Lyke, MD, Professor, and Department of Medicine

Malaria is the deadliest parasitic infectious disease, responsible for over 600,000 deaths annually. Despite eliciting immune responses to acute infection, the lack of durable immunity hinders the development of highly efficacious vaccines. This study aims to unravel the mechanisms governing malaria susceptibility, the generation and maintenance of *Plasmodium falciparum*-specific memory cells, and the impact of parasitic co-infections on the immune response, by employing a transcriptomics approach to analyze peripheral blood mononuclear cells (PBMCs) collected from children in Mali, West Africa, a country with hyperendemic seasonal malaria.

To pinpoint host determinants of susceptibility during the development of acquired immunity, we examined PBMCs from Malian children who differ in susceptibility to clinical malaria. Blood samples were collected at the onset, peak, and conclusion of the malaria season from children aged 4-6 years. We characterized the immune cell composition and cytokine secretion for a subset of 20 children per timepoint (10 children with no symptomatic malaria age-matched to 10 children with $\geq$2 symptomatic malarial illnesses), and gene expression patterns for six children (three per cohort) per timepoint.

We noted higher frequency of HLA-DR$^+$ CD4 T cells in protected children during the peak of the malaria season and comparable levels cytokine secretion after stimulation with malaria schizonts across all three time points. Additionally, we observed differences in the expression of genes related to cell death and inflammation; in particular, inflammatory genes such as CXCL10 and STAT1 and apoptotic genes such as XAF1 were upregulated in susceptible children before the transmission season began. This suggests that differences in apoptotic and inflammatory gene expression patterns can predict susceptibility to clinical malaria.

While *P. falciparum* is highly prevalent in Mali, it is crucial to recognize that this parasite does not exist in isolation. Mali exhibits a high prevalence of multiple infectious pathogens ranging from viruses to parasites. Notably, *Schistosoma haematobium*, with an infection prevalence reaching 50% in children before the age of 16, significantly contributes to the burden of infection diseases experienced by individuals in this area. To investigate the impact of a chronic *S. haematobium* infection on immune responses during acute *P. falciparum* infection and convalescence, we utilized single-cell RNA-sequencing on PBMCs from 20 Malian children. We successfully identified distinct subsets of T cells, B cells, natural killer (NK) cells, and myeloid cells. Notably, gene expression differences were observed due to the presence of a *P. falciparum* infection, while *S. haematobium* co-infection did not significantly impact gene expression. Additionally, we analyzed gene expression profiles in numerous CD4 T cell subsets and identified a unique cytotoxic CD4 T cell population. Differential expression analysis revealed increased expression of lymphocyte activation gene 3 (LAG3), basic leucine zipper ATF-like transcription factor (BATF), interferon, and interleukin 18 (IL18) receptor genes across distinct CD4 T cell

populations during an acute malaria episode. Furthermore, we observed upregulation of the NR4A family of transcription factors in *P. falciparum*-negative, malaria-exposed children, suggesting their potential role in T cell dysfunction which may explain sub-optimal immunity observed during a secondary *P. falciparum* infection. This study provides valuable insights into immune responses in children exposed to *P. falciparum* and sheds light on potential regulatory networks involving BATF and NR4A family members. The dynamic gene expression patterns suggest a complex response to antigenic factors, highlighting the need for further research to understand the mechanisms shaping immune responses to infection and, particularly, co-infection.

Host Immunotranscriptomics during Malaria Infection and Malaria-Schistosomiasis Co-infection in Malian Pediatric Cohorts

by
Gillian Mbambo

Dissertation submitted to the Faculty of the Graduate School of the
University of Maryland, Baltimore in partial fulfillment
of the requirements for the degree of
Doctor of Philosophy
2023

Dedication

To my family, Sheila Mbambo, McEwan Mbambo, Nelly Kobe, Hazel Mbambo, Isaac Mbambo, Blake Kobe, Malaika Kobe, and Nahla Kobe. Thank you for your love and support.

Dedication, hard work plus patience. The sum of all my sacrifice.

~Nipsey Hussle

Acknowledgements

Thank you to my mentors, Joana C. Silva, and Kirsten E. Lyke for all you have taught me during this journey. Your patience, support, and guidance meant everything to me! To my thesis committee, Tonya Webb, David Serre, Vincent Bruno, and Robert Seder, thank you for your thoughtful comments and feedback.

To my cohort, Anya O'Neal, and Jessica Allen, so glad I got to experience this journey with you both, it was a hoot!

My closest friends, Jumoke Akinola, Zalak Shah, Sarah Robbins, Christina Stennet, and Abifolowa Shitta-Bey, you all were my support system, listened to me vent and gave me your unconditional love and support.

To my lab and PhD community, Emily Smith, Hanover Matz, Katie Gwilliam, Alex Soare, Brianna Young, Ankit Dwivedi, Kemi Ifeonu, Yiwei Yang, Ryan Scalsky, Wilson Tavares, and Thomas Stabler, I am so thankful for you all.

Table of Contents

List of Tables

List of Figures

List of Abbreviations

ADCC	Antibody Dependent Cellular Cytotoxicity
ADT	Antibody-derived tag
AMA1	Apical Membrane Antigen 1
AP-1	Activator Protein-1
APC	Antigen Presenting Cells
BACH2	Broad Complex-tramtrack-bric a brac and Cap‘n’collar Homology 2
BATF	Basic Leucine Zipper Transcription Factors
BCL	Base Call
BCL6	B Cell Lymphoma 6
BCR	B Cell Receptor
BSA	Bovine Serum Albumin
BTLA	B- and T-Lymphocyte Attenuator
$CaCl_2$	Calcium Chloride
CCL	CC Chemokine Ligand
CCR	CC Chemokine Receptor
CD	Cluster Differentiation
cDC	Classical Dendritic Cells
cDNA	Complementary Deoxyribose Nucleic Acid
CITE	Cellular Indexing of Transcriptomes and Epitopes
CSF	Cerebral Spinal Fluid
CSP	Circumsporozoite Protein
CTL	Cytotoxic T Lymphocyte

CTLA4	Cytotoxic T lymphocyte-associated molecule 4
COVID-19	Coronavirus Disease 19
CXCL	C-X-C Chemokine Ligand
CXCR	C-X-C Chemokine Receptor
CyTOF	Cytometry by Time of Flight
DA	Differential Abundance
DAVID	Database for Annotation, Visualization, and Integrated Discovery
DDX11	DEAD/H-Box Helicase 11
DC	Dendritic Cell
DCR	Dead Cell Removal
DNA	Deoxyribonucleic Acid
DPBS	Dulbecco's Phosphate Buffered Saline
DS	Differential State
ELISA	Enzyme-Linked Immunosorbent Assay
FBS	Fetal Bovine Serum
FCS	Fetal Calf Serum
FCS	Flow Cytometry Standard
FDR	False Discovery Rate
FOXP3	Forkhead Box P3
G6PD	Glucose-6-Phosphate Dehydrogenase
GATA3	GATA Binding Protein 3
gEAR	Gene Expression Analysis Research
GEM	Gel Bead in Emulsion

GBP	Guanylate Binding Protein
GIMAP	GTPase Immune Associated Protein
GRCh38	Genome Research Consortium Human Build 38
GSEA	Gene Set Enrichment Analysis
GZMA	Granzyme A
GZMB	Granzyme B
GZMH	Granzyme H
GZMK	Granzyme K
HbC	Hemoglobin C
HbS	Hemoglobin S
HGF	Hepatocyte Growth Factor
HISAT	Hierarchical Indexing for Spliced Alignment of Transcripts
HIV	Human Immunodeficiency Virus
HLA	Human Leukocyte Antigen
HTseq	High-throughput Sequence Analysis
ICOS	Inducible T-Cell Co-Stimulator
IFI	Interferon Induced Protein
IFITM	Interferon Induced Transmembrane Protein
IFN	Interferon
IFNG-AS1	Interferon Gamma Antisense RNA 1
IKZF2	IKAROS Family Zinc Finger 2
IL	Interleukin
IRF	Interferon Regulatory Factor

iRBC	Infected Red Blood Cell
ISG	Interferon Stimulated Genes
JAK	Janus Kinase
KEGG	Kyoto Encyclopedia of Genes and Genomes
KLRB1	Killer Cell Lectin Like Receptor B1
LAG3	Lymphocyte Activation Gene-3
LEF1	Lymphoid Enhancer-binding Factor 1
LFC	Log Fold Change
ICOS	Inducible T Cell Co-stimulator
iRBC	Infected Red Blood Cell
MAIT	Mucosal-Associated Invariant T Cells
MHC	Major Histocompatibility Complex
NFKB	Nuclear Factor Kappa B Subunit
NFKB	Nuclear Factor Kappa B Subunit Inhibitor Epsilon
NK	Natural Killer
NKG7	Natural Killer Cell Granule Protein 7
NR4A	Nuclear Receptor 4A
NTD	Neglected Tropical Diseases
PBMC	Peripheral Blood Mononuclear Cells
PBS	Phosphate Buffered Saline
PCA	Principal Component Analysis
PCR	Polymerase Chain Reaction
pDC	Plasmacytoid Dendritic Cells

PDCD1	Programmed Cell Death Protein 1
PD-1	Programmed Cell Death Protein 1
Pf	*Plasmodium falciparum*
PfEMP1	*Plasmodium falciparum* Erythrocyte Membrane Protein 1
Pfsz	*Plasmodium falciparum* Schizonts
PRF1	Perforin
RNA	Ribonucleic Acid
RORC	RAR-related Orphan Receptor C
RT	Reverse Transcriptase
RTS,S	Repeat T-cell Epitope Surface Antigen
RUNX3	Runt-related Transcription Factor 3
SEB	*Staphylococus* Enterotoxin B
scRNA-seq	Single cell RNA sequencing
Sh	*Schistosoma haematobium*
SLAM	Signaling Lymphocytic Activation Molecule
STAT	Signal Transducer and Activator of Transcription
T-bet	T-box expressed in T Cells
TBX21	T-Box 21
TCF7	T Cell Factor 7
TCR	T Cell Receptor
T_{CM}	Central Memory T Cells
T_{EM}	Effector Memory T Cells
T_{FH}	T Follicular Helper

TGF	Transforming Growth Factor
TGFBR	Transforming Growth Factor Beta Receptor
TH	T Helper
TIGIT	T Cell Immunoreceptor with Ig and ITIM domains
TLR	Toll-like Receptor
TNF	Tumor Necrosis Factor
TNFAIP3	Tumor Necrosis Factor Alpha Induced Protein-3
TNFSF	Tumor Necrosis Factor Superfamily Member
TNFRSF	Tumor Necrosis Factor Receptor Superfamily Member
TOX	Thymocyte Selection Associated High Mobility Group Box
Treg	Regulatory T Cells
TXK	Tyrosine Kinase
UMAP	Uniform Manifold Approximation and Projection
V(D)J	Variable, Diversity, and Joining Gene Segments
XAF1	XIAP Associated Factor 1
ZAP70	Zeta Chain of T Cell Receptor Associated Protein Kinase 70

Chapter 1: Introduction

1.1 Malaria

Malaria is a major global health threat that affects over 200 million people annually[1]. Clinical symptoms of malaria, a parasitic disease caused by *Plasmodium* species, are most prevalent in children and are characterized by fever, headaches and, in severe cases, severe anemia and cerebral malaria[2]. Service disruptions during the COVID-19 pandemic resulted in a 12% rise in deaths in 2020[3]. Over 600,000 people die of malaria annually, the vast majority of whom are children[1]. Despite its global distribution throughout the tropical and subtropical regions, 93% of malaria cases occur in sub-Saharan Africa[1]. Progress has been made in malaria vaccine development efforts. In 2019, the first malaria vaccine (RTS, S, commercially sold as Mosquirix^{TM}) was approved by the World Health Organization (WHO) for use in children[4]. In 2023 a second vaccine, R21/Matrix-M, based on the same *Plasmodium* antigen as RTS,S was also endorsed by the WHO[5–7]. Despite these key developments, much remains to be understood regarding mammalian immune responses to infection, particularly regarding differences in host susceptibility and responses to naturally acquired parasitic malaria infection and co-infections.

1.2 *Plasmodium falciparum*

Five different *Plasmodium* species infect the human host, including *P. knowlesi, P. ovale, P. vivax, P. malaria* and, the deadliest species, *P. falciparum.* The *Plasmodium* life cycle in the human host begins when an infected mosquito takes a blood meal and injects sporozoites into the capillaries within the skin; these sporozoites migrate to the liver where they infect hepatocytes[8]. Within the hepatocytes, sporozoites mature into schizonts which rupture and release 30,000-40,000 merozoites into the bloodstream[8]. In the bloodstream,

each merozoite infects a new erythrocyte and matures from early to late trophozoite, eventually maturing into a schizont which encompasses much of the red blood cell causing it to rupture and release a dozen or more merozoites, which proceed to infect more red blood cells[8]. The rupturing of red blood cells coincides with the symptoms associated with clinical malaria[9]. During the blood-stage of infection, a small number of merozoites are triggered to differentiate into gametocytes which are then taken up by a female *Anopheles* mosquito during a blood meal[8]. Once the gametocytes mature into gametes, the parasite goes through sexual reproduction within the midgut of the secondary mosquito host where the male and female gametes mate and produce zygotes that mature to form ookinetes[8]. Mobile ookinetes cross the midgut to form sporozoite-filled oocysts within the basal lamina[8]. Sporozoites released from the oocyst eventually invade the salivary glands and are positioned to infect human skin during the next *Anopheles* blood meal[8]. The life cycle of *Plasmodium* is similar across species; however, some species such as *P. ovale* and *P. vivax* have dormant stages that can persist within the liver[8]. Species such as *P. vivax* are highly prevalent in Southeast Asia and South America, while *P. falciparum* is the most prevalent species in sub-Saharan Africa, responsible for 95% of documented malaria cases in the region[10,11].

1.3 Malaria Susceptibility

Susceptibility to malaria is influenced by multiple factors ranging from the human host to the parasite genetics, host behavior, and environmental factors. Individuals in high transmission, malaria-endemic regions are continuously exposed to diverse *P. falciparum* strains and associated malaria antigens. This repeated exposure can lead to acquired immunity to clinical malaria[12]. The behavior of the human host plays a crucial role in

whether they acquire infection. The decision to use bed net, the choice of where to work, and the conditions under which children play outside, all contribute to behavioral conditions that increase susceptibility to malaria. Nutrition and access to resources also contribute to the likelihood of getting a symptomatic malaria infection; studies show that children with malnutrition are more likely to have severe cases of malaria infection compared to their healthy counterparts. Specifically, children who are anemic and supplement with iron pills are more likely to get established malaria infections due to the presence of iron in the blood stream[13,14] . Host genetic factors, including those related to red blood cell disorders (HbS, HbC, G6PD, alpha-thalassemia), are known to contribute to resistance to malaria, while some HLA alleles are associated with increased susceptibility to malaria infection[15,16]. In addition to the described behavioral, environmental and genetic factors, exposure to other infectious pathogens can also play a role in susceptibility to clinical malarial disease[17–19].

Plasmodial parasites exhibit genetic diversity and have evolved an array of immune evasion mechanisms that significantly influence host susceptibility to infection. During the liver stage of infection, the parasite expresses surface molecules, such as the circumsporozoite protein (CSP), that interact with Kupffer cell surface proteins. This interaction can inhibit Kupffer cell defense mechanisms and induce apoptosis, thereby allowing the infection to progress[20]. At the erythrocytic stage of infection, antigenic variation plays a pivotal role in the parasite's immune evasion strategies. As the parasite matures from merozoite to schizont, it sequentially expresses a range of different proteins that are exposed to the host immune system[20,21]. Extracellular merozoites express surface proteins with high levels of polymorphism, making it difficult for neutralizing antibodies

to recognize and target these variants effectively[21]. Furthermore, a significant proportion of proteins found on the surface of infected red blood cells (iRBCs) belongs to multigene families, with the *var* gene family, encoding the *P. falciparum* erythrocyte membrane protein 1 (*Pf*EMP1) class of proteins, being predominant. This family exhibits a dynamic process of silencing and switching, resulting in the parasite expressing different genes from the *var* family as it matures[21]. These multifaceted immune evasion strategies collectively contribute to the parasite's ability to persist and thrive within the host.

1.4 Immune response to malaria

Host immunity factors, including the history of exposure and the quality of previous immune responses contribute to the severity of malaria episodes[22]. In addition, being immunocompromised, or having an underlying autoimmune illness, may impact the response to malaria infections[23,24]. In a healthy host, responses to *Plasmodium* infection are dependent on parasite life cycle stage and location within the host, and both innate and adaptive arms of the immune system play an important role in the control of infection.

1.4.1 Innate Immune Responses to *P. falciparum*

Innate immune responses to *P. falciparum* are critical during the initial stages of infection and play a role in controlling the parasite density[25]. Innate cells, such as macrophages and dendritic cells (DCs), recognize conserved molecules on the surface of *Plasmodium* parasites, while natural killer (NK) cells recognize the absence of self-molecules from infected hepatocytes[25,26]. Tissue-resident macrophages, Kupffer cells, can phagocytize and eliminate infected hepatocytes, secrete anti- and pro-inflammatory molecules, as well as hepatocyte growth factor (HGF) to induce apoptosis of liver cells[27,28]. During the erythrocytic stage of infection, macrophages recognize surface molecules such

as *P. falciparum* erythrocyte membrane protein 1 (*Pf*emp1) through innate receptors, CD36 and Toll-like receptors (TLRs) to endocytose infected cells and secrete cytokines and chemokines to recruit more immune cells to the site of infection and initiate specific CD4 T cell immune responses[25]. The role of liver-resident DCs during infection is poorly understood; however, studies show that circulating blood DCs can enter the liver and phagocytose infected liver cells[29,30]. Like macrophages, DCs recognize *Plasmodium* surface molecules during the erythrocytic stage of infection to phagocytize and secrete cytokines[25,29]. DCs and macrophages also have antigen presenting capacity and prime adaptive immune responses through MHC class I and II in both the liver and blood-stage[25,27,29].

Although the mechanism is poorly understood, studies show that NK cells are an early source of interferon gamma (IFN-γ) production in both *Plasmodium* mouse models and stimulated peripheral blood mononuclear cells (PBMCs)[31,32]. The role of IFN-γ in malaria immunity has been extensively studied. Although some negative effects are associated with the presence of this highly inflammatory cytokine, multiple studies demonstrate how this cytokine is critical for survival during both murine and human models of infection[33,34]. NK cells also play a role after initiation of the adaptive antibody immune response via antibody dependent cellular cytotoxicity (ADCC)[35,36].

Gamma delta T cells (γδ T cells) represent a distinctive subset of T cells at the interface of innate and adaptive immune responses[37,38]. In the context of *Plasmodium* infection, these cells secrete pro-inflammatory molecules, such as IFN-γ, TNF-α, and granzyme B, while also directly killing merozoites during the blood-stage of the infection[37]. These T cells are an integral component of the early immune response to blood-

stage malaria. Previous studies show that Vγ9Vδ2 γδ T cells, the predominant γδ T cell population in humans, expand during an acute primary infection; however, after each subsequent infection this population contracts[38,39]. In contrast, the less prevalent Vδ1 γδ T cell subset matures through repeated exposure, coinciding with the acquisition of immunity[40]. Although γδ T cells have been associated with a protective role, certain investigations propose that the inflammatory cascade initiated by these cells might contribute to the manifestation of severe symptoms observed during primary infection[41,42]. Encouragingly, the severity of these symptoms tends to diminish during subsequent infections, which could potentially be attributed, at least in part, to the diminishing populations of contracted γδ T cells[43,44].

1.4.2 Adaptive Immune Responses to *P. falciparum*

During the liver-stage of infection, antigen presenting cells (APCs) such as DCs and macrophages play a pivotal role in priming and activating $CD8^+$ T cells. These activated $CD8^+$ T cells are crucial in targeting and eliminating infected hepatocytes[6]. $CD4^+$ T cells appear to play a role in priming CD8 T cells, through the production of IFN-γ, though the mechanism behind this priming has not been characterized.[38] T cell responses during the blood-stage of infection are complicated by the lack of major histocompatibility complex (MHC) expression in erythrocytes, allowing for an immune-evading environment for the parasite. The immune response mounted against blood-stage malaria is characterized by the production of antibodies that exhibit the capacity to neutralize and opsonize *Plasmodium* antigens. These antigens are either displayed on the surface of infected red blood cells or on the surface of merozoites which are found in the bloodstream[45–47]. A critical aspect of antibody production is an effective T cell-mediated immune response that

facilitates the differentiation of B cells into antibody-producing plasma cells and eventually, memory B cells. Both Th1- and Th2-mediated $CD4^+$ T cell responses are pivotal in regulating and resolving parasitic infections peripherally[7,8].

Th1-mediated immune responses are critical during the early stages of infection, where cytokines including IFN-γ, TNF-α, IL-2, and IL-12 confer pro-inflammatory responses that control the parasite load[7]. Although the mechanism is poorly understood, rodent studies show that the deletion of IL-12 and IFN-γ results in increased *Plasmodium* parasitemia[48,49]. Moreover, the secretion of IFN-γ and IL-2 by Th1 $CD4^+$ T cells is correlated with the activation of macrophages and NK cells which facilitate endocytosis and lysis of infected erythrocytes[50].

Th2-mediated $CD4^+$ T cell immune responses, characterized by the secretion of anti-inflammatory cytokines such as IL-4, IL-5, and IL-13, are critical during an established blood-stage infection[50–52]. This $CD4^+$ T cell subset promotes B cell clonal expansion, somatic hypermutation, and isotype switching. Additionally, the production of IL-4 is critical for memory T cell production and regulating inflammation during later stages of infection[53].

Distinct $CD4^+$ T cell subsets, such as T follicular helper cells (T_{FH}), regulatory T cells (Tregs), and cytotoxic CD4 T cells (CD4 CTL), contribute to the regulation of *Plasmodium* parasite density and clearance[38]. In alignment with the Th2 subset, T_{FH} cells actively promote B cell germinal center responses, leading to the generation of malaria-specific plasma cells and memory B cells[38]. Tregs, a subset of immunosuppressive $CD4^+$ T cells, secrete anti-inflammatory molecules IL-10 and transforming growth factor (TGF)-β, and express the co-inhibitory receptor cytotoxic T lymphocyte-associated molecule 4 (CTLA-

4) to prevent excessive inflammation during immune responses to infection[38,54]. However, it is notable that expanded Treg populations have been linked to heightened parasitemia in certain individuals from malaria-endemic regions[55].

Despite this association, findings from mouse studies demonstrate that Treg depletion can result in excessive inflammation, highlighting the pivotal role of Tregs in immune response regulation following *Plasmodium* infection[54]. The presence of Tregs serves as an essential mechanism for maintaining immune balance[56]. Notably, the timing of Treg expansion emerges as a critical factor in orchestrating effective immune modulation[54].

Longitudinal studies have observed an age-related effect on cytokine production, such that younger children and malaria-experienced adults have higher serum levels of pro-inflammatory and regulatory cytokines when compared to older children (7-10 years old)[57,58]. Meanwhile, transcriptomic analysis from whole blood cells derived from malaria-naïve and malaria-experienced individuals show that upon infection with *P. falciparum*, naïve individuals have a higher pro-inflammatory cytokine response when compared to their malaria-experienced counterparts[59].

Humoral immunity represents the hallmark of protection against malaria infection[60]. *Plasmodium*-specific B cells engage in germinal center reactions, a process encompassing somatic hypermutations, affinity maturation, and class-switch recombination[61]. This complex series of events results in the differentiation of B cells into high-affinity antibody-producing plasma cells and long-lived memory B cells[61]. *Plasmodium*-specific antibodies serve as critical effectors during the blood stage of infection[60]. These antibodies possess the capacity to recognize and neutralize merozoites, blocking their ability to invade new red blood cells[60]. Additionally, they can opsonize infected red blood cells, initiating

phagocytosis and promoting complement-mediated clearance of parasitized cells[60]. B cells that undergo differentiation into memory B cells play a pivotal role in long-term immunity[60]. Upon re-exposure to the parasite during a secondary infection, these memory B cells are rapidly mobilized, ensuring a swift and effective clearance of the pathogen[60].

1.4.3 T cell memory responses to malaria

Long-term immunity to malaria is a crucial subject within malaria research, with a focus on understanding the mechanisms of memory cell generation and their maintenance over time. This topic holds significant importance for the development of effective malaria vaccines. Prior investigations into the acquisition of natural immunity to malaria in individuals residing in endemic regions have shown that repeated exposure to malaria antigens results in the mitigation of clinical symptoms, without conferring complete sterile immunity[22,62–64]. However, this immunity tends to wane when an individual leaves an endemic region, suggesting impaired development or durability of memory cells generated against malaria antigens, which require constant stimulation from *P. falciparum* proteins. Some studies have suggested the involvement of *Plasmodium*-encoded genes in impairing the development of memory T cells during malaria infection[65].

Memory CD8 T cells have been extensively studied in the context of vaccine-induced immunity to liver-stage *P. falciparum*. Due to the inherent challenge of studying liver-stage infection in human models, a substantial portion of our understanding of the mechanisms behind the formation of memory against liver-stage *P. falciparum* infection has been revealed through mouse or primate models of *Plasmodium* infection. CD8 memory T cells responding to liver-stage *P. falciparum* can be categorized into three main groups; tissue-resident (T_{RM}) cells, circulating effector memory (T_{EM}) cells, and secondary lymphoid

organ localized central memory (T_{CM}) cells[66]. T_{RM} are a non-circulating T cell subset characterized by the expression of integrins CD103 and CD49a, chemokine receptor CXCR6, and early activation marker CD69[67,68]. The functionality and protective potential of liver T_{RM} cells are of particular interest in the context of malaria, as studies have demonstrated their significance in protection and effector molecule production[69–72]. T_{CM} and T_{EM} are a subset of $CD45RA^{-}/CD45RO^{+}$ cell populations, further differentiated by the presence of CD62L and CCR7 on their cell surface, with T_{CM} cells expressing these markers while T_{EM} cells do not. Both subsets are recalled during subsequent *Plasmodium* infection[73].

Secondary *P. falciparum* blood-stage infections elicit the recall of both humoral and T cell-mediated memory immune responses. Long-lived plasma cells, memory B cells, CD4 T_{EM} cells, and T_{CM} cells have been observed in PBMCs from both human and rodent models of *Plasmodium* infection[22,74–76]. The memory CD4 T cell compartment encompasses diverse CD4 lineages, including Th1 (Tbet), Th2 (GATA3), and T_{FH} (BCL6), all of which been identified in effector memory CD4 T cells from individuals exposed to malaria[77–81]. Studies in other infectious pathogens suggest variations in the survival of memory Th lineages[82–84], yet this aspect has not been thoroughly explored in the context of *P. falciparum* infection. While the importance of memory Th1 and T_{FH} lineages in efficient parasite clearance during secondary infections is evident, most of these observations are derived from rodent models of infection. Further research is needed to investigate the role and presence of distinct CD4 lineages during human malaria infection. The significance of memory $CD4^{+}$ T cells extends beyond effector molecule production and the recruitment of macrophages and DCs during secondary infections. $CD4^{+}$ T cell-

derived cytokines play a crucial role in the generation and maintenance of both B cell and $CD8^+$ T cell memory responses[85–87]. For both CD8 and CD4 T cells, multiple studies underscore the importance of tissue-derived IL-7 and IL-15 cytokines in the survival and maintenance of pathogen-specific memory populations in the absence of antigen exposure after infection resolution. However, it remains an area of ongoing investigation to elucidate the factors that govern the production of these crucial cytokines, as well their interactions with receptors on the surface of memory cells.

1.5 Co-infection and malaria susceptibility

Malaria-endemic regions are characterized by a high prevalence of infectious pathogens and diseases, leading frequently to co-infections[88,89]. The immunological impact of co-infections is multifaceted, affecting both individuals and populations. At the individual level, co-infections lead to diminished vaccine and drug efficacy and altered disease transmission. On a population level, they can result in reduced economic productivity[90–94]. Notably, in sub-Saharan Africa, co-infections involving *P. falciparum* with other *Plasmodium* strains and various bacterial, viral, and parasitic species, including *Mycobacterium tuberculosis*, Human Immunodeficiency Virus (HIV), and dengue virus, have been observed and their impact on disease severity and immune responses assessed.

Co-infections involving *P. falciparum* and HIV have been the subject of extensive research due to their widespread occurrence and substantial clinical implications. Previous investigations have revealed an increased prevalence of severe malaria among individuals co-infected with HIV, as well as a notable reduction in malaria-specific antibody concentrations among HIV-positive pregnant women with placental malaria[95,96]. While the potential influence of HIV on the severity of malaria disease is more obvious given the

pivotal role of $CD4^+$ T cells in the immune response against *P. falciparum* and the specific cellular tropism of HIV, the broader impact of *P. falciparum* co-infections with less investigated yet highly prevalent parasites remain inadequately studied.

The agents of neglected tropical diseases (NTDs) represent a group of pathogens highly prevalent in tropical regions, contributing to over one billion infections in sub-Saharan Africa[97]. This diverse array of NTD-causing pathogens encompasses viruses, bacteria, fungi, and parasites, with some of the most widespread ones including leishmaniasis, soil-transmitted intestinal helminths (ascariasis and hookworm), schistosomiasis, and Chagas disease[98]. Parasitic infections account for nearly 60% of all NTD cases, often sharing a geographical overlap with *P. falciparum*[97]. This proximity raises the potential for parasitic coinfections, thereby impacting malaria pathogenesis. For instance, leishmaniasis, a parasitic NTD that targets immune cells such as macrophages and DCs, annually affects nearly one million individuals[99]. Studies involving co-infection with malaria in rodent models have revealed a *Leishmania* spp.-specific influence on the severity of malaria[100].

Soil-transmitted intestinal helminths, responsible for over one billion infections worldwide, have demonstrated the ability to induce immunosuppression when co-infected with *P. falciparum*[101,102]. However, whether this immunosuppression exacerbates malaria-associated pathology remains unclear. Investigations into helminths, which infect distinct cell populations compared to *P. falciparum* have shed light on the significant impact of co-infection on the host's immune response to infection. This, in turn, prompts the pertinent question: how does *Schistosoma* spp., blood flukes with a preference for blood vessels, influence the host's immune response to *P. falciparum*, a parasite that primarily infects circulating red blood cells throughout the body?

1.6 Schistosomiasis

In 2019, the World Health Organization reported an estimated 240 million cases of schistosomiasis[103,104]. Among these cases, more than 40% were attributed to ***Schistosoma haematobium*** (***Sh***)[105–107]. Schistosomiasis, a neglected tropical disease caused by multicellular eukaryotic parasites of the genus *Schistosoma*, is a significant global health concern. This is a disease associated with poverty. The genus *Schistosoma* includes several species that commonly infect humans, such as *Schistosoma haematobium*, *Schistosoma mansoni*, *Schistosoma japonicum*, *Schistosoma mekongi*, *Schistosoma intercalatum* and *Schistosoma guineensis*. These *Schistosoma* species, excluding *S. haematobium*, primarily cause intestinal schistosomiasis, while *S. haematobium* is responsible for urogenital disease.

1.6.1 *Schistosoma haematobium* life cycle and pathology

In sub-Saharan Africa, *S. haematobium* is the most prevalent and debilitating *Schistosoma* species, accounting for over 90 percent of all schistosomiasis cases[104]. The *Schistosoma* lifecycle requires both a primary human host and an intermediate snail host. Infection begins when cercariae larvae, in fresh water, directly penetrate the host skin and become schistosomulae. Schistosomulae enter venous circulation and end up in the liver where they mature into adult worms. Male and female adult worms pair off and migrate to the venous plexus of the urinary bladder where they mate for life and produce eggs within 4-6 weeks. A mating pair of adult worms can last up to 30 years. Eggs are normally excreted in the urine but can aberrantly migrate and can be retained in tissue leading to chronic schistosomiasis as the result of granulomas that form around this foreign body. Eggs shed from the human host hatch into miracidia and penetrate fresh-water snails.

Within the snail, miracidia mature into sporocysts which produce cercariae larvae that are released into fresh water and infect the next human host to continue the transmission cycle.

Schistosomiasis symptoms can manifest within days or weeks to months after infection depending on the exposure history of the individual. Acute schistosomiasis, known as Katayama fever, is usually prevalent in tourists or individuals from non-endemic regions, with symptoms ranging from mild, such as dermatitis, headache, fever, painful urination to more severe cases such as diarrhea, labored breathing, hepatomegaly, chronic kidney disease, and abdominal pain[108]. Chronic schistosomiasis is asymptomatic and prevalent in individuals who live in an endemic setting. However, studies show that chronic *S. haematobium* infection contributes to genito-urinary disease, leading to complications such as bladder cancer and infertility in Africa[109,110].

1.6.2 Immune responses to helminths

Host immune responses to schistosomiasis are complex and vary depending on the life cycle of the *Schistosoma*, antigens present, and the location within the host. Our understanding of immune responses to helminth infections relies on mouse models due to the limitations of human immunology. Although progress in human immune models has been made, studies on schistosomiasis are limited due to its neglected nature.

Although type 2 immune responses dominate during helminthic infections, the primary response to an initial infection is mediated by type 1 immune cells. $CD4^+$ Th1 cells produce pro-inflammatory cytokines such as IFN-γ and TNF-α during the early stages of infection to recruit DCs and macrophages to facilitate parasite clearance. Th1 immune responses are directed towards the early forms of the parasites (schistosomulae and adult worms). As the infection progresses and the worms produce eggs, CD4+ Th2 cells produce effector

molecules such as IL-4, IL-5, and IL-13 which help recruit and activate mast cells, eosinophils, and fibroblasts. However, prolonged type 2 responses lead to the formation of granulomas around schistosome eggs that progress to hepatic and bladder fibrosis[111,112]. During the chronic phase of infection, Tregs play an important role in modulating the immune responses and preventing excessive fibrosis by producing anti-inflammatory cytokines, such as IL-10 and TGF-β, to moderate Th2 immune responses[111,112].

1.7 Malaria and schistosomiasis co-infection

Studies estimate that the prevalence of malaria-schistosomiasis co-infection among children in sub-Saharan Africa can be as high as 30-50% in regions where both diseases are endemic[113,114]. The high prevalence of both malaria and schistosomiasis in sub-Saharan Africa as well as disease prognosis make these two diseases an important model to study parasitic co-infection in an endemic setting.

Much of our understanding about the immunological response to malaria co-infections derives from research using mouse models. These studies have demonstrated that helminth-malaria co-infections lead to suppressed Th1 responses that result in increased *Plasmodium* parasitemia in mice[115–117]. However, there are several limitations to these studies in terms of how well they represent human *Pf-Sh* co-infection. Most experimental models of helminth-malaria co-infection use intestinal, soil-transmitted helminths such as roundworms and hookworms, but do not address the impact of helminths that are blood-borne, such as *Sh*. Moreover, rodent *Plasmodium* species are distantly related to *Pf*[118], *Plasmodium* species that infect humans do not infect rodents, and there are well-established differences in biology between *Pf* and rodent *Plasmodium* species[119,120]. Although these models serve as a foundation to understand co-infections, the results are not always

translatable to human infection. Human studies on co-infection have reported conflicting results; some studies suggesting that pre-existing *Schistosoma* infections lead to increased malaria susceptibility[89,121], while more recent, prospective studies have shown that *Schistosoma* can reduce the severity of subsequent *Plasmodium* infections through the modulation of host immune responses[11,122–124].

Our group has previously studied the impact of malaria-schistosomiasis co-infection in humans using PBMCs collected prospectively from Malian children who were actively followed for nine months. These studies showed that co-infection with *Sh* promotes the maintenance of *Pf*-specific B and T cell memory responses, and alters regulatory T cell response[122,123,125]. Furthermore, these data provide evidence of a correlation between IL-4 cytokine expression derived from central memory T cell (T_{CM}) populations and *Sh*-positivity in children[122]. Research shows that T_{CM} are long-lived when compared to effector memory T cell (T_{EM}) populations[126,127], consistent with the importance of the former to long-term memory acquisition. Cytokines such as IL-4, IL-7, IL-15, and IL-21 have been identified as critical for the maintenance of memory T cells[128–132]. However, it is currently unknown whether *Sh* infection impacts expression of genes encoding molecules critical for memory cell survival.

1.8 Specific Aims

Aim 1: Immunogenomic profile at baseline predicts hosts susceptibility to clinical malaria.

Objective: To identify key determinants of susceptibility and protection to malaria in children from malaria endemic regions.

Hypothesis*: In areas of high malaria transmission, children who do not manifest clinical disease throughout a transmission season can control infection better than those who experience two or more symptomatic malaria episodes during the same period. We hypothesize that this difference is reflected in their PBMC transcriptomic profiles.*

Approach: Utilizing PBMCs collected from children aged 4-6 years at the onset, peak, and conclusion of the malaria season, this aim will (1) employ a transcriptomics approach to investigate gene expression dynamics over the course of a single malaria transmission season and (2) conduct immunophenotyping and cytokine secretion analysis to identify key cell types and cytokine secretion patterns explaining differences in malaria susceptibility.

Aim 2: Dynamics of T cell responses during malaria infection in *Schistosoma haematobium*-negative and *Schistosoma haematobium*-positive individuals.

Objective: To explore the dynamics of immune responses during acute *Plasmodium falciparum* infection and assess the impact of a pre-existing *Schistosoma haematobium* co-infection.

Hypothesis*: A pre-existing S. haematobium (Sh) co-infection modulates host immune responses to secondary P. falciparum infections, leading to the generation and maintenance of responsive memory CD4 T cells in the human host.*

Approach: Using single-cell RNA-sequencing on PBMCs from children aged 4-8 in a highly malaria-endemic region in Mali, this aim will (1) identify and characterize distinct cell population present in *Sh+ and Sh-* children exposed to *P. falciparum* and (2) compare cell composition and gene expression differences induced by *P. falciparum* infection while assessing the influence of co-infection.

Significance:

This research aims to provide valuable insights into immune responses in children exposed to *P. falciparum*, potentially identifying novel markers for susceptibility, and elucidating regulatory networks governing T cell dysfunction during malaria infection and co-infection. The outcomes will contribute to our understanding of disease tolerance establishment and protective outcomes associated with malaria infection, guiding the development of targeted interventions and vaccine strategies against malaria.

Chapter 2: Immunogenomic profile at baseline predicts hosts susceptibility to clinical malaria.

2.1 Abstract

Host gene and protein expression impact susceptibility to clinical malaria, but the balance of immune cell populations, cytokines and genes that contribute to protection, remains incompletely understood. To identify determinants of host susceptibility to clinical malaria at a time when acquired immunity is developing, we analyzed PBMCs collected from children who differed in susceptibility to clinical malaria, all from a small town in Mali. PBMCs were collected from children aged 4-6 years at the start, peak and end of the malaria season. We characterized the immune cell composition and cytokine secretion for a subset of 20 children per timepoint (10 children with no symptomatic malaria age-matched to 10 children with $\geq$2 symptomatic malarial illnesses), and gene expression patterns for six children (three per cohort) per timepoint. We noted higher frequency of HLA-DR$^+$ CD4 T cells in protected children during the peak of the malaria season and comparable levels cytokine secretion after stimulation with malaria schizonts across all three time points. We also observed differences between the two groups of children in the expression of genes related to cell death and inflammation; in particular, inflammatory genes such as CXCL10 and STAT1 and apoptotic genes such as XAF1 were upregulated in susceptible children before the transmission season began. This suggests that differences in apoptotic and inflammatory gene expression patterns can predict susceptibility to clinical malaria.

---

225. Mbambo, G. *et al.* Immunogenomic profile at baseline predicts host susceptibility to clinical malaria. *Frontiers in Immunology* **14**, (2023).

2.2 Introduction

Malaria remains a major global health concern that impacts over 200 million people annually, causing an estimated 619,000 deaths in 2021[10]. Despite its global distribution throughout the tropical and subtropical regions, 95% of malaria cases occur in sub-Saharan Africa, and are caused primarily by *Plasmodium falciparum*[10]. Individuals in malaria-endemic regions with high transmission are repeatedly exposed to diverse *P. falciparum* strains and their associated antigens; these successive exposures can lead to acquired immunity to clinical malaria[133]. However, children with similar levels of malaria exposure can vary in susceptibility to clinical disease. Several host factors, including those related to red blood cell disorders (HbS, HbC, G6PD and alpha-thalassemia), are known to be associated with protection, while some HLA alleles are associated with increased susceptibility to malaria infection[15,16]. Nevertheless, much remains to be understood, particularly regarding differences in the host response to infection[134].

Previous studies have implicated the activation of the type 1 interferon pathway in mitigating severe disease to mild malaria and FN-γ secretion with protection from clinical disease[135]. However, other studies suggest a role for IFN-γ in exacerbating severe malaria episodes (cerebral malaria), implying that a delicate balance of inflammatory cytokines is critical to regulate malarial disease and pathogenesis[33]. T cell-mediated immune responses play an important role in controlling pro- and anti-inflammatory immune responses during blood stage malaria[50]. Type 1 helper CD4 T cells (Th1) produce inflammatory cytokines such as IFN-γ and TNF-α that shape the early adaptive immune response to *Plasmodium* infection. These inflammatory responses are controlled by regulatory T cells (Tregs) that produce cytokines such as IL-10 and TGFβ[58]. Later in infection, Type 2 helper CD4 T cells

(Th2) dominate and aid in antibody production, which is characteristic of a protective response to blood stage *Plasmodium* infection[52].

Transcriptomic analysis from whole blood cells has shown that naïve individuals >13 years old have a higher pro-inflammatory cytokine response when compared to their malaria-experienced counterparts upon infection with *P. falciparum*[59]. This may indicate a dampened immune response in individuals with pre-existing immunity to malaria, which could impact the clinical presentation of the disease. Some studies suggest exhausted B and T cells play a role in the lack of robust immune responses in individuals with recurrent exposure to *P. falciparum*[136]. However, it remains to be determined how molecular pathways correlate with malaria exposure history in children with distinct levels of susceptibility to clinical malaria, and which immunoprofiles characterize a protective response. Gene expression studies are increasingly used to decipher molecular mechanisms and pathways associated with malaria infection using either PBMCs or whole blood[59,137], and to analyze gene expression patterns in immune cells during malaria infection only[59,138]. Here, we compare the longitudinal transcriptional profiles of two cohorts of location and age-matched children, ages 4 to 6 years old, who differ in the degree of malaria susceptibility, to better understand the protective immune response to malaria at a time when acquired immunity is developing.

We hypothesize that in an area of high malaria transmission, children who do not manifest clinical disease throughout an entire transmission season can control infection better than those who experience two or more symptomatic malaria episodes during the same period (either by preventing erythrocytic infection or by controlling symptoms), and that this difference is reflected in their PBMC transcriptomic profiles. To address this

hypothesis, we compared PBMC gene expression profiles derived from a subset of children categorized as "susceptible" versus "non-susceptible/protected" to malaria, and who were part of the control arm of a malaria vaccine trial in Mali[139]. An improved understanding of the host immune response to malaria, and in particular the identification of immune cell subpopulations that may play a role in a protective immune response, may identify those at increased risk and inform preventative treatment.

2.3 Methods and Sample Collection

2.3.1 Ethics

Sample processing was conducted with review and oversight by the University of Maryland, Baltimore's Human Research Protection Office. The primary study was reviewed and approved by the Institutional Review Boards of the University of Maryland, Baltimore and the University of Bamako, Mali. Village permission to conduct research was obtained from village chiefs, government officials, and traditional healers prior to study initiation. Individual written informed consent was obtained from the parent or legal guardian of each child prior to screening and enrollment in accordance with the Declaration of Helsinki. Child assent was also obtained prior to study conduct.

2.3.2 Study Design

After obtaining informed parental consent, PBMCs from children who were part of a randomized, controlled, double-blind Apical Membrane Antigen 1 (AMA1) malaria vaccine trial in Bandiagara, Mali, West Africa, were cryopreserved on site using standardized procedures and transported to the University of Maryland, Baltimore (UMB), utilizing a tightly controlled cold chain. Registration on ClinicalTrials.gov (NCT00460525) and full study details have been previously described[139]. Bandiagara,

Mali, is a Sahelian town of approximately 14,000 inhabitants with highly prevalent and seasonal malaria transmission (June to December)[122,140]. There is no significant variability in the socio-economic state in this remote community. The prevalence of HIV is extremely low, and previous screening of children aged 3 months to 14 years revealed no concomitant infections with filaria. While *S. haematobium* is endemic, prevalence is typically low for children aged 2-6 years. At the time of the study conduct, children under 6 years of age routinely acquired 1-4 symptomatic malaria infections per season. All children were provided government-issued, insecticide-treated bed nets with 61% of control participants reporting use[139]. Participants were continuously monitored through passive case detection and the rate of loss to follow-up was less than 7%. The Bandiagara research center served as the primary source of western medical care for most children in the village, and few had access to pharmaceuticals for intermittent malarial therapy. A subset of children (n = 25) ages 4-6 was selected from the control arm (three doses of human diploid-cell rabies vaccine (RabAvert, Chiron Vaccines)) based on age, number of clinical malaria episodes, and availability of sample across all three timepoints[139]. We examined PBMCs from this cohort (Supplementary Table 2.1). The original study followed children during a single malaria transmission season (6 months) and PBMCs were collected at day 0 (beginning of transmission season), day 90 (peak transmission season), and day 150 (end of transmission season) (Supplementary Figure 2.1A). For this analysis, children with at least two clinical malaria episodes throughout the transmission season were classified as "susceptible" and were age-matched to children with no clinical malaria episodes throughout the same transmission season; the latter were classified as "protected" (Supplementary Figure 2.1B). Malaria episodes were acquired by susceptible participants between day 8 and 146. The

timing of illness varied among participants, with the majority experiencing their first episode before the day 90 timepoint, except for one participant (Supplementary Figure 2.1C). Clinical malaria was defined as a symptomatic infection consistent with malaria (e.g., fever, headache, malaise) and evidence of parasitemia in the absence of an alternative clinical diagnosis. None of the children met the definition of severe malaria. Only children with PBMC available at all three time points were eligible for analysis. Serum samples were collected for each child at the same timepoints and kept at -80ºC.

2.3.3 Peripheral Blood Mononuclear Cells (PBMC) Stimulation

Cryopreserved PBMCs were thawed with fetal calf serum (FCS) enriched media (RPMI, Gibco, Grand Island, New York) and incubated at 37ºC/5% CO_2 overnight. After incubation, PBMCs were washed and partitioned into three $1x10^6$ cell aliquots. One aliquot was stimulated with *P. falciparum* schizonts (Pfsz; derived from a Malawian source and cultured *in vitro* at UMB) at a 3:1 ratio (3 schizonts/cell) and incubated at 37ºC/5% CO_2 for 4 hours. The other two aliquots served as negative (media) and positive (stimulation with 10 mg/ml *Staphylococcus* enterotoxin B (SEB); Sigma, St. Louis, MO) controls and incubated at 37ºC/5% CO_2 for 2 hours. Golgi blockade (BD Pharmingen) was added at 0.5 mL/tube and incubated overnight (16 hours) at 37ºC/5% CO_2. As the addition of Golgi blockade compromised RNA integrity, a finding not previously noted in the literature, samples from 6 unique randomly selected children that met the age and malaria episode criteria were immediately extracted after stimulation for RNA sequencing without the addition of Golgi blockade.

2.3.4 Regulatory T cell (Tregs) depletion

PBMCs were thawed as described above. A portion of the cells were partitioned to serve as negative and positive controls. The remaining PBMCs were split into two aliquots that were either mock depleted or depleted of CD25 cells using Dynabeads Pan Mouse IgG or CD25 magnetic beads, respectively (Invitrogen, Carlsbad, California) at a bead to PBMC ratio of 5:1 as described[125]. PBMCS were stimulated with media, schizonts and SEB as described above.

2.3.5 Staining Protocol

PBMCs were stained with viability marker, Cisplatin ($Pb^{194/195}$) (Sigma Aldrich, Indianapolis) at 1.25 mL per 500 mL for a final concentration of 25 mM. After a 1-minute incubation, PBMCs were washed with PBS supplemented with 10% FCS then incubated with one of two optimized (13-21 cell surface markers) panels (Supplementary Tables 2.2-2.3) for 20 minutes. Cells were then fixed using IC fixation buffer (eBioscience) and permeabilized using Caltag Reagent B (Invitrogen, Oregon) along with an intracellular staining cocktail (Supplemental Tables 2.1-2.2), followed by the addition of DNA intercalator Iridium 191 (Ir-191 intercalator, NA). Cells were then washed 2x with cell staining media (0.2 mg/mL sodium azide in low-barium PBS supplemented with 2% FCS) and resuspended in Milli-Q water for assessment by mass cytometry. Before analysis, a viability dye, $Cisplatin^{141}$ and the DNA metalointercalator $^{191/193}Ir$ to identify individual cells, was used to complete the panel.

2.3.6 Generation of RNAseq data

Immediately after PBMC stimulation, Roche Protector RNase inhibitor (3335399001; MilliporeSigma, Burlington, Massachusetts, USA) was added to each

sample. RNA was isolated using QIAzol (Qiagen 79306; Hilden, Germany) and the Direct-zol RNA Mini Prep Plus Kit (Zymo Research, Irvine, California, USA) per manufacturer's instructions. RNA quality was assessed using the Agilent Bioanalyzer 2100, and only samples with RNA integrity numbers (RIN) greater than 7 or total RNA concentration greater than 100 ng were selected for RNA sequencing (Supplementary Table 2.4). PolyA-enriched, strand-specific RNA libraries were constructed and 100bp paired-end reads were sequenced on an Illumina NovaSeq 6000 platform. Reads were assessed for quality, trimmed if PHRED scores fell below 20, and any remaining adapter sequences were removed. These processed paired-end reads were aligned to human reference genome GRCh38 using HISAT2, and counts were generated using the HTseq analysis package[142–144]. Reads that successfully mapped to the reference genome were used for downstream analyses. The data are available under bio-project ID (PRJNA603324).

2.3.7 Differential Gene Expression Analyses

To perform differential gene expression analyses, we used DEseq, EdgeR and Cuffdiff R packages[142–145]. Any genes with counts per million (CPM) values of less than 10 in 86% of the samples (or 45 of all 53 samples analyzed) were excluded from the analyses. Hemoglobin genes (the most expressed genes after those encoding rRNAs) were removed to improve power. This cutoff was selected to account for the low sample size and to ensure that each group had at least two samples present for differential expression analyses. For visualization of differentially expressed genes, normalized read counts generated by DEseq were input for the software gEAR (https://umgear.org/multigene_curator.html) to create volcano plots, implemented using the Dash Bio suite of bioinformatics components (v0.6.1 - https://github.com/plotly/dash-

bio). Welch's t-test was used to determine significance[146], and was computed using the python package diffxpy (v0.7.4 - https://github.com/theislab/diffxpy).

2.3.8 Pathway and functional analysis

Pathway enrichment analysis was conducted with the output from deseq2. Differentially expressed genes with a false discovery rate (FDR) <0.05, and a log fold change (LFC) >1, were used. Genes that passed these cutoffs were submitted to DAVID web-based tool (https://david.ncifcrf.gov/tools.jsp)[147–149]. Bar plots were created with GraphPad Prism v9. Further functional analyses were performed using GSEA[149], using normalized expression values from all genes as the input.

2.3.9 Mass cytometry data processing

FlowJo v.10.8.0 Software (BD Life sciences, Ashland, Oregon, USA) was used to select intact ($Ir191^+$, $Ir193^+$), live ($PT195^-$), singlet, $CD14/CD19^-$ and $CD3^+$ cells. Specimens were included in the analysis if (*i*) the cell viability was >80% after thawing and (*ii*) cells were shown to be functionally active as determined by the production of IFN-γ by at least 0.2% $CD3^+$ cells after stimulation with SEB. A response was considered specific if (*i*) the differential in the number of positive events in the stimulant pool compared to the media control was significantly increased by Chi-square analyses; and (*ii*) the net percentage of cytokine producing cells was >0.1% in stimulant pool as compared to the media control. A response was considered positive if the production of one or more cytokines, meeting the pre-defined criteria, was measured in response to antigen stimulation of PBMCs. A mean of ~200,000 cells per sample were analyzed by the CyTOF® Mass Cytometer, with 71%-98% of the cells intact. After gating, $CD3^+$ populations were exported via FlowJo to create new FCS files containing only the intact,

live, $CD3^+$ cell populations. FCS files were further analyzed in R version 2021.09.2 +384 using flowCore[150] and CATALYST[151,152] packages. FlowCore package was used to read the FCS files into R and CATALYST package was used to create a single cell experiment and transform the data with arcsinh cofactor 5. FlowSOM[153] and ConsensusClusterPlus[154] packages were used to perform high dimension clustering and generate 20 clusters using the cell surface marker panel (Supplementary Table 2.2). UMAP was used to perform high dimension reduction to visualize the clusters generated. Clusters were manually annotated based on cell surface marker expression.

2.3.10 Differential analysis of mass cytometry data

Differential analysis was performed using *diffcyt* (https://bioconductor.org/packages/3.15/bioc/html/diffcyt.html), an R package that utilizes *edgeR, limma* and *voom* methods as part of the workflow[155]. We used the *diffcyt* differential abundance (DA) method to test for differences in cell type abundance between our two study groups and the *diffcyt* differential states (DS) method to test for differences in intracellular marker expression within each identified cell population between protected and susceptible individuals. We used an FDR cutoff of <0.05 to identify differentially expressed cell types and cytokines.

2.3.11 Differential antibody responses to PfEMP1 microarray

A protein microarray featuring 257 PfEMP1 protein fragments from reference and clinical infections was probed with sera collected before the malaria transmission season (day 0), from 19 children in the same cohort. Samples were randomly selected to include children whose PBMCs were processed via RNA sequencing and mass cytometry. Nine serum samples were from protected children while 10 serum samples were from

susceptible children. Sera from a pool of North American malaria-naïve adults was used as a negative control while sera from Malian adults from the same study site collected under a different study protocol were used as positive control[156]. Slide preparation and serum probing were performed as described elsewhere[157–159]. Fluorescence intensity was defined as the raw signal intensity reduced by the mean for the no-DNA negative controls for each serum sample. For each protein fragment, we compared the distribution of fluorescence intensities between sera of susceptible and protected children with a two-tailed Wilcoxon rank-sum test.

2.4 Results

2.4.1 Quality control of data and experimental samples

PBMCs were processed from 26 Malian children. Cells from 6 individuals were processed through RNA sequencing and cells from 20 distinct children were profiled via mass cytometry. Study groups were assigned based on the number of clinical malaria episodes experienced during a single malaria transmission season.

RNAseq data was generated for six children for each of the three timepoints, and for each of the three stimulation conditions (media, schizonts and SEB), for a total of 54 samples. One SEB stimulated sample from day 150 did not pass QC and was not included in the analyses. For each sample, an average of 30 million Illumina reads were generated (Supplementary Table 2.5).

Mass cytometry data was generated for 20 different children from the same cohort. For each of the three time points, and each of the three conditions, an average of 200,000 cells were processed. Samples were functionally active if SEB stimulated controls had at least a 0.2% increase in IFN-γ production relative to unstimulated cells.

2.4.2 Gene expression differences exist between susceptible and protected groups at baseline

To assess if gene expression differences are present between malaria-protected and malaria-susceptible children, we performed a pair-wise comparison of bulk RNA sequence data to identify genes that were either significantly up-regulated or down-regulated at day 0 (start of malaria transmission season) before and after PBMC stimulation with malaria antigen. At baseline, we observed 78 genes significantly differentially expressed based on our analysis parameters (Figure 2.1A). We observed 74 downregulated and 4 upregulated genes in protected relative to susceptible children. Baseline differences in gene expression at the beginning of the malaria season suggest that differences already exist between children who later develop clinical malaria episodes and those who do not. Of interest, genes upregulated in susceptible children compared to protected children included CXCL10, STAT1, STAT2, IRF1, XAF1 and GZMB. CXCL10, STAT1 and STAT2, all genes that are downstream of interferon signaling, and IRF1, XAF1 and GZMB, which participate in apoptotic processes. Next, we evaluated gene expression patterns in Pfsz-stimulated PBMCs and observed 11 differentially expressed genes, of which 9 were downregulated and 2 upregulated in protected children relative to susceptible children. We observed some overlap in upregulated genes in susceptible children before and after antigen stimulation (Figure 2.1B, Supplementary Figure 2.2A). One gene, DDX11, was upregulated in protected children before and after Pfsz stimulation (Figures 2.1A,B and Supplementary Figure 2.2B). DDX11 encodes a helicase and plays a role in DNA repair[160]. However, the direct role of this gene in regulating immune responses is not known.

To determine if the expression patterns observed were restricted to individual genes or whether, instead, they reflect broader differences at the pathway level, we searched for enriched biological, functional, and immunological pathways at day 0, with DAVID, using genes upregulated in susceptible children (FDR < 0.05; LFC >1) as input. Relative to protected children, we observed enrichment in "Type I interferon signaling," "interferon-gamma signaling," and "apoptotic" pathways in susceptible children (Figure 2.1C,D). Further analysis using gene set enrichment analysis (GSEA) showed enrichment in IFN-γ and apoptotic pathways (Supplementary Figure 2.3).

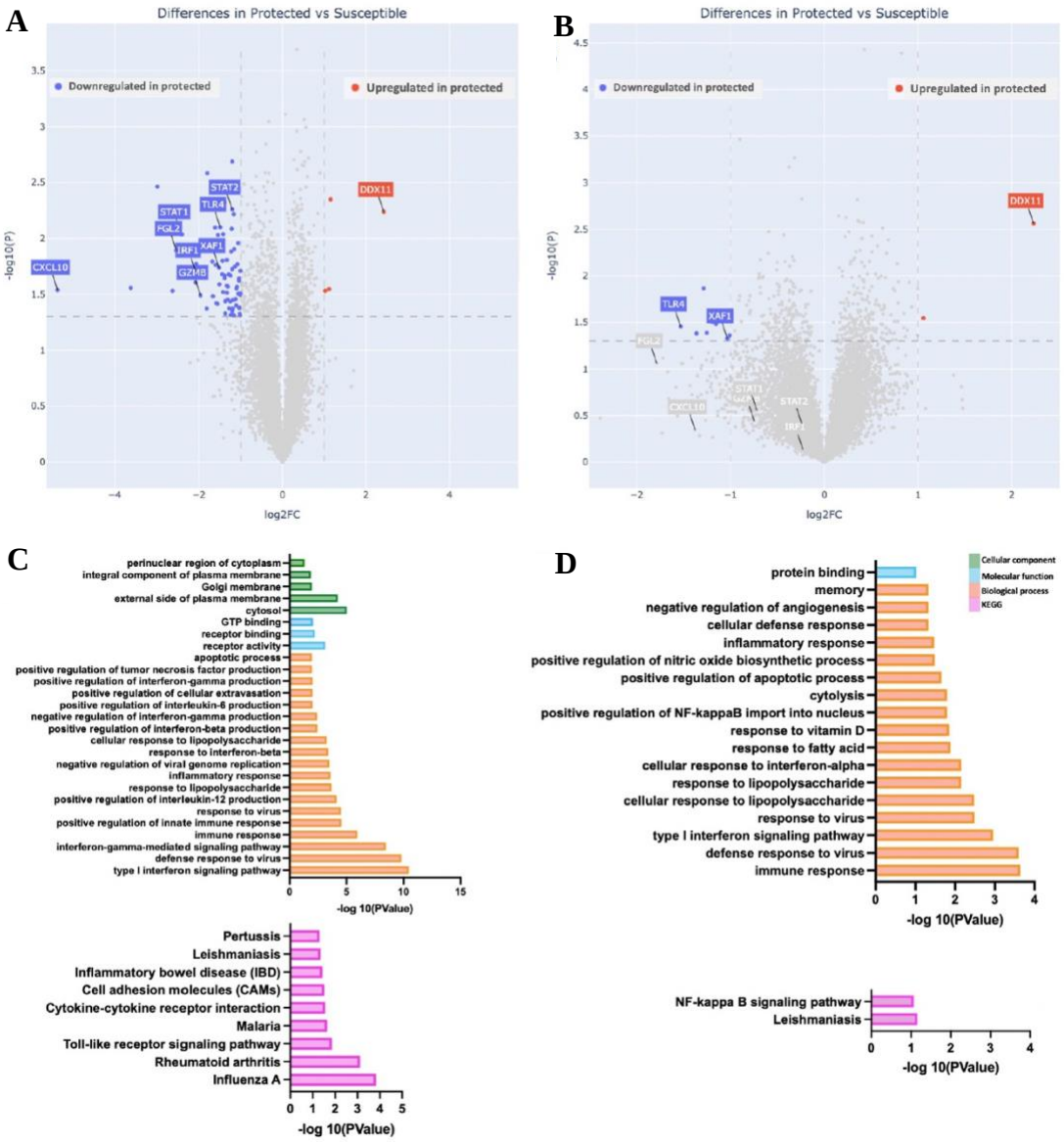

Figure 2.1. Differences in gene expression and immune pathways exist at baseline.

(**A-B**) Depicted is a volcano plot of differential gene expression, with significant differences shown (blue, red), based on Welch's Test (log10(pval) is plotted against the log2 foldchange; significance: P value <0.05). (**A**) Unstimulated PBMCs. (**B**) PBMCs stimulated with malaria antigen (*P. falciparum* schizont, Pfsz) . (**C-D**) Pathway enrichment analysis on differentially expressed genes (False discovery rate, FDR<0.05; gene expression log-fold change, LFC>1), using pathway enrichment software DAVID[148]. (**C**) Pathways enriched in susceptible children before antigen stimulation . (**D**) Pathways enriched in susceptible children after Pfsz stimulation. Enrichment analyses were performed on differentially expressed genes that met the FDR and LFC thresholds; no genes overexpressed in protected children met this threshold.

To determine whether the observed differences in gene and pathway expression were based on different levels of pre-existing immunity to malaria between the susceptible and protected groups, we probed a protein microarray populated with 257 fragments of *P. falciparum* erythrocyte membrane protein-1s (PfEMP1s) with sera from day 0 timepoint. Increased responses to PfEMP1 have been associated with recent malaria exposure[161–163]. We compared the PfEMP1 serologic responses between the two groups and observed no differences in antibody responses to 99.2% of the fragments (255/257 PfEMP1 fragments; Supplementary Figure 2.4B). Additionally, we compared the proportion of individuals within each group with serorecognition of each protein fragment (defined as a fluorescence intensity greater than the mean plus two standard deviations for a serum panel from 10 malaria-naïve North American adults probed on the microarray). We observed that across extracellular PfEMP1 fragments, there was a trend towards greater proportions of protected children with serorecognition of these fragments than susceptible children [68.1% of extracellular PfEMP1 fragments(65/204)]. Interestingly, for 19 of the 20 intracellular PfEMP1 fragments on the microarray, a higher proportion of the susceptible group had serorecognition of the intracellular PfEMP1 fragment than the protected group (Supplementary Figure 2.4C). Our group previously found that serologic responses to the intracellular region of PfEMP1s is associated with greater malaria exposure[162], suggesting that the susceptible group may have had more malaria exposure than the protected group. In addition, we analyzed previously published ELISA data for Apical Membrane Antigen 1 (AMA1), another important blood stage *P. falciparum* antigen, the responses to which decrease over time since a previous clinical malaria episode[164], for individuals in the same study. A comparative analysis of 25 samples for which data was available, twelve of which

were from protected and 13 of which were from susceptible children, showed no significant differences in the baseline AMA1 antibodies present in the serum collected from the children in either cohort (Supplementary Figure 2.5). The lack of differences in antibody responses to PfEMP1 and AMA1, two major blood stage malaria antigens, suggest that the differences in gene and pathway expression between groups are not due to differences in malaria exposure between the two groups. Finally, we investigated the possibility of ongoing subclinical malaria infections in susceptible children at baseline. To this effect, we analyzed previously generated data on a screen to detect the presence of parasites based on PCR amplification of the AMA1 gene from the day 0 timepoint[139]. Although 2/12 individuals from the protected group were asymptomatically positive at baseline compared to 0/13 individuals from the susceptible group, we observed no statistically significant differences (Fisher's exact test) in the percent of individuals testing positive for malaria for each study group (Supplementary Figure 2.6A-B), consistent with the hypothesis that the observed patterns are not caused by differences in ongoing or recent malaria exposure.

2.4.3 Gene expression at peak malaria transmission

To evaluate how increased natural exposure to malaria impacts the differences observed at baseline, we evaluated gene expression differences between the two groups at day 90 (peak malaria transmission). At this time point, we identified 73 differentially expressed genes in the unstimulated PBMCs; 61 were downregulated while 12 were upregulated in PBMCs from protected children relative to susceptible children (Figure 2.2A,B). Pathway enrichment analyses revealed significantly enriched "inflammatory response" among biological processes, in susceptible children (Figure 2.2C,D). We also observed enrichment in other biological processes in this group, including "chemotaxis"

and “response to IFN-γ,” as well as enrichment in molecular functions including “chemokine activity” and “receptor activity” (Figure 2.2C,D). KEGG pathway analysis revealed multiple enriched pathways in susceptible children, including the “malaria” pathway (Figure 2.2C,D). Consistent with pre-stimulation observations, the biological process “inflammatory response” was significantly enriched, after Pfsz-stimulation, in susceptible children compared to protected children (Figure 2.2D).

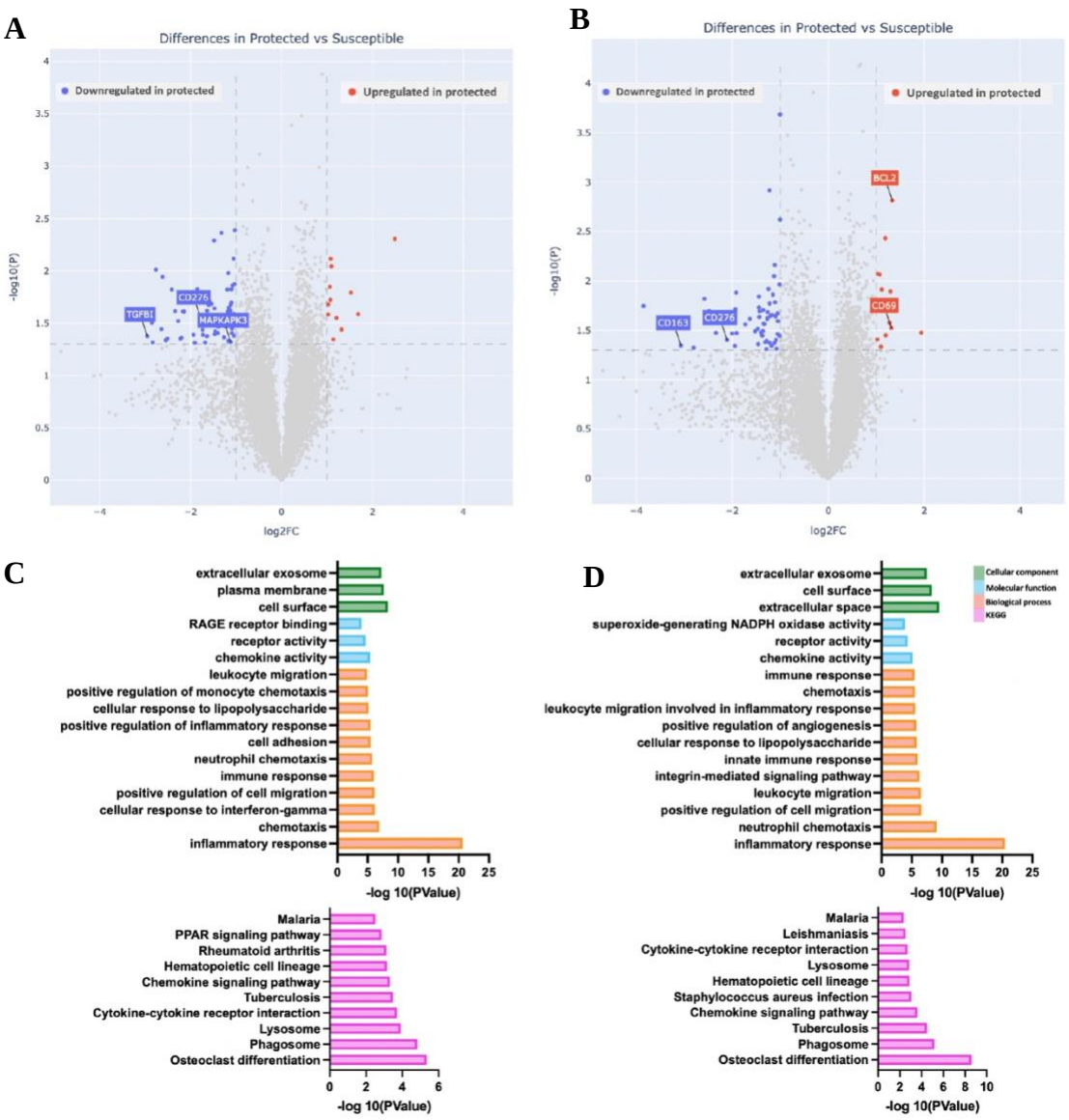

Figure 2.2. Gene expression differences during peak malaria transmission.

(**A**-**B**) Depicted is a volcano plot of differential gene expression, with significant differences shown (blue, red), based on Welch's Test (log10(pval) is plotted against the log2 foldchange; significance: P value <0.05). (**A**) Unstimulated PBMCs. (**B**) PBMCs stimulated with malaria antigen (*P. falciparum* schizont, Pfsz). (**C**-**D**) Pathway enrichment analysis on differentially expressed genes (False discovery rate, FDR<0.05; gene expression log-fold change, LFC>1), using pathway enrichment software DAVID[148]. Bar graphs depict Gene Ontology; Cellular component, molecular function, and biological processes that are enriched and KEGG pathways enriched at day 90. (**C**) Pathways enriched in susceptible children before antigen stimulation. (**D**) Pathways enriched in susceptible children after Pfsz stimulation. Enrichment analyses were performed on differentially expressed genes that met the FDR and LFC thresholds.

2.4.4 Reduced gene expression differences at the end of the malaria transmission season

We evaluated gene expression differences between the two groups at day 150 (end of the transmission season). We observed the fewest differences at this time point, with a total of 11 genes differentially expressed between the two groups. Six genes were downregulated compared to five genes upregulated in protected versus susceptible children (Figure 2.3A). Upregulated genes include the chemokine ligand CCL24, while downregulated genes included STAT1 and CD163. Pathway enrichment analysis revealed increased chemokine activity in susceptible children compared to protected children (Figure 2.3C,D). Chemokines play an important role during the host immune response to infection, as they recruit immune cells to the site of infection by binding chemokine receptors on the surface of immune cells[165]. In malaria, high serum chemokine levels are associated with high parasite density and in some cases, severe malaria[166,167].

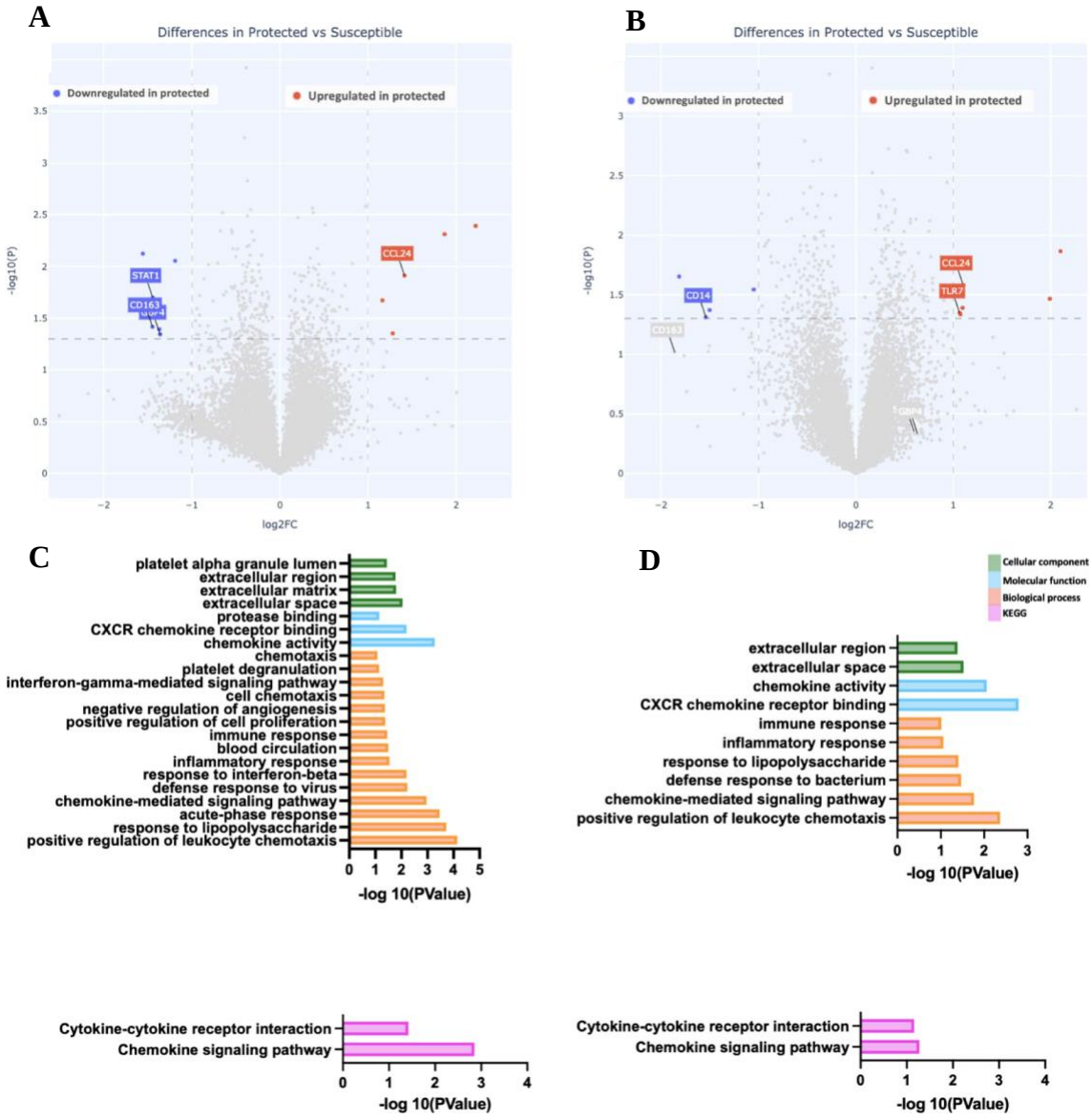

Figure 2.3. Reduced gene expression differences at the end of the malaria transmission season.

(**A**-**B**) Depicted is a volcano plot of differential gene expression, with significant differences shown (blue, red), based on Welch's Test (log10(pval) is plotted against the log2 foldchange; significance: P value <0.05). (**A**) Unstimulated PBMCs. (**B**) PBMCs stimulated with malaria antigen (P. falciparum schizont, Pfsz). (**C**-**D**) Pathway enrichment analysis on differentially expressed genes (False discovery rate, FDR<0.05; gene expression log-fold change, LFC>1), using pathway enrichment software DAVID148. Bar graphs depict Gene Ontology; Cellular component, molecular function, and biological processes that are enriched and KEGG pathways enriched at day 150. (**C**) Pathways enriched in susceptible children before antigen stimulation. (**D**) Pathways enriched in susceptible children after Pfsz stimulation. Enrichment analyses were performed on differentially expressed genes that met the FDR and LFC thresholds; no genes overexpressed in protected children met this threshold.

2.4.5 Similar immune cell population clustering patterns between protected and susceptible children

To identify additional distinguishing properties between children with varying malaria susceptibility, we also investigated the phenotypes of immune cell populations. PBMCs were stimulated and analyzed via mass cytometry (see Methods). Using a panel specific for effector function $CD4^+$ T cell profiling (Supplementary Table 2.2), we performed high dimensional clustering on $CD3^+$ PBMCs collected at each timepoint and identified distinct cell populations (Figure 2.4A-C). Across all three timepoints, we were able to successfully identify $CD8^+$, γδ and naïve and memory $CD4^+$ T cell populations, as well as a cluster annotated as "T cells" for cells that were not positive for either $CD4^+$, $CD8^+$ or γδ TCR antibodies. Memory cell populations became more defined as the transmission season progressed. By day 150, we identified distinct memory $CD4^+$ T cell populations, including central memory (T_{CM}) ($CD4^+CD45RA^-CCR7^+$), effector memory (T_{EM}) ($CD4^+CD45RA^-CCR7^-$), and $CD45RA^+$ effector memory populations (T_{EMRA}) in both protected and susceptible individuals (Figure 2.4B,C). For each identified cluster, we performed both differential cell type abundance and differential state analyses using *diffcyt* package. We observed variable cell type abundances across all individuals regardless of protected or susceptible status (Figure 2.4D-F, Supplementary Figure 2.7A-F). Differential state analysis did not detect any significant differences in intracellular marker abundance between protected and susceptible children; however, we observed slightly elevated levels of Programmed Cell Death 1 (PD-1) at day 0 and day 90 (Figure 2.5A-B), elevated IL-4 across all three timepoints (Figure 2.5A-C) and elevated IL-6 at day 150 within all PBMCs in susceptible children compared to protected children (Figure 2.5C). Within this small

subset, we did not observe significant differences in cytokine production within $CD4^+$ or $CD8^+$ T cells alone (Supplementary Figure 2.8).

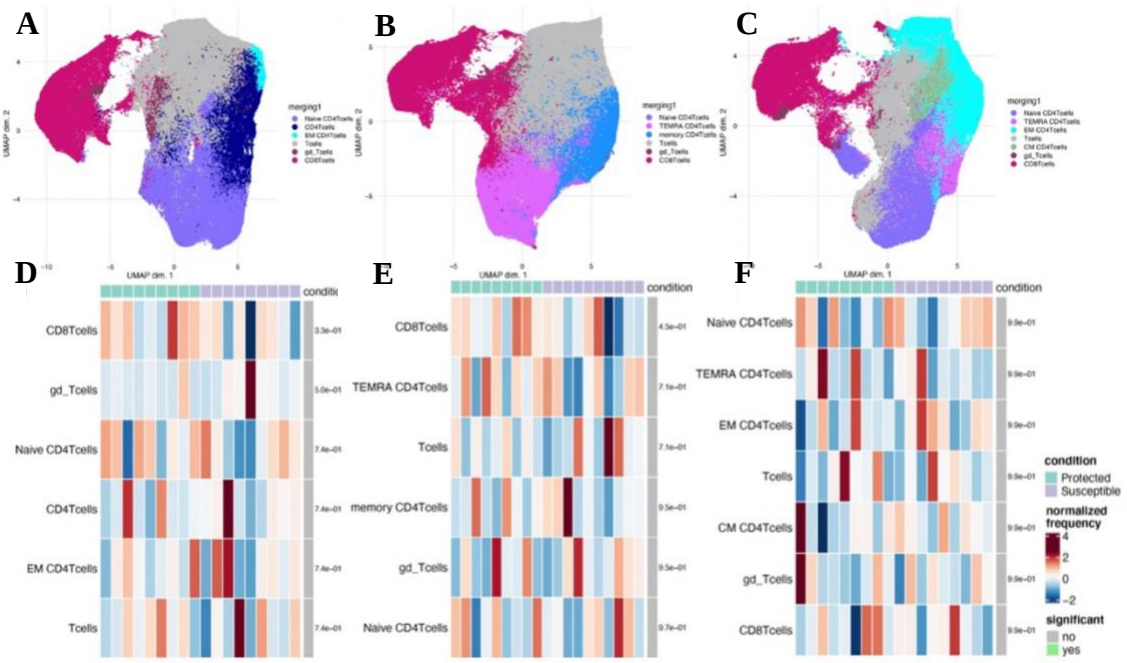

Figure 2.4. Phenotyping of CD3+ immune cell populations to assess effector function and cell type abundance across a single malaria transmission season.

(**A-C**) UMAP plots displaying immune cell populations identified though unsupervised clustering based on cell surface marker expression. (**A**) Clustering of cells from samples collected at the day 0 timepoint. (**B**) Cells from sampled collected at day 90. (**C**) Cells from samples collected at the day 150 timepoint. (**D-F**) Heatmap showing cell type frequencies of $CD3^+$ T cell populations present in protected (green) and susceptible (purple) children. High frequency populations are displayed in dark red and lowest frequencies are in dark blue. Population frequencies that are significantly different (FDR < 0.05) between protected and susceptible children are marked with a green bar. (**D**) Heatmap of cell type frequencies at day 0. (**E**) Heatmap of cell type frequencies at day 90. (**F**) Heatmap of cell frequencies at day 150.

The presence of slightly elevated levels of PD1 in the mass cytometry data along with the enrichment of cell death pathways in susceptible children prompted us to investigate the role of Tregs at baseline and across the transmission season. Previous studies show that the presence of Tregs may promote increased *P. falciparum* parasitemia due to a reduction in host responses to infection, and that these effects are reversed under CD25 depleted conditions[125,168]. To probe how Tregs from protected and susceptible

children behave as exposure to *P. falciparum* increases, we stained stimulated PBMCs with a regulatory T cell panel (Supplementary Table 2.3). We assessed cell composition and cytokine secretion patterns of stimulated $CD3^+$ cells in the presence and absence of Tregs ($CD4^+CD25^+$). We were able to successfully identify a small subset of Tregs (200-1200 cells) at all three timepoints and, as expected, these cells were absent under the CD25 depleted conditions (Figure 2.6A-F). Additionally, we identified an HLA-DR^+ $CD4^+$ population across all three timepoints in both $CD25^+$ present and depleted conditions (Figure 2.6A-F). HLA-DR is a human MHC class II molecule that is expressed on a variety of lymphocytes, including activated T cells[169]. Differential abundance and state analyses for PBMCs stained with the regulatory panel revealed differences in the frequency of HLA-DR^+ $CD4^+$ T cells at day 90, when protected children had a higher frequency of this population relative to susceptible children (Figure 2.6G-L). We did not observe significant differences in intracellular marker expression between the two groups (Supplementary Figure 2.9). Comparison of intracellular cytokine production in PBMCs before and after CD25 depletion revealed individual-specific changes, with no significant trend noted within the entire group (Supplementary Figure 2.10A-F). Some individuals, patients 4, 6, 9, and 10 experienced slight increase in IFN-γ and IL-2 levels at day 0 while patients 2, 3, and 13 experienced decrease in these cytokines at the same time point (Supplementary Figure 2.10 A,D). These data demonstrate inter-individual variation present in samples collected from individuals in an endemic setting.

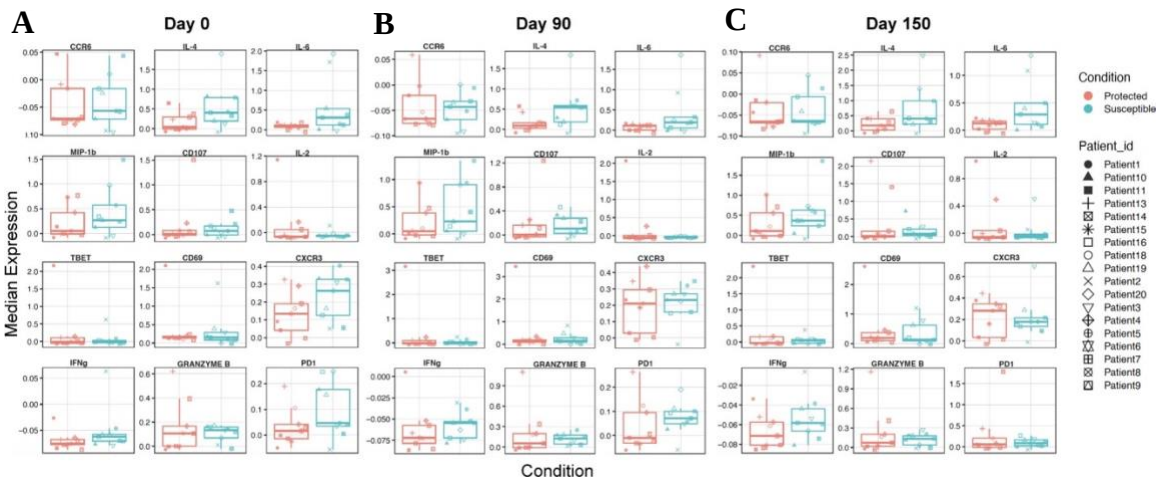

Figure 2.5. Characterizing overall expression of intracellular molecules and induced chemokine receptors in CD3+ cells across a single transmission season.

(**A-C**) Box plots displaying overall median expression of intracellular molecules and chemokine receptors from all T cells ($CD3^+$) in each Pfsz stimulated sample. Expression values were subjected to Z-score scaling, transforming the values to have a mean of 0 and a standard deviation of 1 across all cells. Negative expression values indicate that the average expression of a marker is lower relative to the other markers and positive expression values indicate that the average expression of a marker is higher relative to the other markers. Expression levels for protected children are indicated in red and expression levels for susceptible children are indicated in teal. Expression values from each child are indicated by a unique shape (**A**) Median expression for molecules at day 0. (**B**) Median expression for molecules at day 90. (**C**) Median expression for molecules at day 150.

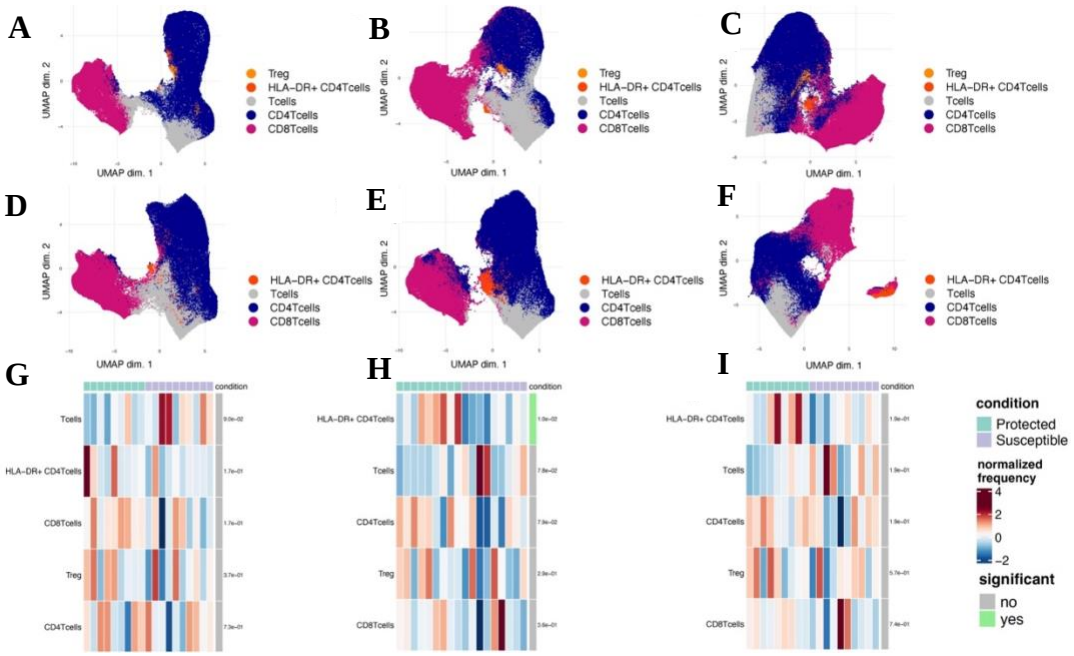

Figure 2.6. Phenotyping of CD3+ immune cell populations to assess regulatory functions across a single malaria transmission season.
(**A-C**) UMAP plots displaying immune cell populations identified though unsupervised clustering based of PBMCs stained with the regulatory panel. (**A**) Day 0, (**B**) Day 90, and (**C**) Day 150. (**D-F**) UMAP plots displaying immune cell populations identified though unsupervised clustering of CD25-depleted PBMC stained with the regulatory panel. (**D**) Day 0, (**E**) Day 90, and (**F**) Day 150. (**G-I**) Heatmap showing cell type frequencies of $CD3^+$ T cell populations present in children from each of two conditions (protected, teal; susceptible, purple). High frequency populations are displayed in dark red and lowest frequencies are in dark blue. Population frequencies that are significantly different (FDR<0.05) between protected and susceptible children are marked with a green bar (to the right of heat map). (**G**) Day 0, (**H**) Day 90, and (**I**) Day 150.

2.5 Discussion

In this study, we used both bulk RNA sequencing and mass cytometry to identify host immune gene and protein expression patterns associated with varying susceptibility to clinical malaria disease. We used samples from a cohort of children who have high exposure to malaria, but who are early in the trajectory of acquiring immunity to malaria. We performed RNA sequencing on PBMCs to characterize gene expression patterns of children with different levels of malaria susceptibility. Through gene expression analyses, we identified higher baseline expression of CXCL10, STAT1, STAT2, GZMB, XAF1 and IRF1 in susceptible children relative to protected children. Our findings suggest that

existing differences in gene expression, already in place before a malaria transmission season may impact susceptibility to subsequent infection. However, a new study with a larger cohort is needed to enable a study design with stronger statistical power and establish definitive conclusions. Furthermore, utilizing a regression approach can help determine the association between the number of malaria events and the enrichment of specific pathways.

Interferon gamma-induced protein 10 (CXCL10), a pro-inflammatory chemokine induced by multiple cytokines including IFN-γ, has been previously identified as a marker of malaria disease severity[170–172]. A study of CXCL10 wildtype (WT) and knockout (KO) mice showed efficient parasite control in KO mice while WT mice progressed to cerebral malaria[170]. Additionally, a field study in Ghana found higher CXCL10 levels from postmortem cerebral spinal fluid (CSF) in cerebral malaria patients[173]. Another gene downstream of IFN-γ signaling, STAT1, was also significantly overexpressed in the susceptible group relative to the protected group. STAT1 is a transcription factor activated by multiple interferons, and it regulates various cellular processes including cell proliferation and differentiation[174,175]. Although we did not see differential expression between groups with IFN-γ cytokine expression, we found evidence of gene expression differences for molecules downstream of IFN signaling, suggesting that gene expression studies may detect changes that are missed by cytokine studies.

Our pathway-level analyses revealed an enrichment of the apoptotic pathway in susceptible children. These observations are consistent with previous studies that have demonstrated increased apoptosis of immune cells (lymphopenia) in individuals with malaria infection[176,177]. Additional studies have found that malaria infection increases apoptotic processes, mediated through FAS, FASL and Tumor Necrosis Factor (TNF)[178–

[180]. Although we did not observe increased expression of these specific genes, we observed higher expression of pro-apoptotic genes XAF1 and IRF1 in susceptible children at baseline. XAF1 is a transcriptional co-activator of IRF1, a protein that negatively regulates anti-apoptotic genes and promotes FASL expression in immune cells[181–184]. The RNA-seq data were supported by mass cytometry results of slightly higher levels of PD-1 in susceptible children.

High dimension reduction and differential analysis of mass cytometry data identified higher frequencies of HLA-DR^{+}CD4^{+} T cells in protected children when compared to susceptible children. HLA-DR is a late activation marker that is upregulated on the surface of either memory or naïve T cells after antigen encounter. Although the function of HLA-DR on the surface of T cells is poorly understood, studies on infectious pathogens including *Mycobacterium tuberculosis* (the causative agent of tuberculosis, or TB) and Human Immunodeficiency Virus (HIV), show that HLA-DR^{+}CD4^{+} T cells have the ability to persist longer in the periphery and are more resistant to suppression mechanisms initiated by Tregs[185–187].

Our data shows that inherent differences in inflammatory and apoptotic gene expression already exist at baseline between children who will go on to have two or more malaria episodes throughout a malaria season and those who will not experience clinical malaria. Recent studies report on the importance of baseline immune signatures on the subsequent response to disease progression, vaccine efficacy, and treatment failure or success[188]. Tsang et. al showed a correlation between the extent of an immune response to influenza vaccination and the pre-vaccination status of an individual[189]. Additionally, the importance of baseline immunity has been noted in cancer, where studies show that the

presence of certain immune genes influences the activity of some immunotherapies as well as cancer metastasis[190]. These studies also emphasize the importance of a systems approach to understanding overall immune signatures .

Our current study corroborates and extends previous findings. We compared children with two or more episodes of clinical malaria (susceptible cohort) to age- and location-matched children without clinical malaria (protected cohort). Although the cohorts had similar risk of malaria exposure, we identified differences in gene expression patterns assessed before the onset of the malaria transmission season between the cohorts. This study emphasizes the importance of understanding the initial gene expression repertoire to accurately interpret clinical and immunological implications of field studies with human subjects. In conclusion, this study identifies potential genes and cell populations associated with, and which may play a causal role in, predicting malaria susceptibility.

Chapter 3: Dynamics of T cell immune responses during malaria infection in *Schistosoma haematobium*-negative and *Schistosoma haematobium*-positive individuals

3.1 Abstract

This study aimed to characterize immune cell populations in children aged 4-8 during acute *Plasmodium falciparum* infection and several months following clearance, while also assessing the influence of a pre-existing *Schistosoma haematobium* co-infection on immune cell composition and gene expression. Using single-cell RNA-sequencing, we analyzed peripheral blood mononuclear cells (PBMCs) from 20 children in a highly malaria-endemic region in Mali. We successfully identified distinct populations of T cells, B cells, natural killer (NK) cells, and myeloid cells. Notably, gene expression differences were observed due to *P. falciparum* infection, while *S. haematobium* co-infection did not significantly impact gene expression. Additionally, we explored CD4 T cell lineages and discovered a unique cytotoxic CD4 T cell population enriched in Th1 cells. Differential expression analysis revealed increased expression of lymphocyte activation gene 3 (LAG3), basic leucine zipper ATF-like transcription factor (BATF), interferon, and interleukin 18 (IL18) receptor genes across distinct CD4 T cell populations during an acute malaria episode. Furthermore, we observed upregulation of the NR4A family of transcription factors in *P. falciparum*-negative, malaria-exposed children, suggesting their potential role in T cell dysfunction which may explain sub-optimal immunity observed during *P. falciparum* infection. This study provides valuable insights into immune responses in children exposed to *P. falciparum* and sheds light on potential regulatory networks involving BATF and NR4A family members. The dynamic gene expression

patterns suggest a complex response to antigenic factors, highlighting the need for further research to understand the mechanisms shaping immune responses to infection and, particularly, co-parasite.

3.2 Introduction

Tropical regions are known to be endemic to a variety of infectious disease pathogens, often leading to cases of co-infections in human populations[88,89]. These co-infections can impose significant immunological burdens on individuals, affecting vaccine and drug effectiveness, modifying disease transmission dynamics and, at a broader level, diminished economic productivity[90–94]. Among the prevalent parasitic infections in sub-Saharan Africa, malaria and schistosomiasis stand out, accounting for a combined total of over 400 million infections annually[1,192]. Notably, co-infection rates are substantial, with studies suggesting that co-occurrence of malaria and schistosomiasis can reach up to 30-50% in sub-Saharan African children residing in areas where both diseases are widespread[113,114]. Given their high prevalence and clinical significance, these two most prevalent pathogens, *Plasmodium falciparum* (*Pf*) and *Schistosoma haematobium* (*Sh*), present an ideal model for investigating parasitic co-infections in tropical regions where both diseases are endemic.

Immune responses to parasites are intricate and variable, influenced by the parasite's life cycle, the presence of specific antigens, and in-host dynamics. The kinetics of responses to malaria, caused by an intracellular parasite, are distinct from responses to schistosomiasis, caused by an extracellular parasite that usually presents as a chronic disease.

Although T helper (Th) Type 2 immune responses dominate during helminthic infections, the primary response to an initial infection is mediated by $CD4^+$ Th1 cells[112]. Th1 produce pro-inflammatory cytokines such as IFN-γ, TNF-α, IL-2, and IL-12 during the early stages of infection to recruit dendritic cells and macrophages to facilitate parasite clearance[111,112]. Th1 immune responses are directed towards the early forms of the parasites (schistosomulae and adult worms). As the infection progresses and the worms produce eggs, $CD4^+$ Th2 cells secrete cytokines like IL-4, IL-5, and IL-13 against the schistosome egg antigen, which in turn facilitate the activation and recruitment of mast cells, eosinophils, and fibroblasts[112,193]. However prolonged Th2 responses lead to the formation of granulomas around schistosome eggs that progress to hepatic fibrosis[111,112]. In the context of persistent infections, Tregs play a pivotal role by modulating immune responses and mitigating excessive fibrosis[112]. Tregs release anti-inflammatory cytokines like IL-10 and TGF-β, thereby tempering Th2 and Th1 immune responses. While we understand the role of Tregs, Th1 and Th2 CD4 T cells during *S. haematobium* infection[111,112], we have yet to characterize the memory compartment and how this pathogen interacts with other parasites.

In contrast, acute malaria infections trigger a highly proinflammatory Th1 immune response. These cytokines promote the recruitment and activation of macrophages and NK cells, facilitating the clearance of infected red blood cells and controlling *Plasmodium* parasitemia[25]. As the malaria infection progresses, CD4 Th2 immune responses emerge, with IL-4 and IL-5 aiding B cell germinal center reactions that promote the production of malaria-specific B cell immunoglobulin isotypes and facilitate the development of memory B cells. Importantly, a portion of the initial effector Th1 and Th2 cells undergo

differentiation into central memory (T_{CM}) and effector memory (T_{EM}) populations[38]. These memory subsets become crucial in subsequent infections, as they contribute to rapid responses and play a pivotal role in the development of essential humoral responses[38,77,78]. Eventually, Tregs expand and secrete anti-inflammatory molecules IL-10 and TGF-β to control the proinflammatory immune responses and induce apoptosis of effector T cells[38,54]. Some studies propose that elevated Treg populations correlate with heightened parasitemia in specific individuals from malaria-endemic regions[55]. These observations are supported by murine studies that observed increased survival of *Plasmodium* infected mice lacking regulatory T cells[168,194]. The prevailing immunosuppressive nature of Treg responses combined with the potential decrease in memory $CD4^+$ T cell proportions in chronic schistosomiasis is seemingly at odds with the need for a pro-inflammatory response in an acute malaria infection. This stark contrast raises a pertinent question: how do these two infections interact and influence each other within the intricate immune landscape?

Our research group has previously conducted investigations into the impact of malaria-schistosomiasis co-infection in humans utilizing prospectively collected PBMCs from Malian children under active observation for nine months, through the end of *S. haematobium* transmission. Our findings illuminated how co-infection with *S. haematobium* enhances the persistence of *Pf*-specific B and T cell memory responses while inducing modifications in regulatory T cell reactions[122,123,125]. Furthermore, these insights revealed a correlation between IL-4 cytokine expression from T_{CM} cell populations and Schistosoma positivity in children[122]. To comprehend how chronic schistosomiasis influences immune cell mechanisms in individuals exposed to malaria, we executed single-

cell RNA sequencing on PBMCs obtained from both *S. haematobium*-positive and -negative Malian children during active malaria infection and subsequent clearance.

3.3 Materials and Methods

3.3.1. Study Design and PBMC Selection

Children participating in this study were residents of Bandiagara, a town situated in Mali, West Africa. During the field study, Bandiagara had a population of approximately 13,600 and experienced marked seasonal transmission of both malaria and schistosomiasis. *P. falciparum* accounted for 95% of all malaria cases in this region, with children experiencing an average of 1.54 clinical malaria cases per transmission season[195]. The prevalence of *S. haematobium* in this region is 25% in children aged 4-14 years of age and 50% in adults[11].

Children aged between 4 and 14 years underwent screening for the presence of *S. haematobium* eggs in the urine and intestinal helminth eggs in stool samples. Asymptomatic *S. haematobium*-infected children were carefully selected to avoid co-morbidities and matched for age and geographical location with healthy counterparts who tested negative for *S. haematobium* and exhibited no signs of acute or chronic illness or pregnancy. Prior to study initiation, all children were treated with albendazole to eliminate intestinal helminths. Throughout the malaria transmission season (wet season), children were monitored on a weekly basis for acute malaria symptoms, with passive follow-up available at all times of the day and night. PBMCs were collected from each participant at the time of their first symptomatic, blood smear-positive malaria infection. Subsequently, PBMCs were collected again during the dry season, eight weeks after standing water pools had dried up. At this point, children received praziquantel treatment for *S. haematobium*

infection. PBMC samples in this study were collected over the span of two malaria transmission seasons in 2002 and 2003, as well as two post-malaria transmission (dry) seasons in 2003 and 2004. Approximately 11 Schistosoma-negative children acquired *S. haematobium* during the trial interim and samples were censored from immunological analyses.

Out of the 654 children who were matched by age and location and completed the parent study, we selected 20 children, ages 4-8, based on the availability of both wet and dry season PBMC samples, the occurrence of clinical malaria episodes, and age. Of these 20 children, ten were positive for *S. haematobium* (*Sh*+) while the other ten were negative for *S. haematobium* (*Sh*-) (Supplementary Table 3.1). Both groups of experienced symptomatic *P. falciparum* infections in the wet season (*Pf*+) and were blood smear negative and seemingly healthy in the dry season (*Pf*-) (Supplementary Table 3.1).

3.3.2 PBMC Thawing and Dead Cell Removal

For each single-cell RNA sequencing (scRNA-seq) run, four cryopreserved PBMC samples (one each from a different participant) were thawed in a 37°C water bath for two minutes (min) and transferred into 10 mL of pre-warmed (37°C) AIM V media. Cells were centrifuged at 400 g, 4°C for 5 min, the supernatant was removed, and the pellet was resuspended in 10 mL of DPBS supplemented with 0.2% BSA. Resuspended cells were centrifuged at 400 x g, 4°C for 5 min and the pellet was resuspended in 1 mL of thawing buffer (DPBS supplemented with 0.2% BSA) then filtered through a 40 μm nylon cell strainer (Falcon, Durham, NC USA).

To assess viability, 5 μL of resuspended cells were added to 100 μL of propidium iodide (PI) solution and incubated at room temperature for 5 min. Following incubation,

60 μL of the cell solutions in PI were added to Moxi GO II flow cassette and assessed on a Moxi GO II Next Generation Coulter-Principle Flow Cytometer. A count of the number of viable cells, dead cells and percent red blood cell contamination was provided. Samples with less than 95% cell viability were treated with a dead cell removal kit. PBMCs were centrifuged and supernatant was discarded. Then, the pellet was resuspended in thawing buffer at 100 uL/5,000,000 cells and transferred into a pre-wetted polystyrene tube. Annexin V Dead Cell Removal (DCR) cocktail (5 uL) was added to cells followed by five uL Biotin cocktail. Cells were incubated at room temperature for 3 min. DCR (10 uL) beads (vortexed during the three-minute incubation) were added to the cells followed by 2.4 mL of buffer (PBS supplemented with 0.5 mM CaCl2 and 2% FBS). Cells were placed on the stem cell magnet and incubated at room temperature for 3 minutes. Following incubation, the supernatant was retained and transferred to a new pre-wetted polystyrene tube. Cells were centrifuged at 400 g for 5 min and the supernatant was discarded. Cells were resuspended in 1 mL thawing buffer and filtered through a 40 μm nylon cell strainer and viability of the remaining cells was assessed again as described above.

3.3.3 PBMC multiplexing and staining

One million cells from each sample were aliquoted into new pre-wetted polystyrene tubes and centrifuged at 400 g for 5 min and resuspended in 50 uL of Cell Staining Media (BioLegend cat#420201). BioLegend TruStain FcX Fc receptor blocking solution (5 uL) was added to each sample and incubated for ten minutes on ice. During incubation TotalSeq-C hashtags 1-4 (BioLegend cat#394661, #394663, #394665, #394667) were centrifuged at 14,000 g at 4^{o}C for ten minutes. Hashtag working solution was diluted with cell staining media for a final concentration of 0.1 ug/uL. After incubation, 50 uL of each

hashtag working solution was added to each sample and incubated for 30 min on ice. During incubation, lyophilized TotalSeq C human universal cocktail (BioLegend cat #399905) and was reconstituted per manufacturer's instructions. Following incubation, 3.5 uL of BioLegend cell staining buffer was added and gently mixed with the hashtagged cells. Cells were centrifuged at 400 g for 5 min and resuspended in 50 uL of cell staining media. To multiplex cells, 6.25 uL from each sample of hashtagged cells were aliquoted to a new pre-wetted polystyrene tube for a total of 25 uL. 25 uL of reconstituted TotalSeq C universal cocktail was added to the multiplexed cells for a total volume of 50 uL and incubated on ice for 30 min. Following incubation, cells were washed three times with cell staining media and resuspended in 500 uL of PBS supplemented with 0.04% of BSA and submitted to Maryland Genomics (Institute for Genome Sciences' genomics center) for sequencing.

3.3.4 Sequencing of cellular indexing of transcriptomes and epitopes (CITE), CITEseq

Single-cell immune profiling was performed using Chromium Next GEM Single Cell 5′ Reagent Kits v2 (10x Genomics, Inc). Following the recommended 10x protocol, 10,000 multiplexed and stained cells were combined with a reverse transcriptase master mix (RT Reagent B, Poly-dT RT primer, Reducing agent B, RT Enzyme C, and nuclease-free water), 5′ Gel beads and partitioning oil and loaded onto a Chromium Next Gen Chip K to generate GEMs (Gel Bead in Emulsion) such that each oil droplet contained, on average, a single cell. As part of the amplification reaction, within each GEM, the cell was lysed, and poly-adenylated mRNA transcripts were reverse transcribed into cDNA. Simultaneously, a Gel Bead primer complementary to the capture sequence on the DNA-

tagged antibodies (cell surface markers and hashtags) was used to generate a 10x barcoded DNA sequence. The cDNA and cell surface DNA was further amplified to generate three sequencing libraries, one each for gene expression, TCR/BCR V(D)J sequences, and cell surface markers. TCR and BCR libraries were generated by enriching TCR and BCR sequences using primers specific for the constant region of the TCR and BCR, respectively. Libraries were sequenced on NovaSeq platform (Illumina).

3.3.5 Single cell data analysis

Illumina base call files (BCLs) were demultiplexed using cellranger mkfastq pipeline to generate FASTQ files. FASTQ files were demultiplexed using the cellranger multi pipeline to assign cells to samples. STAR aligner, part of cellranger multi, was used to perform splice-aware alignment of reads to the reference human genome (hg38). Seurat (version 4.0.5) was used to read the sample feature matrix file into R (version 4.0.3) to perform filtering and downstream analysis. Cells with less than 200 genes or more than 6,000 genes, as well as those with more than 7.5% mitochondrial genes and 5% hemoglobin genes were excluded from downstream analyses.

Cell surface markers, detected with an antibody-derived tag (ADT counts), were normalized using centered log-ratio transformation and RNA counts were normalized using SCT transformation. To identify anchors between *Sh*+ and *Sh*- samples from the wet and dry seasons, we utilized the FindIntegrationAnchors function in Seurat and, to integrate the data, the IntegrateData function was applied[196]. To perform principal component analysis (PCA) on the gene expression data, we retained the first 50 dimensions and used the RunPCA function. Clustering was performed on the integrated single cell data using the FindClusters function in Seurat. To visualize the clusters, we employed the RunUMAP

function to perform Uniform Manifold Approximation and Projection (UMAP) analysis. Cell clusters were manually annotated using a combination ADT cell surface markers and gene expression, enabling the identification of canonical cell-identifying markers. A secondary sub-clustering analysis with 30 dimensions was performed on CD4 T cell clusters, and new clusters were annotated with the same strategy described above.

3.3.6 Gene Signature Scoring

To evaluate the enrichment of helper T cell lineages and functional states, we employed the AddModuleScore_UCell function from the R package Ucell[197] to calculate gene signature scores for each single cell. Helper T cell lineage signatures were obtained from literature[198] and gene sets from (https://www.gsea-msigdb.org/gsea/index.jsp) were utilized to assess functional states[149].

3.3.7 Cell Proportions

To assess the abundance of cell proportions, we calculated the percentage each annotated cell type constituted within the entire population. Paired statistical analysis was conducted using Wilcoxon rank sum test to detect differences in proportions. Proportion data was visualized using the R package ggplot2.

3.3.8 Differential Gene Expression Analysis and Pathway Enrichment

The annotated Seurat object was converted to a single cell experiment using R package SingleCellExperiment[199]. Genes expressed in less than ten cells were excluded and read counts for each sample were aggregated across all the cells from annotated clusters using aggregate.Matrix function of Matrix.utils R package. For each cluster, genes with counts per million (CPM) values of less than 10 in 50% of the samples were excluded from the analyses. Accounting for inter-individual cell count variation, read counts were

normalized and, pseudo-bulk differential gene expression analyses were carried out using DESeq2[200]. To perform enrichment analysis, we selected all differentially expressed genes, regardless of fold-change, and used the DAVID functional analysis web software to identify enriched biological processes within each group[148].

3.4 Results

3.4.1 Immune cell composition in *S. haematobium*- positive and *S. haematobium* -negative children during and after acute *P. falciparum* infection

To investigate the immune cell phenotype of individuals exposed to malaria, we assessed the transcriptomes and cell composition of PBMCs obtained from Malian children with and without pre-existing chronic *S. haematobium* infection. Samples were collected in the wet season; during an active symptomatic malaria infection and in the dry season; months after the infection was cleared. We performed unsupervised clustering on 123,414 cells based on gene expression and identified clusters present in *Sh*+ and *Sh*- samples from both the wet and the dry season (Figure 3.1A). Clusters were annotated based on the expression of canonical cell surface markers from the ADT assay, further annotation was done based on gene expression (Figure 3.1B,C). A total of 22 distinct clusters were identified, including nine T cell clusters, comprising four CD4+, three CD8+, two gamma delta (γδ), one mucosal-associated invariant T cell (MAIT)/CD8+, and a Natural Killer T cell (NKT) cluster, as well as four myeloid clusters comprising CD16 and CD14 monocytes, classical dendritic cells (cDC), and plasmacytoid dendritic cells (pDC), a B cell cluster comprising plasmablasts, naïve, memory, and atypical B cells, two NK cell clusters and one platelet cluster (Figure 3.1A). We observed heterogenous distribution of cell populations across *Sh*+ and *Sh*- from the wet and dry season (Figure 3.1D). Surprisingly, at both time points,

we observed comparable proportions of plasmablasts, γδ T cells, and naïve and effector CD4 T cells (Figure 3.1D). Plasmablasts are short-lived[201] and VD2 γδ T cells subsets are known to expand during infection[38], therefore, the proportions of these subsets are expected to vary in disease and convalescence.

Next, we sought to evaluate the correlation between the presence of cell surface protein markers and the expression of their encoding gene, as well as determine the extent of overlap between cells expressing the cell surface marker and the corresponding gene. For each cell-identifying marker, we observed that ADT expression was consistently detected in approximately 96% of the corresponding cells, in contrast to gene expression, which was observed in approximately 83% of the cells (Supplementary Table 3.2). Importantly, this difference in expression did not adversely affect our clustering analysis, as cells were primarily clustered based on gene expression and still exhibited the expected cell surface marker expression profiles. This discrepancy in expression levels of the gene and protein can be attributed to the possibility that the expression of genes encoding cell surface markers ceases once the cell acquires its phenotype. However, it is important to note that the limit in the of number of transcripts assayed per single cell could lead to errors in the inference of transcript presence/absence. Nevertheless, this observation suggests that while ADT expression patterns appear to be more robust, the repertoire of genes expressed within a cell is adequate for distinguishing cell types and appropriately annotating clusters.

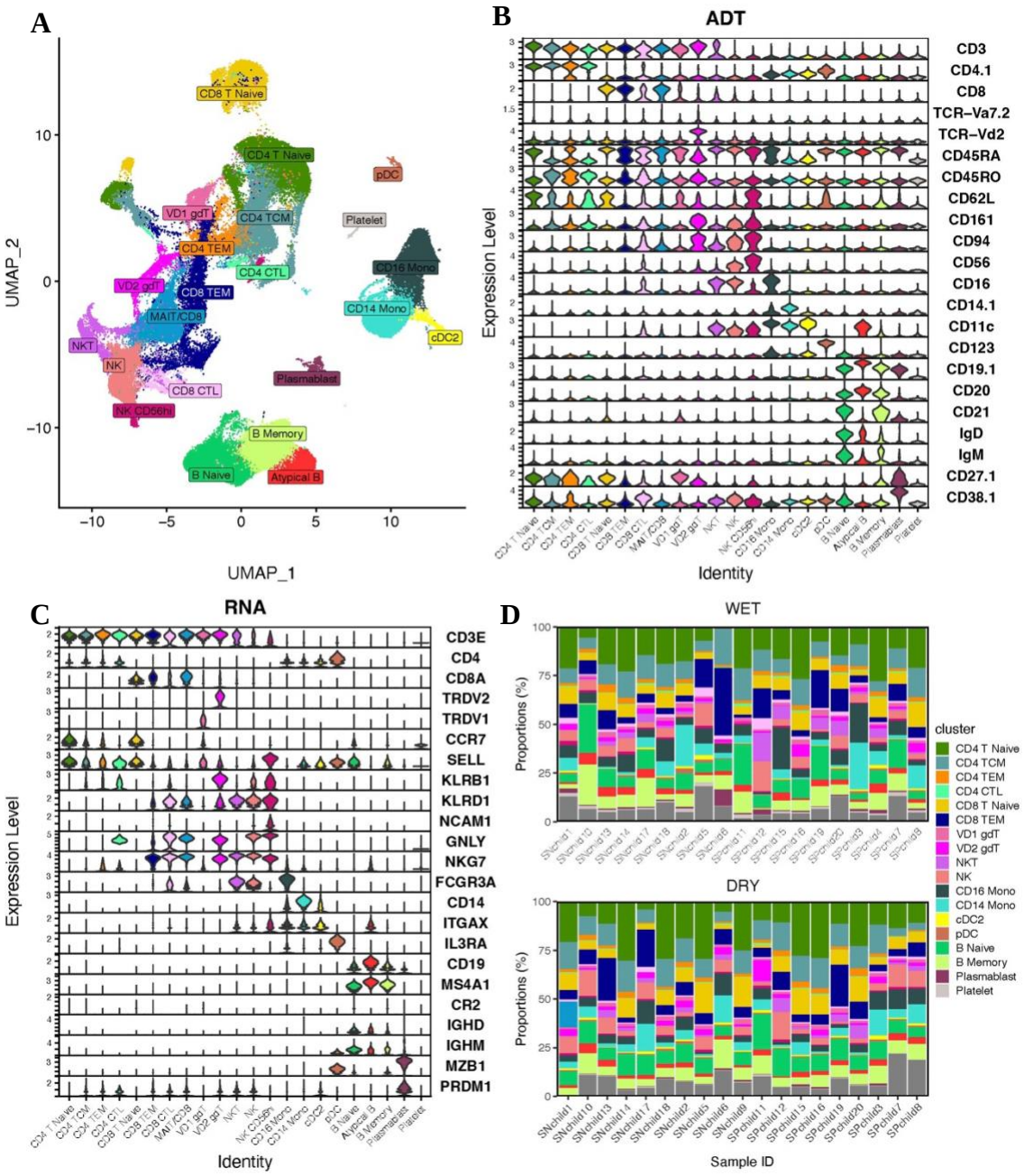

Figure 3.1. Classification of peripheral blood mononuclear cell populations present in P. falciparum-exposed S. haematobium-positive and -negative children.

(**A**) UMAP plots displaying immune cell populations identified though unsupervised clustering. (**B**) Violin plots depicting canonical cell surface markers used to annotate clusters. (**C**) Violin plots depicting canonical gene markers used to annotate clusters. (**D**) Stacked bar plot depicting relative distribution of PBMC subsets across individuals in the wet and dry season.

3.4.2 CD4 T cell sub-clustering: Unraveling cell heterogeneity and composition dynamics

In our previous study, we observed significant differences within the memory CD4 T cell compartment between *Sh*+ and *Sh*- children upon re-stimulation with *Pf* antigen[122]. In this study, we sought to elucidate the underlying mechanism by examining gene expression patterns before re-stimulation. To characterize the $CD4^+$ T cell compartment within this cohort, we conducted sub-clustering analysis on 39,068 $CD4^+$ T cells and utilized a combination of gene expression and protein surface marker profiles to further categorize the cells. Using CD45RA and CD45RO cell surface protein expression and CCR7 gene expression, we differentiated naïve cells from memory and effector sub-populations. We identified 6 distinct CD4 T cell populations present in PBMCs from *Sh*+ and *Sh*- children at both time points. These CD4 sub-populations included cytotoxic T lymphocytes (CTL), Tregs, T_{CM}, T_{EM}, transitioning T cells, and naïve cells (Figure 3.2A).

CD4 CTLs were CD45RO positive and exhibited high expression of cytotoxic genes GZMK, GZMA, GZMM, NKG7, KLRB1, PRF1, and cytotoxic lymphocyte regulator CST7 (Figure 3.2B and Supplementary Figure 3.1A). Additionally, this population also showed high expression of Th1-associated genes, including chemokine ligand CCL5, transcription factors RUNX3 and STAT4, and cytokine receptors IFNGR1 (Supplementary Figure 3.1A,B). Tregs were characterized by the expression of genes encoding transcription factors FOXP3 and IKZF2, cytokine receptors IL2RA and IL10RA, and co-inhibitory receptor TIGIT, as well as cell surface protein expression of CD25 and CD39 (Figure 3.2B,C and Supplementary Figure 3.1C,D). In comparison to other annotated subpopulations, Tregs exhibited lower expression of both the IL7R gene and

protein (Figure 3.2B and Supplementary Figure 3.1E). T_{CM} cells were CD45RO positive and expressed stem-like markers CCR7, TCF7, LEF1, IL7R, and CD69 (Figure 3.2B and Supplementary Figure 3.1F). Similarly, T_{EM} cells were CD45RO positive but lacked CCR7 gene expression and displayed high levels of S100 family proteins (S100A10, S100A11, S100A6, S100A4) and co-stimulatory molecule TNFRSF4 (OX40) and CD69 (Figure 3.2B,C and Supplementary Figure 3.1F). Naïve and transitioning CD4 T cells exhibited similar gene expression profiles, both expressing stem-like markers such as CCR7, TCF7, LEF1, IL7R, and the surface protein CD45RA (Figure 3.2B,C). Notably, naïve cells were characterized by high CD62L surface protein expression, while transitioning cells had lower CD62L surface protein expression and high expression of early T cell signaling gene CD44, and transcription factor BACH2 (Figure 3.2B,C and Supplementary Figure 3.1D).

Our clustering analysis revealed distinct nodes within our dataset. To discern the factors contributing to the divergence of CD4 T cell nodes, we employed the FindMarkers function in Seurat for the identification of genes enriched in each cluster. Our observations indicate that the branching patterns are primarily influenced by variations in the expression of T cell receptor β variable (TRBV) gene segments (Supplementary Figure 3.2). Notably, the naive branches exhibited distinct TRBV profiles, encompassing TRBV5-1, TRBV19, TRBV2, TRBV6-1, TRBV7-9, TRBV6-5, TRBV3-1, TRBV7-2, and TRBV30. Among these, TRBV9 emerged as the predominant gene segment in both naïve and non-naïve CD4 subsets (Supplementary Figure 3.2).

3.4.3 Deciphering CD4 T cell lineages and exploring cell composition dynamics

To assess whether CD4 subpopulations were enriched for Th1 (TBX21 (encoding T-bet), RUNX3, and STAT4), Th2 (GATA3, STAT6, and IL4R), Th17 (RORC, IL17RA, IL17RB), and T_{FH} (BCL6, CXCR5) we used UCell to calculate gene signature scores. We observed Th1 and Th2 enrichment across all six subpopulations, with CD4 CTLs displaying the highest enrichment in Th1 and T_{EM} displaying the highest enrichment in Th2 (Figure 3.2D). This observation suggests that CD4 CTLs in malaria-exposed individuals are derived from the Th1 lineage and expand to an extent that they can form a distinct cluster that is maintained past the transmission season. Interestingly, Th17 and T_{FH} gene signatures were not enriched in any of the CD4 T cell subpopulations (Figure 3.2D).

Figure 3.2. Classification of CD4 T cell populations present in P. falciparum-exposed S. haematobium-positive and -negative children.

(**A**) UMAP plots displaying CD4 T cell populations identified though secondary unsupervised clustering. (**B**) Violin plots depicting gene markers used to identify CD4 T cell subsets. (**C**) Violin plots depicting cell surface markers used to identify CD4 T cell subsets. (**D**) Violin plots depicting gene signature scores of CD4 helper lineages. (**E**) Stacked bar plot depicting relative distribution of CD4 subsets across individuals in the wet and dry. (**F**) Boxplot comparing cluster proportions between *Sh*+ and *Sh*- children in the wet and dry season. Statistical significance tested using Wilcoxon rank-sum test.

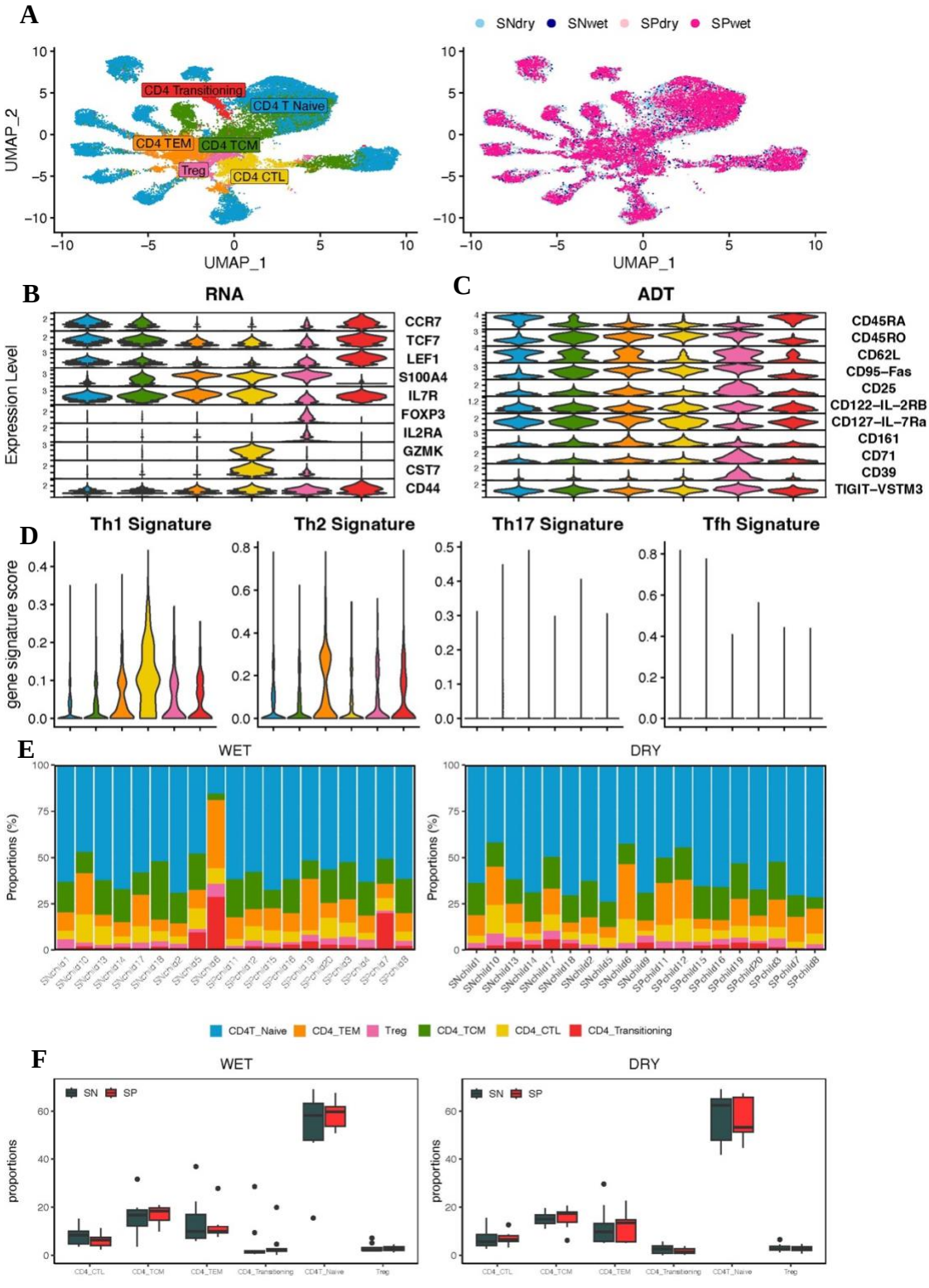
A
SNdry
SNwet
SPdry
SPwet
CD4 Transitioning
CD4 T Naive
CD4 TEM
CD4 TCM
Treg
CD4 CTL
UMAP_2
UMAP_1
B
RNA
Expression Level
CCR7
TCF7
LEF1
S100A4
IL7R
FOXP3
IL2RA
GZMK
CST7
CD44
C
ADT
CD45RA
CD45RO
CD62L
CD95–Fas
CD25
CD122–IL–2RB
CD127–IL–7Ra
CD161
CD71
CD39
TIGIT–VSTM3
D
Th1 Signature
Th2 Signature
Th17 Signature
Tfh Signature
gene signature score
E
WET
DRY
Proportions (%)
CD4T_Naive
CD4_TEM
Treg
CD4_TCM
CD4_CTL
CD4_Transitioning
F
WET
DRY
SN
SP
proportions
CD4_CTL
CD4_TCM
CD4_TEM
CD4_Transitioning
CD4T_Naive
Treg

CD4 T cells are critical in both *S. haematobium* and *P. falciparum* infections; studies have demonstrated that upon antigen recognition, this population undergoes expansion and differentiation to mediate pathogen-specific immune responses[25,38,112]. This led us to investigate whether the composition of CD4 T cells was impacted by the presence of an acute *P. falciparum* infection and chronic *S. haematobium* co-infection. To assess this, we performed a paired analysis comparing the proportions of the six identified CD4 T cell populations between the wet season (*Pf*+) and the dry season (*Pf*-) and observed no statistically significant differences in the frequency of the six identified CD4 T cell populations (Figure 3.2E,F). Subsequently, we investigated whether the presence of a *S. haematobium* co-infection had an impact on cellular composition during either the wet or dry season (Figure 3.2E,F). Our findings indicated that co-infection and acute *P. falciparum* infection did not significantly alter cellular composition.

3.4.4 Gene expression patterns of CD4 effector populations during and after acute *P. falciparum* infection

In addition to expanding upon antigen recognition, CD4 T cells secrete pro-inflammatory molecules during an acute infection and exhibit recall responses in subsequent *P. falciparum* infections[22,38,112]. To elucidate the mechanisms behind these processes, we explored whether gene expression patterns within CD4 effector populations were influenced by an acute *P. falciparum* infection and a chronic *S. haematobium* co-infection. To this end, we used PBMCs from both the wet season (collected during a clinical malaria episode) and the dry season, when malaria cases were no longer present but prior to treating *Sh*+ children for *S. haematobium* infection. First, we performed principal component analysis on each non-naive CD4 T cell cluster and found that a large

fraction of the variation in gene expression (38% in T_{CM}, 37% in T_{EM}, 31% in CTL and 22% in Tregs) in our dataset was explained by differences in *P. falciparum* infection status between the wet and dry season Figure 3.3A,B,C,D. Notably, there were no distinct grouping patterns associated with *S. haematobium* infection (Figure 3.3A,B,C,D).

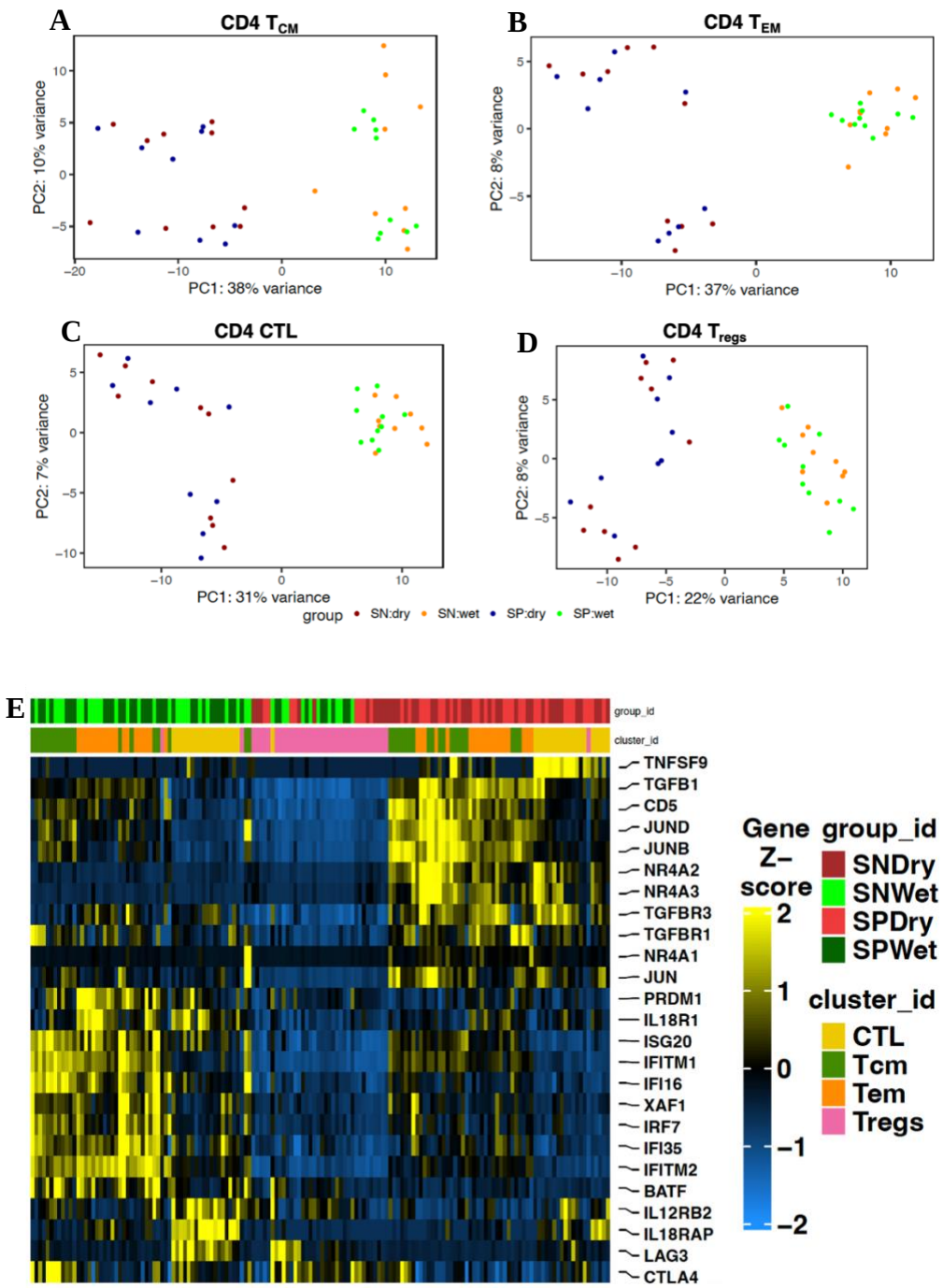

Figure 3.3. Pseudo-bulk analysis reveals grouping based on season.

(**A-D**) Principal component analysis on non-naïve CD4 T cells. (**A**) PCA of TCM plots displaying CD4 T cell (**B**) PCA of TEM. (**C**) PCA of CTL (**D**) PCA of Tregs. (**E**) Heatmap depicting differentially expressed genes that overlap across two or more non-naïve CD4 T cell subsets.

We then performed pseudo-bulk differential gene expression analysis between samples from the wet season (*Pf*+) and dry season (*Pf*-). This analysis revealed 2491 differentially expressed genes within T_{CM} cells, 2116 within T_{EM} cells, 1433 within CD4 CTL, and 679 within Tregs (Figure 3.3E). To assess if gene expression within *Pf*-exposed CD4 T cells was impacted by the presence of a *S. haematobium* infection, we compared the expression patterns of genes between *Sh*+ and *Sh*- children from the wet season. Surprisingly, our analysis revealed no significant differences in global gene expression between the two pediatric groups during an active malaria episode (data not shown). Furthermore, we assessed whether there were any differences in gene expression patterns between *Pf*-/*Sh*- and *Pf*-/*Sh*+ children during the dry season. At this time point, we observed no variations in the expression of genes within any of the annotated CD4 T cell subpopulations (data not shown). These findings indicate that the *S. haematobium* did not significantly impact the gene expression profiles in CD4 T cells at either time point.

Our comparative analysis of CD4 T cell populations between the wet and dry season showed ubiquitously differentially expressed genes, with an overlap in gene sets that were differentially expressed across different non-naïve CD4 populations. Cells from the wet season expressed higher levels of interferon signaling genes (IFI16, IFI35, IFITM1, IFITM2, IRF7, ISG20, XAF1), transcription factor BATF, T cell co-receptors LAG3 and CTLA4 (T_{CM}, T_{EM}, CD4 CTL), and inflammatory cytokine receptor IL12RB2 (T_{CM}, CD4 CTL, and Tregs) (Figure 3.3E).

Furthermore, wet season T_{CM} cells, T_{EM} cells, and CD4 CTLs, which were collected during an ongoing clinical malaria episode (*Pf*+), exhibited a substantial upregulation of key signaling molecules, including STAT1, ZAP70, TXK, and JAK2 (Supplementary

Figure 3.3). This suggests an enhanced activation of T cell receptor signaling pathways during *P. falciparum* infection in the wet season. In contrast, CD4 T cell populations from the dry season displayed a distinct gene expression profile. Notably, NR4A family transcription factors NR4A1 (in T_{EM} and CD4 CTL), NR4A2, and NR4A3, as well as AP-1 transcription factors JUN (in T_{EM} and CD4 CTL), JUNB, and JUND, were expressed at higher levels across multiple CD4 populations (Figure 3.3E).

Previous studies have established that NR4A transcription factors are downstream targets of NFAT signaling. To explore this further, we investigated NFAT expression and observed a moderate upregulation (fold change ~1.33) of NFATC3 in CD4 CTLs and Tregs and low upregulation of NFATC1 and NFATC2 in T_{CM} cells during the dry season (Supplementary Figure 3.3). Additionally, the negative regulator of T cell receptor signaling, CD5, and TGFB cytokine and receptor genes (TGFB1, TGFBR3, and TGFBR1) were upregulated in T_{CM}, T_{EM}, and CD4 CTL cells (Figure 3.3E). The upregulation of CD5 and TGFB-related genes, whose proteins have immunosuppressive properties, suggests downregulation of signaling during the dry season. Moreover, in T_{EM} and CD4 CTL cells collected during the wet season, we observed higher expression of co-stimulatory molecule TNFSF9 (4-1BB ligand), the inflammatory cytokine receptor IL18R1, and its accessory protein IL18RAP Figure 3.3E). The upregulation of the IL18 receptor has been associated with IFN-γ production, and co-expression with IL-12 receptor promotes the differentiation into the Th1 lineage[202,203]. These findings suggest that T_{EM} cells and CD4 CTLs from the

wet season have the potential to produce IFN-γ in response to *P. falciparum* antigen stimulation during natural infection.

Figure 3.4. Distinct differential expression patterns from non-Naïve CD4 T cell subsets.

(**A-D**) Violin plots depicting significantly differentially expressed genes upregulated in the wet season (shown in red) or the dry season (shown in blue) (**A**) Violin of T_{CM}. (**B**) Violin of T_{EM}. (**C**) Violin of CTL (D) Violin of Tregs. (**E-H**) Enrichment analysis on differentially expressed genes (FDR < 0.05) using DAVID functional annotation software. Displayed here are GO Biological Processes enriched in the wet season (teal) and dry season (gold) (**E**) Bar plot of genes enriched in TCM. (**F**) Bar plot of genes enriched in TEM. (**G**) Bar plot of genes enriched in CTL (**H**) Bar plot of genes enriched in Tregs**.**

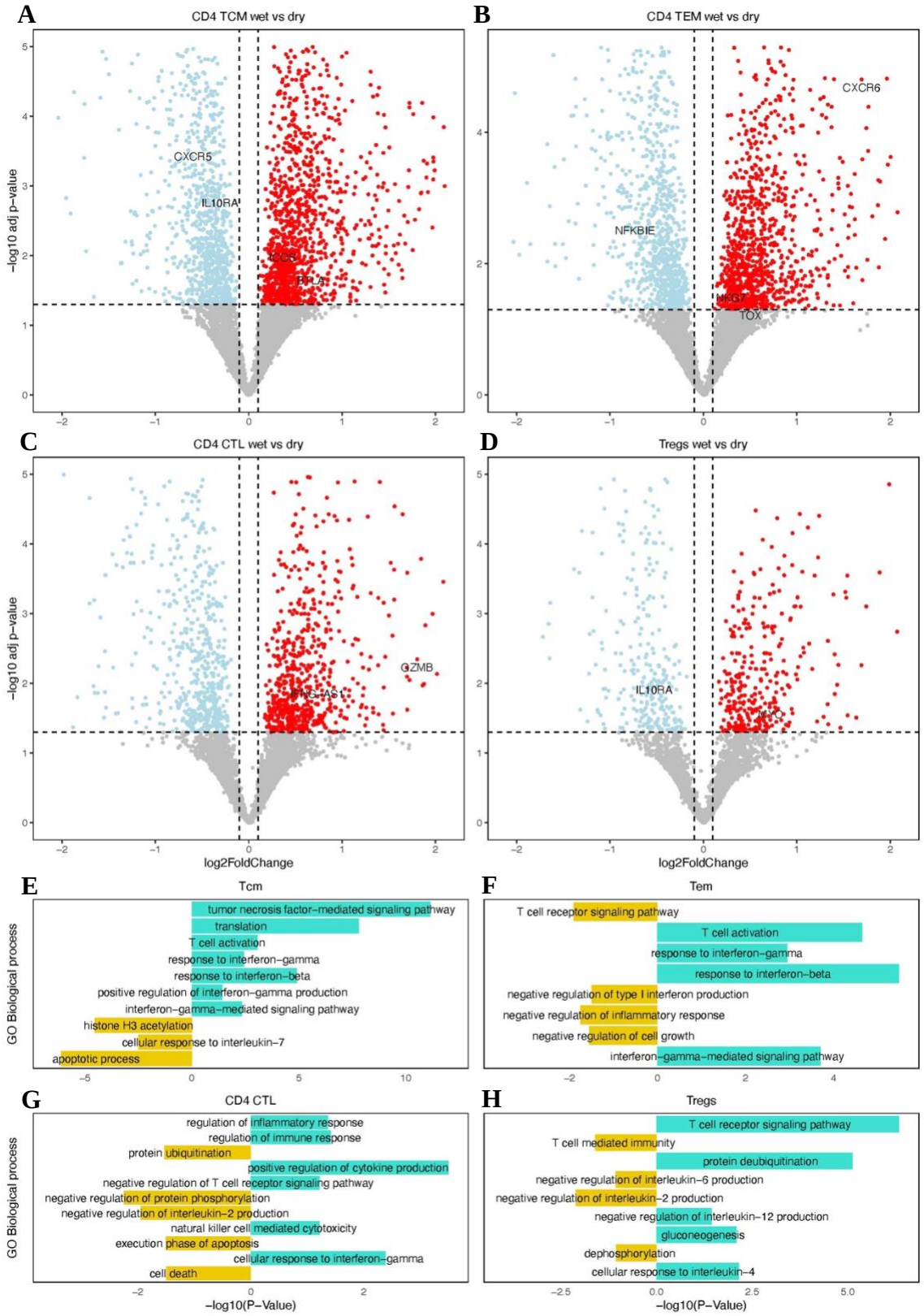
A
CD4 TCM wet vs dry
CXCR5
IL10RA
ICOS
PTPN7
−log10 adj p−value
B
CD4 TEM wet vs dry
CXCR6
NFKBIE
IKZF3
TOX
C
CD4 CTL wet vs dry
GZMB
IFNG−AS1
log2FoldChange
D
Tregs wet vs dry
IL10RA
MYO
log2FoldChange
E
Tcm
tumor necrosis factor−mediated signaling pathway
translation
T cell activation
response to interferon−gamma
response to interferon−beta
positive regulation of interferon−gamma production
interferon−gamma−mediated signaling pathway
histone H3 acetylation
cellular response to interleukin−7
apoptotic process
GO Biological process
F
Tem
T cell receptor signaling pathway
T cell activation
response to interferon−gamma
response to interferon−beta
negative regulation of type I interferon production
negative regulation of inflammatory response
negative regulation of cell growth
interferon−gamma−mediated signaling pathway
G
CD4 CTL
regulation of inflammatory response
regulation of immune response
protein ubiquitination
positive regulation of cytokine production
negative regulation of T cell receptor signaling pathway
negative regulation of protein phosphorylation
negative regulation of interleukin−2 production
natural killer cell mediated cytotoxicity
execution phase of apoptosis
cellular response to interferon−gamma
cell death
GO Biological process
−log10(P−Value)
H
Tregs
T cell receptor signaling pathway
T cell mediated immunity
protein deubiquitination
negative regulation of interleukin−6 production
negative regulation of interleukin−2 production
negative regulation of interleukin−12 production
gluconeogenesis
dephosphorylation
cellular response to interleukin−4
−log10(P−Value)

To identify distinct patterns associated with cells collected during the wet or the dry season, we conducted a detailed analysis of gene expression variation in individual cell populations between timepoints (Figure 3.4A,B,C,D). In wet season T_{CM}, we observed an upregulation of two important T cell co-receptor genes, ICOS and BTLA, while T_{CM} cells from the dry season displayed an upregulation of the chemokine receptor CXCR5 (Figure 3.4A). Subsequent pathway enrichment analysis revealed that wet season T_{CM} cells were enriched in pathways related to "T cell activation", "translation", "interferon-gamma mediated signaling pathway", and "response to interferon-gamma". Conversely, dry season T_{CM} cells exhibited enrichment in pathways associated with "chromatin remodeling", "apoptosis processes" and "cellular response to interleukin-7 (Figure 3.4E).

When we investigated differentially expressed genes in wet season T_{EM}, our analysis identified high expression of the cytotoxic molecule NKG7 and the co-inhibitory molecule TOX (Figure 3.4B). In contrast, dry season T_{EM} cells displayed elevated expression of the inflammatory cytokine TNF and the NFKB inhibitor NFKBIE (Figure 3.4B). Pathway enrichment analysis for these populations indicated that wet season T_{EM} cells were enriched in pathways related to "T cell activation", "interferon-gamma-mediated signaling pathway" and "response to interferon gamma" while dry season cells exhibited enrichment in pathways associated with "negative regulation of cell growth", "T cell receptor signaling pathway", and "negative regulation of inflammatory response" (Figure 3.4F).

Finally, we probed for differences in gene expression within Th1 enriched CD4 CTLs and observed higher expression of the protease GZMB and IFN-γ regulator IFNG-AS1 (Figure 3.4C). Enrichment analysis revealed an enrichment of "natural killer cell

mediated cytotoxicity", "regulation of inflammatory response", "apoptotic processes", and "negative regulation of T cell receptor signaling pathway" in wet season CD4 CTLs while "negative regulation of interleukin-2 production", "negative regulation of protein phosphorylation", and "protein ubiquitination" in dry season CTLs (Figure 3.4G). Analysis of regulatory T cells revealed an increase in transcriptional regulator MYC and enrichment in "cellular response to interleukin-4", "negative regulation of interleukin-12 production", and "gluconeogenesis" in the wet season while dry season cells revealed upregulation of "negative regulation of interleukin-6 production", "negative regulation of interleukin-2 production", and "dephosphorylation" (Figure 3.4D,H).

3.5 Discussion

In this study, we sought to interpret our previous findings of altered immunological responses to *P. falciparum* in children with or without *S. haematobium* using transcriptomic analysis. We characterized immune cells from individuals at the time when they had an acute *P. falciparum* infection and months after clearing the infection and to assess whether a pre-existing co-infection with *S. haematobium* provided enough of a stimulatory effect *in vivo* to influence immune cell composition and gene expression. Through single-cell RNA-sequencing, we profiled PBMC from *Sh*+ and *Sh*- children who lived in a region in Mali with high seasonal malaria endemicity. Our study successfully delineated distinct populations of T cells, B cells, natural killer (NK) cells, and myeloid cells in the peripheral blood of these children. Moreover, we conducted pseudo-bulk differential gene expression analysis and identified gene signatures of *P. falciparum* infection. We demonstrated differences in gene expression due to *Pf* infection status, but not due to *Sh* infection status. This study offers invaluable insights into the gene patterns

common to children exposed to *P. falciparum* in a region with high prevalence of malaria and schistosomiasis.

Due to their central role in host immune responses to *P. falciparum* and in facilitating B cell mediated protection, we performed further analyses on CD4 T cells. Through comprehensive analyses on this critical cell population, we provide an understanding of the landscape of Th lineages, their distribution across different CD4 compartments and begin to elucidate how protection is conferred by assessing the longitudinal expression profiles of effector populations. In addition to T_{CM}, T_{EM}, and Tregs, our study also revealed the presence of novel cytotoxic CD4 T cells which had previously not been characterized in *P. falciparum* exposed individuals. Compared to other CD4 T cell helper lineages, Th1 enriched CD4 CTLs made up a large enough population to generate a distinct cluster during our UMAP clustering analysis. These cells, identified at both time points, represent a highly differentiated population of effector/memory CD4s that have the capacity to secrete cytotoxic molecules[204]. CD4 CTLs have previously been identified in cancer, autoimmunity, and chronic infection where they have been shown to mediate apoptosis of infected cells through the perforin and granzyme B mechanisms[205,206]. We identified differences in this population between *Pf*+ and *Pf*- children, with CD4 CTLs from the malaria-positive timepoint expressing more GZMB, and exhibiting enrichment in T cell receptor signaling, metabolic, proteasome and ribosome pathways, suggesting that the cells are translationally active in response to stimuli. Since blood-stage *Pf* parasites infect MHC-free erythrocytes, functional studies with *P. falciparum* are needed to determine the role and mechanism of this population in during malaria and whether this

cytotoxic population contributes to the immunopathology associated with blood-stage *Pf* infection.

Although we identified immune populations that were consistently present at both time points and with minimal variations in their relative frequencies between the wet and dry seasons, these populations exhibited marked phenotypic variability, giving rise to discernible differences in gene expression patterns at the timepoints with and without malaria infection. Our differential gene expression analyses revealed differences across all non-naïve CD4 T cell populations, with a high degree of overlap of differentially expressed genes across cell populations, suggesting that distinct CD4 T cell population share similar gene signatures when responding to infection.

We observed increased expression of interferon genes across all non-naïve CD4 T cells and increased expression of IL18 receptor genes in T_{EM} and CD4 CTLs. Our data is consistent with multiple studies that have shown that interferon-related cytokines, genes, and pathways are upregulated during malaria infection and that these molecules are critical for protection[33,207,208]. Moreover, levels of IL18, the cytokine that binds IL18R, are known to be increased during *Pf* infection and in some cases are associated with severe disease[209,210]. Cytokine cell surface receptors are usually upregulated in a positive-feedback mechanism in response to cytokine binding[211], which would suggest relatively higher serum cytokine levels of IL18 during an active malaria episode when compared to malaria-cleared timepoints. Moreover, our gene expression observations were supported by enrichment analyses that revealed enrichment in IFN-γ mediated responses and signaling in T_{CM} and T_{EM} during malaria infection.

We also discovered a significant upregulation of the transcription factors NR4A1, NR4A2, and NR4A3 in individuals exposed to malaria, several months after clearing the infection. Notably, these orphan nuclear receptors have been implicated in T cell dysfunction[212,213]. Prior research has shown that NR4As, which are downstream of NFAT signaling, exert antagonistic effects on AP-1 transcription factors by competing for binding sites[212,214]. Liu et al. reported downregulation of AP-1 transcription factors, FOS and JUN in NR4A-high/tolerant cells[212], while NR4A-low cells exhibited upregulation of GZMB and BATF. In line with these findings, our study also observed enrichment of GZMB and BATF in NR4A-low cells from the wet season. BATF is a transcription factor that is induced during TCR signaling and is known to counter T cell exhaustion and promote cell survival[215,216]. In malaria, BATF expression has been observed in the context of Type 1 regulatory T cells (Tr1), where it is co-expressed with LAG3 , ICOS, and CTLA4[217–219] as observed within some of our memory populations. The upregulation of BATF in wet season samples relative to dry season suggests an immune mechanism that involves this transcription factor to sustain T cell responses over the duration of an acute *P. falciparum* infection.

In contrast, our investigation revealed an upregulation of JUNB and JUND in cells collected during the dry season, with increased expression of NR4A transcription factors. An earlier study demonstrated JUND's role in mediating the activation of NR4A1, suggesting that the expression of JUND is required for NR4A1 expression[220]. Furthermore, our study observed elevated expression of CXCR5 in T_{CM} cells from the dry season, a chemokine receptor recently detected in exhausted, chronically stimulated CD8 T cells[221,222]. Nevertheless, further investigation is required to understand the dynamics of

expression and co-expression of these transcription factors to elucidate how these feedback mechanisms are regulated and which stimuli determine the extent of expression.

Our findings suggest a dynamic regulation of genes involved in T cell receptor signaling. During active infection, high BATF expression may drive the differentiation of Th lineages and maintain T cell activity. In contrast, NR4As are highly expressed in the absence of infection, indicating their role in promoting a quiescent state in T cells. This dynamic balance of gene expression underlines the complexity of immune responses during and after *P. falciparum* infection.

Surprisingly, our study did not detect differences in memory CD4 T cells between *Sh*+ and *Sh*- children as observed by Lyke et al[122,125]. Lyke et al noted a higher percentage of IFN-γ, TNF-α, and IL-2 production in *Sh*+ individuals during the dry season in response to stimulation with *Pf* and *Sh* antigens[122]. Key differences in study design and characteristics of randomly selected samples between our current study and theirs may contribute to the contrasting results. Notably, the time to first malaria episode was shorter in *Sh*+ relative to *Sh*- children in our subset (Supplementary Figure 3.4A), whereas the parent study (n = 327) demonstrated a longer time to first infection in *Sh*+ individuals within the same age range[11]. The differences in timing of first *P. falciparum* infection could potentially contribute to the differences in the observations.

Moreover, our current study assessed gene expression differences without *ex vivo* stimulation, contrary to Lyke et al[122,125]. The absence of *ex vivo* stimulation in our study may allow for accurate interpretation of gene expression during the dry season when memory cells are in quiescent state. Furthermore, consistent with the primary study, we also observed lower parasitemia in *Sh*+ children from this subset (Supplementary Figure

3.4B). Additionally, despite evidence suggesting a Treg-enriched environment in response to chronic *S. haematobium*[111,112], we found no significant differences in proportions and gene expression within Tregs between *Sh*+ and *Sh*- children. This unexpected result, which differs from the larger parent study, hints at the complex dynamics of co-infection, suggesting a need for further exploration.

One limitation of our study is the lack of PBMCs from a baseline timepoint, hindering our ability to track immune cell dynamics before, during and after a *P. falciparum* infection. Additionally, our analysis is confined to effector populations in the periphery, we are unable to capture details of recently activated T cells and T_{CM} found in secondary lymphoid organs or tissue-resident cells found in the liver where $CD8^+$ T cells may play a larger role[223,224]. Despite these limitations, our study offers a comprehensive profile of peripheral responses from PBMCs acquired in children with a chronic *S. haematobium* infection and the dynamics during a naturally acquired *P. falciparum* infection.

In conclusion, our study demonstrates that a chronic asymptomatic *S. haematobium* infection, in this small subset, does not significantly alter gene expression in contrast to a symptomatic *P. falciparum* infection. We also highlight the importance of considering various factors, such as timing of infections and *ex vivo* stimulation, when interpreting immune responses in co-infected individuals. By constructing a comprehensive immune landscape, we have illuminated the transcriptomic profile of CD4 T cells in this context, making a substantial contribution to our understanding of immune responses in the presence of malaria and co-infections. Our findings suggest a complex regulatory network involving BATF and NR4A family members, along with their interactions with key

transcription factors such as NFAT and AP-1, potentially contributing to T cell dysfunction in individuals exposed to malaria. Furthermore, the observed variations in gene expression patterns indicate a dynamic response to antigenic factors, underscoring the importance of further research to fully unravel the mechanisms at play and assess how these transcription factors influence malaria disease tolerance and immune responses to subsequent infections.

Chapter 4: Conclusion and Discussion

4.1 Study Summary

The goals of this study were to identify the determinants of malaria susceptibility by assessing factors that contribute to varying immune responses in a Malian cohort (Aim 1) and to characterize the mechanisms behind T cell memory formation in malaria-exposed individuals in addition to assessing the impact of a pre-existing *S. haematobium* co-infection on *P. falciparum* immune responses (Aim 2). To address these aims, mass cytometry, microarray, single-cell and bulk RNA sequencing, and secondary data analyses were used to interpret immunological responses using peripheral blood mononuclear cells collected from children who reside in malaria-endemic regions. These tools enabled cutting-edge analyses to identify genes that were differentially expressed in individuals with varying susceptibility to clinical malaria and cell composition and signatures associated with P. *falciparum* infection.

4.1.1 Aim 1 Significant Findings and Limitations

In *Aim 1* (Chapter 2) we compared gene expression and cytokine profiles in PBMCs obtained from children who experienced one to two clinical malaria episodes (susceptible) over the course of a single transmission season with those from children who experienced no clinical malaria episodes (protected) within the same time frame. We conducted a comprehensive analysis of samples collected at different timepoints: day 0 (baseline), day 90 (peak transmission) and day 150 (end of the transmission season). At each timepoint, we compared immune responses between protected and susceptible children. The results of this Chapter underscore the importance of baseline immune signatures in predicting disease progression, vaccine efficacy, and treatment outcomes in the context of malaria.

Here, we demonstrated that high expression of interferon signaling genes (CXCL10, STAT1, STAT2, GZMB, XAF1, IRF1) prior to the transmission season is associated with an increased likelihood of symptomatic malaria[225]. While interferon genes are necessary for effective clearance of *P. falciparum*, excessive production of highly inflammatory cytokines, and the subsequent recruitment of macrophages and dendritic cells, contribute to some of the adverse symptoms associated with acute and severe malaria[33,226]. Furthermore, this chapter reveals that children who subsequently acquire symptomatic malaria are enriched in both type I and type II interferon signaling and apoptotic pathways[225], indicating that systematic differences at baseline contribute to susceptibility in this cohort. Moreover, we observed higher proportions of HLA-DR$^+$CD4$^+$ T cells in the peripheral blood of protected children upon stimulation with *P. falciparum* schizonts[225]. HLA-DR, a cell surface marker upregulated during infection, is associated with resistance to infectious pathogens[185–187]. Higher HLA-DR expression on the surface of CD4 T cells from protected children may account for the absence of clinical malaria within this group.

However, a major limitation of this aim is the sample size for the bulk RNA sequencing analysis portion of the present study. While we identified gene signatures common to susceptible individuals, a larger study is needed to validate these findings. This limitation was primarily due to the limited availability of PBMCs, as most of the samples initially collected from each cohort participant were utilized during the primary study. Unfortunately, some samples processed for RNA-sequencing had low quality due to the addition of Golgi blockade – a phenomenon not previously reported in the literature, and, consequently, were unusable. Through our work, we demonstrated that the addition of

Golgi blockade to PBMCs compromises the quality of RNA and needs to be accounted for in future work involving PBMC stimulation.

Another potential limitation to consider is the choice of stimulant. We used *P. falciparum* schizonts from a Malawian strain adapted to culture. These schizonts are derived from an East African strain, whereas the study samples originate from Mali, West Africa. Genomic diversity in *P. falciparum* strains across geographic regions is well documented, with W. African strains being distinct from those in E. Africa and across Asia[227–229]. Consequently, stimulating with these schizonts may have led to indiscriminate upregulation of genes and proteins in both susceptible and protected children, making the differentiation of these groups through RNA-seq and mass cytometry analysis challenging. The RNA-seq data revealed substantial differences between the two groups at baseline timepoints prior to stimulation, but these distinctions diminished as the transmission season progressed or after stimulation with *P. falciparum* schizonts. This suggests that the fading of differences in PBMC gene expression between susceptible and protected children halfway through the malaria season, in the absence of *ex vivo* stimulation, may be due to natural stimulation by exposure to parasites in the field.

Regardless of these nuances, the study successfully identified gene expression differences in children of similar age and geographic location who exhibited distinct clinical outcomes over the course of a single transmission season. In summary, *Aim 1* highlights the significance of baseline gene expression patterns in understanding malaria susceptibility. It not only identifies potential genes and cell populations that may aid in predicting malaria susceptibility but also underscores the necessity of adopting systems-

level approaches to comprehend immune responses in the context of human subjects and natural infection.

4.1.2 Aim 2 Significant Findings and Limitations

In *Aim 2* (Chapter 3), we compared cell proportions and cell-specific gene expression profiles of children during and after an acute malaria episode. We also assessed the impact of a chronic *S. haematobium* infection on immune responses to *P. falciparum* and *P. falciparum* exposed peripheral CD4 T cells. We demonstrated that balancing negative and positive feedback loops are essential aspects of host immune responses to *P. falciparum* infection. We showed that the relative levels of immune activating and inhibiting genes change in response to natural *P. falciparum* infection. This study substantially advances our comprehension of the immune gene signatures associated with clinical malaria, the dynamics of co-infection, and the heterogeneity of immune cell populations. Nevertheless, to further enrich the existing body of knowledge in this field, future investigations employing diverse study designs are warranted.

First, this study corroborates previous findings by demonstrating increased expression of interferon genes and elevated expression of IL18 receptor genes across different CD4 T cell sub-populations during *P. falciparum* infection. The role of IL18 in promoting Th1 and IFN-γ production has been well-established, and the production of inflammatory cytokines during *P. falciparum* infection noted in conjunction with malaria symptoms[33]. These prior observations validate our findings since we are observing expected changes induced by *P. falciparum* infection. Furthermore, we also observed the presence of a novel cytotoxic CD4 T cell population within PBMCs of malaria-exposed children. This population has also been shown to produce highly inflammatory

cytokines[230]. However, the presence of CD4 CTLs in individuals exposed to *P. falciparum* infection raises questions about their potential role in protection against malaria and their possible involvement in the immunopathology associated with *P. falciparum* infection. Follow up studies are warranted to assess the mechanism of this cell population during malaria, especially considering that red blood cells lack MHC molecules, which raises questions about the T cell functionality and cytotoxic phenotype, specifically whether they produce IFN-γ but do not release cytolytic granules containing perforin and granzyme.

During a clinical malaria episode in the wet season, we observed significant upregulation of BATF, LAG-3, and CTLA4 in children from this cohort. The co-expression of these molecules has been observed in type 1 regulatory T cells (Tr1) during human malaria[217–219]. This subset of FOXP3-negative CD4 T cells is capable of producing both Th1 mediated cytokine, IFN-γ, and regulatory immunosuppressive cytokine, IL-10 [217–219]. The upregulation of Tr1 gene signatures in the wet season samples points to the potential role of this cell subset in simultaneously promoting parasite clearance and reducing *P. falciparum*-associated pathology. Some mouse studies suggest that this population is derived from Th1 and shares an immune gene signature with this lineage[231,232]; further studies with human samples are needed to validate these findings. To gain insight into the presence and function of this subset in our cohort, we could stimulate PBMCs with a *P. falciparum* antigen and gate on Tbet^{+} CD4 T cells, and then assess the presence of IFN-γ /IL-10 dual-positive cells, although this would require a substantial number of cells. As a follow up, performing single-cell RNA sequencing on sorted CD4 T cells from *P. falciparum*-infected children could allow the acquisition of enough cells from each individual to generate distinct clusters for each Th lineage. This would enable the

characterization of each lineage and understand their immune signature during symptomatic malaria and convalescence.

Furthermore, we detected significant upregulation of the NR4A family of transcription factors in individuals exposed to malaria, several months after infection clearance. These transcription factors are known to be involved in exhaustion and are part of a feedback loop in both B cells and T cells that promotes the expression of inhibitory molecules[233–236]. Notably, CXCR5, identified as upregulated in dry season T_{CM}, has been implicated in exhaustion when co-expressed with PD1 and TCF1[221]. Additionally, Lyke et. al, in a study under review, observed upregulation is this chemokine in a repetitive challenge model of *P. falciparum*, associated with a dampening of clinical symptoms related to malaria disease. Collectively, these findings, in conjunction with our study, suggests a role for CXCR5 in dampening symptoms and suppressing the development of immunity to *P. falciparum*. Furthermore, these pathways may contribute to the well-described phenomenon of "tolerance" to *P. falciparum*, where children can tolerate parasitemia with minimal symptoms, but rarely achieve sterile immunity[12]. Some studies suggest that upregulated expression of proteins encoded by these genes correlates with changes in chromatin accessibility by promoting accessibility of gene sites that code for inhibitory molecules[212,216]. Interestingly, these studies also point to the antagonistic function of NR4A and BATF[212,216], a molecule which was upregulated in wet season cells relative to the dry season cells. Both these molecules are shown to be part of the NFAT signaling pathway, where NR4A proteins promote NFAT binding the promoter in the absence of AP-1 transcription factors which leads to expression of inhibitory genes, while BATF promotes NFAT/AP-1 binding, terminating exhaustion pathways[215,216]. A critical

follow-up to our study would be to investigate the mechanism behind NR4A-mediated immunosuppression during malaria. It is well documented that protective immune responses to malaria are not long-lasting, but the mechanism is poorly understood[22,237]. Whether NR4A plays a role in this phenomenon has yet to be addressed. To address this, we can perform an assay for transposase-accessible chromatin sequencing (ATAC-seq) experiment to assess chromatin accessibility for gene sites that are suspected to be inhibited or promoted by NR4A proteins. Assessing these sites during both a clinical malaria episode and months after clearance can shed a light on whether malaria-exposed memory T cells are targeted for exhaustion through the NR4A-mediated pathway.

Another goal of our study was to assess the impact of a pre-existing *S. haematobium* infection on immune responses to *P. falciparum* and the development and maintenance of memory populations. In contrast to previous findings by Lyke et al[122], our study surprisingly revealed no discernible differences in memory CD4 T cell populations between *Sh*+ and *Sh*- children. Lyke et al. reported a higher proportion of IFN-γ, TNF-α, and IL-2 production in *Sh*+ individuals during the dry season in response to both *Pf* and *Sh* antigens[122], which contrasted with our observations. Notably, our current study and the earlier investigation differ significantly in study design and the characteristics of randomly selected samples used for analysis. While the time to first malaria episode was shorter in *Sh*+ children within our subset (Supplementary Figure 3.4A), the larger parent study (n = 327) exhibited a longer time to initial infection in *Sh*+ individuals within the same age range[11]. Variations in the timing of first *P. falciparum* infection suggest that the participants in the two studies might not be representative of the same baseline cohort, which may account for the discrepancies in our observations.

Furthermore, our current study evaluated gene expression differences without *ex vivo* stimulation as performed in the previous studies, which might be essential to induce distinct cellular phenotypes in quiescent cells from the dry season. Consistent with the primary study, we also observed lower parasitemia in *Sh*+ children within this participant subset (Supplementary Figure 3.4B). Surprisingly, we did not identify differences in proportions and gene expression within Tregs between *Sh*+ and *Sh*- children, despite evidence that chronic *S. haematobium* infection promotes a Treg-enriched environment[111,112]. This finding implies that, contrary to our expectations based on *S. haematobium* mono-infection, the dynamics of co-infection do not conform to conventional patterns and warrant further investigation.

A notable limitation of our study was the absence of PBMCs from the baseline timepoint. Inclusion of such data would have allowed us to track immune cell dynamics both before and after a *P. falciparum* infection, enabling a more comprehensive assessment of immune cell composition in both *Sh*+ and *Sh*- individuals and eliminating the potential for confounders due to baseline differences. Despite these limitations and other limitations, discussed in full below, our study has constructed a comprehensive profile of PBMCs from children with chronic *S. haematobium* infection, revealing the presence of various cell types that respond to natural *P. falciparum* infection, contributing valuable insights into the complex interplay of these infections.

In summary, *Aim 2* has provided a comprehensive characterization of the immune landscape of CD4 T cells and revealed a complex regulatory network involving BATF and NR4A family members. The upregulation or downregulation of these molecules may contribute to T cell dysfunction in malaria-exposed individuals. The observed variation in

gene expression patterns underscores the dynamic response to antigenic factors, emphasizing the need for further research to fully understand the underlying mechanisms and how these transcription factors shape immune responses to subsequent infections.

4.2 Study Limitations and Insights

Studies involving natural human infections face several key limitations. These limitations encompass the inability to control the precise timing of infection, genome-wide differences between infecting strains, parasitemia levels, host behavior, and the challenge of accessing immune cells in crucial sites, such as the liver, spleen, or lymph nodes. Even though PBMC samples were obtained at the onset of diseases symptoms, the manifestation of symptoms in children occurs at variable timepoints following infection. Consequently, the immunological landscape, specifically the composition of immune cells and the differentiation of effector cells, at the time of symptom presentation may give rise to inter-individual variation of specific immune cell subsets. Despite these potential discrepancies, our study controlled for age and its impact towards immune acquisition, therefore any differences observed in our study are not due to differences in age and exposure to *P. falciparum*.

Another major caveat of human studies investigating immune responses to parasites is the inability to capture tissue-resident and lymph node immune cells. While our cohorts from Chapter 1 and Chapter 2 allow us to identify immune cell signatures in the peripheral circulation, we lack information on immune cells residing in tissues and lymph nodes. For instance, in the context of a chronic *S. haematobium* infection, alterations such as aberrant deposition of *S. haematobium* eggs in the liver[238,239] can influence the outcome of *P. falciparum* infection during the liver-stage, affecting parasitemia levels and severity of

symptoms. While this study highlights the central role of CD4 T cells in peripheral immunity, it is important to acknowledge the potential contribution of other cell subsets including CD8 T cells, NKT cells, NK cells, and γδ T cells, may play important roles in other sites that were not captured in this analysis. Another drawback of gene expression studies is our inability to capture differences in transcripts that have already been translated, preventing us from fully capturing the variations attributed to translated and functional proteins.

In conclusion, and despite the potential limitations listed, this thesis sheds light on the importance of a systems-immunology approach to understanding human immune responses to natural *P. falciparum* infection. Our study identified patterns (e.g., interferon enrichment during *P. falciparum* infection) consistent with previous findings in malaria research, affirming that a systems approach can effectively capture signatures observed through cytological assays. *Aim 1* emphasized the importance of understanding baseline immune status, through the characterization of gene expression, for accurately interpreting immunological responses and clinical implications in field studies involving human subjects and identified potential genes and cell populations associated with malaria susceptibility. Aim 2 created a comprehensive picture of the dynamics of CD4 T cells during a clinical malaria episode and elucidated the role of opposing feedback loops that may influence both effector and memory responses. Overall, this study has provided essential insights into the phenotypes of immune cells during *P. falciparum* infection and a potential explanation for the lack of lasting immunity, while contributing to our understanding of clinical disease tolerance observed in malaria-exposed individuals through our transcriptomics analysis. This knowledge can be instrumental in informing on

vaccine efficacy and strategies for malaria protection amongst individuals in endemic settings.

Appendix

A.1 Media Recipe

Thawing Buffer
49 mL DPBS
10 mL 10% BSA

Final Buffer
49.8 mL PBS
0.2 μL 10% BSA

Dead Cell Removal (DCR) Buffer
100 μL 0.5 mM CaCl
1000 μL FBS
Fill to 50 mL with PBS
Filter in 0.2 μm Nalgene filter

A.2 Supplementary Figures and Tables

Supplementary Table 2.1

Volunteer	Group	Assay	Age	Ethnicity	Sex	# of Pf events
Patient 1	Protected	Mass Cytometry/Array	5.24	Peulh	M	0
Patient 4	Protected	Mass Cytometry/Array	4.87	Dogon	F	0
Patient 6	Protected	Mass Cytometry/Array	5.81	Bambara	M	0
Patient 9	Protected	Mass Cytometry	2.52	Dogon	F	0
Patient 11	Protected	Mass Cytometry/Array	5.85	Bambara	F	0
Patient 13	Protected	Mass Cytometry/Array	4.8	Dogon	M	0
Patient 14	Protected	Mass Cytometry	6.78	Dogon	F	0
Patient 15	Protected	Mass Cytometry/Array	4.09	Sonike	M	0
Patient 18	Protected	Mass Cytometry/Array	5.05	Dogon	F	0
Patient 21	Protected	RNA-seq	6.74	Dogon	F	0
Patient 22	Protected	RNA-seq/Array	4.39	Dogon	F	0
Patient 23	Protected	RNA-seq/Array	6.32	Dogon	F	0
Patient 2	Susceptible	Mass Cytometry	4.88	Dogon	F	3
Patient 3	Susceptible	Mass Cytometry	5.78	Dogon	M	2
Patient 5	Susceptible	Mass Cytometry/Array	5.9	Dogon	M	3
Patient 7	Susceptible	Mass Cytometry/Array	6.04	Dogon	M	3
Patient 8	Susceptible	Mass Cytometry/Array	5.22	Dogon	M	2
Patient 10	Susceptible	Mass Cytometry/Array	6.77	Dogon	F	4
Patient 12	Susceptible	Mass Cytometry/Array	4.02	Dogon	F	3
Patient 16	Susceptible	Mass Cytometry	4.11	Dogon	F	2
Patient 19	Susceptible	Mass Cytometry/Array	5.99	Dogon	M	2
Patient 20	Susceptible	Mass Cytometry	4.04	Dogon	F	2
Patient 24	Susceptible	RNA-seq/Array	6.0	Dogon	M	2
Patient 25	Susceptible	RNA-seq	6.09	Dogon	F	2
Patient 26	Susceptible	RNA-seq	4.81	Dogon	F	2

Supplementary Table 2.1: Cohort Demographics.

Table presenting participant information, including participant ID, assigned group condition (protected or susceptible), performed assay, age, sex, ethinicity, and the number of clinical malaria episodes, experienced by each individual.

Supplementary Table 2.2

Fsc colname	Antigen	Marker class
(Pr141)Di	CCR6_141Pr	state
(Nd142)Di	IL_4_142Nd	state
(Nd146)Di	CD8_146Nd	type
(Sm147)Di	HELIOS_IL6_147Sm	state
(Nd150)Di	MIP1b_150Nd	state
(Eu151)Di	CD107_EQ4_151Eu	state
(Sm152)Di	TNF_TCRgd_152Sm	type
(Gd155)Di	CD27_155Gd	type
(Gd158)Di	IL_2_158Gd	state
(Tb159)Di	CD197_159Tb	type
(Gd160)Di	TBET_160Gd	state
(Dy161)Di	CD152_161Dy	type
(Dy162)Di	FOXP3_CD69_162Dy	state
(Dy163)Di	CXCR3_163Dy	state
(Dy164)Di	IL_17_CD161_164Dy	type
(Ho165)Di	IFN_EQ4_165Ho	state
(Tm169)Di	CD45RA_169Tm	type
(Er170)Di	CD3_170Er	none
(Yb171)Di	GRAN_171Yb	state
(Yb174)Di	CD4_174Yb	type
(Lu175)Di	PD1_EQ4_175Lu	state

Supplementary Table 2.2: Antibody Staining for Effector Function Panel

Table displaying cell surface markers and intracellular cytokine staining panel used for effector mass cytometry assay.

Supplementary Table 2.3

Fsc colname	Antigen	Marker class
(Nd146)Di	CD8_146Nd	type
(Sm147)Di	HELIOS_IL6_147Sm	state
(Sm149)Di	CD25_149Sm	type
(Eu151)Di	CD107_EQ4_151Eu	state
(Sm152)Di	TNF_TCRgd_152Sm	state
(Gd155)Di	CD27_155Gd	type
(Gd158)Di	IL_2_158Gd	state
(Gd160)Di	TBET_160Gd	type
(Dy161)Di	CD152_161Dy	type
(Dy164)Di	IL_17_CD161_164Dy	state
(Ho165)Di	IFN_EQ4_165Ho	state
(Er166)Di	IL10_166Er	state
(Er167)Di	GATA3_167Er	type
(Er168)Di	RORGT_168Er	type
(Tm169)Di	CD45RA_169Tm	type
(Er170)Di	CD3_170Er	none
(Yb173)Di	HLA-DR_173Yb	type
(Yb174)Di	CD4_174Yb	type
(Yb176)Di	CD127_176Yb	type

Supplementary Table 2.3: Antibody Staining for Regulatory Function Panel

Table depicting cell surface markers and intracellular cytokines utilized in the regulatory panel.

Supplementary Table 2.4

Sample Name	Group	RIN Value	Concentration (ng/ul)	Volume	Total ng
IGS-MLI-0010rhd1c1	Susceptible	9.5	2.351	50	117.55
IGS-MLI-0010rhd1c4	Susceptible	9.4	1.925	50	96.25
IGS-MLI-0010rhd1c2	Susceptible	9.3	1.158	50	57.9
IGS-MLI-0011rhd1c1	Susceptible	8.2	4.293	50	214.65
IGS-MLI-0011rhd1c4	Susceptible	8.1	3.514	50	175.7
IGS-MLI-0011rhd1c2	Susceptible	8	3.712	50	185.6
IGS-MLI-0012rhd1c1	Protected	9.4	2.87	50	143.5
IGS-MLI-0012rhd1c4	Protected	9.6	2.215	50	110.75
IGS-MLI-0012rhd1c2	Protected	8.5	1.359	50	67.95
IGS-MLI-0013rhd1c1	Protected	8.1	2.465	50	123.25
IGS-MLI-0013rhd1c4	Protected	8.8	0.859	50	42.95
IGS-MLI-0013rhd1c2	Protected	8.4	0.91	50	45.5
IGS-MLI-0010rhd3c1	Susceptible	8.2	3.42	50	171
IGS-MLI-0010rhd3c4	Susceptible	8.4	2.09	50	104.5
IGS-MLI-0010rhd3c2	Susceptible	7.9	2.849	50	142.45

Supplementary Table 2.4, continued

IGS-MLI-0011rhd3c1	Susceptible	7.4	4.281	50	214.05
IGS-MLI-0011rhd3c4	Susceptible	6.9	3.374	50	168.7
IGS-MLI-0011rhd3c2	Susceptible	8	2.401	50	120.05
IGS-MLI-0012rhd3c1	Protected	7.5	4.444	50	222.2
IGS-MLI-0012rhd3c4	Protected	7.4	6.071	50	303.55
IGS-MLI-0012rhd3c2	Protected	6.9	6.529	50	326.45
IGS-MLI-0013rhd3c1	Protected	7.4	5.491	50	274.55
IGS-MLI-0013rhd3c4	Protected	6.7	4.698	50	234.9
IGS-MLI-0013rhd3c2	Protected	7.2	6.693	50	334.65
IGS-MLI-0010rhd2c1	Susceptible	7	4.229	50	211.45
IGS-MLI-0010rhd2c4	Susceptible	7.6	3.501	50	175.05
IGS-MLI-0010rhd2c2	Susceptible	7.9	1.747	50	87.35
IGS-MLI-0011rhd2c1	Susceptible	7.5	0.938	50	46.9
IGS-MLI-0011rhd2c4	Susceptible	8	1.854	50	92.7
IGS-MLI-0011rhd2c2	Susceptible	7.5	2.001	50	100.05
IGS-MLI-0012rhd2c1	Protected	3.1	4.526	50	226.3
IGS-MLI-0012rhd2c4	Protected	5.6	8.63	50	431.5
IGS-MLI-0012rhd2c2	Protected	5.7	10.328	50	516.4
IGS-MLI-0013rhd2c1	Protected	7.1	6.605	50	330.25
IGS-MLI-0013rhd2c4	Protected	7.6	6.401	50	320.05
IGS-MLI-0013rhd2c2	Protected	7	10.975	50	548.75
IGS-MLI-0014rhd1c1	Susceptible	6.3	4.558	50	227.9
IGS-MLI-0014rhd1c4	Susceptible	6.4	8.835	50	441.75
IGS-MLI-0014rhd1c2	Susceptible	6.8	8.191	50	409.55
IGS-MLI-0015rhd1c1	Protected	7.1	1.642	50	82.1
IGS-MLI-0015rhd1c4	Protected	7.3	6.185	50	309.25
IGS-MLI-0015rhd1c2	Protected	7.7	6.38	50	319
IGS-MLI-0014rhd2c1	Susceptible	7	3.74	50	187
IGS-MLI-0014rhd2c4	Susceptible	7.2	2.363	50	118.15
IGS-MLI-0014rhd2c2	Susceptible	7.1	3.907	50	195.35
IGS-MLI-0015rhd2c1	Protected	4.8	2.388	50	119.4
IGS-MLI-0015rhd2c4	Protected	3.3	2.051	50	102.55
IGS-MLI-0015rhd2c2	Protected	5.5	1.558	50	77.9
IGS-MLI-0014rhd3c1	Susceptible	7.4	1.448	50	72.4
IGS-MLI-0014rhd3c4	Susceptible	7.2	1.054	50	52.7
IGS-MLI-0014rhd3c2	Susceptible	7.1	1.26	50	63
IGS-MLI-0015rhd3c1	Protected	7.8	0.255	50	12.75
IGS-MLI-0015rhd3c4	Protected	6.9	1.842	50	92.1

Supplementary Table 2.4, continued

IGS-MLI-0015rhd3c2	Protected	7.9	0.685	50	34.25

Supplementary Table 2.4: RNA Integrity Numbers and Concentration for RNA Sequenced Samples

Table depicting RNA quality and concentration for each sequenced sample.

Supplementary Table 2.5

Sample Name	Total reads	Mapped reads	Percent Mapped	Percent Properly Paired
IGS_MLI_0010rhd1c1	27238560	25895650	95.07	95.98
IGS_MLI_0010rhd1c2	27556062	26118574	94.78	95.97
IGS_MLI_0010rhd1c4	31936084	29741452	93.13	96.29
IGS_MLI_0010rhd2c1	25412166	24028277	94.55	95.59
IGS_MLI_0010rhd2c2	36845900	34774483	94.38	95.77
IGS_MLI_0010rhd2c4	44220630	41368807	93.55	96.17
IGS_MLI_0010rhd3c1	27939058	26623830	95.29	96.39
IGS_MLI_0010rhd3c2	28715580	27238345	94.86	96.09
IGS_MLI_0010rhd3c4	30263134	27891582	92.16	96
IGS_MLI_0011rhd1c1	38824574	36771329	94.71	96.48
IGS_MLI_0011rhd1c2	27080998	25839856	95.42	96.4
IGS_MLI_0011rhd1c4	34282792	31941561	93.17	96.12
IGS_MLI_0011rhd2c1	18990640	17566479	92.5	94.69
IGS_MLI_0011rhd2c2	34437646	32401142	94.09	95.44
IGS_MLI_0011rhd2c4	35257972	32170368	91.24	96.01
IGS_MLI_0011rhd3c1	29552076	27470518	92.96	95.78
IGS_MLI_0011rhd3c2	36212640	34216930	94.49	95.95
IGS_MLI_0011rhd3c4	42739856	39819266	93.17	96.26
IGS_MLI_0012rhd1c1	30192960	28718698	95.12	96.04
IGS_MLI_0012rhd1c2	33478450	31861943	95.17	96.24
IGS_MLI_0012rhd1c4	35243500	33040393	93.75	96.44
IGS_MLI_0012rhd2c1	26623188	23765081	89.26	92.2
IGS_MLI_0012rhd2c2	44049364	41069217	93.23	94.76
IGS_MLI_0012rhd2c4	30112006	27473145	91.24	93.88
IGS_MLI_0012rhd3c1	29320354	27694663	94.46	96.43
IGS_MLI_0012rhd3c2	39436552	37375951	94.77	96.07
IGS_MLI_0012rhd3c4	35704246	32271118	90.38	95.7
IGS_MLI_0013rhd1c1	36317720	34280242	94.39	95.65
IGS_MLI_0013rhd1c2	29664680	27781805	93.65	95.7

Supplementary Table 2.5, continued

IGS_MLI_0013rhd1c4	28742092	26645053	92.7	96
IGS_MLI_0013rhd2c1	24591584	23160706	94.18	95.19
IGS_MLI_0013rhd2c2	39134622	37200357	95.06	96.19
IGS_MLI_0013rhd2c4	22593698	20967976	92.8	96.15
IGS_MLI_0013rhd3c1	28289724	26921378	95.16	95.92
IGS_MLI_0013rhd3c4	31244620	28785976	92.13	95.26
IGS_MLI_0014rhd1c1	35220836	33236955	94.37	95.29
IGS_MLI_0014rhd1c2	33507672	31508824	94.03	95.11
IGS_MLI_0014rhd1c4	47353168	43542121	91.95	95.09
IGS_MLI_0014rhd2c1	35963998	33943651	94.38	95.43
IGS_MLI_0014rhd2c2	31342836	29576035	94.36	95.31
IGS_MLI_0014rhd2c4	44081434	39737715	90.15	94.61
IGS_MLI_0014rhd3c1	31398412	29575428	94.19	95.34
IGS_MLI_0014rhd3c2	31069724	29129743	93.76	95.28
IGS_MLI_0014rhd3c4	34396796	31551391	91.73	95.38
IGS_MLI_0015rhd1c1	30168048	28400885	94.14	95.84
IGS_MLI_0015rhd1c2	30624964	28996006	94.68	95.81
IGS_MLI_0015rhd1c4	22064964	20180743	91.46	95.64
IGS_MLI_0015rhd2c1	29098858	26435418	90.85	92.83
IGS_MLI_0015rhd2c2	35075152	31871983	90.87	92.06
IGS_MLI_0015rhd2c4	25906170	22833398	88.14	92.39
IGS_MLI_0015rhd3c1	40146970	35993893	89.66	94.11
IGS_MLI_0015rhd3c2	34492756	32091822	93.04	94.96
IGS_MLI_0015rhd3c4	32617100	29410653	90.17	95.48
Average	**32580671.43**	**30442560.87**	**93.18679245**	**95.40730769**
Median	**31398412**	**29575731.5**	**93.75**	**95.7**
Total	**1726775586**	**1583013165**	**4938.9**	**4961.18**

Supplementary Table 2.5: Summary Table of Illumina Reads Mapped to Reference Genome

Table depicting total reads mapped to the human reference genome.

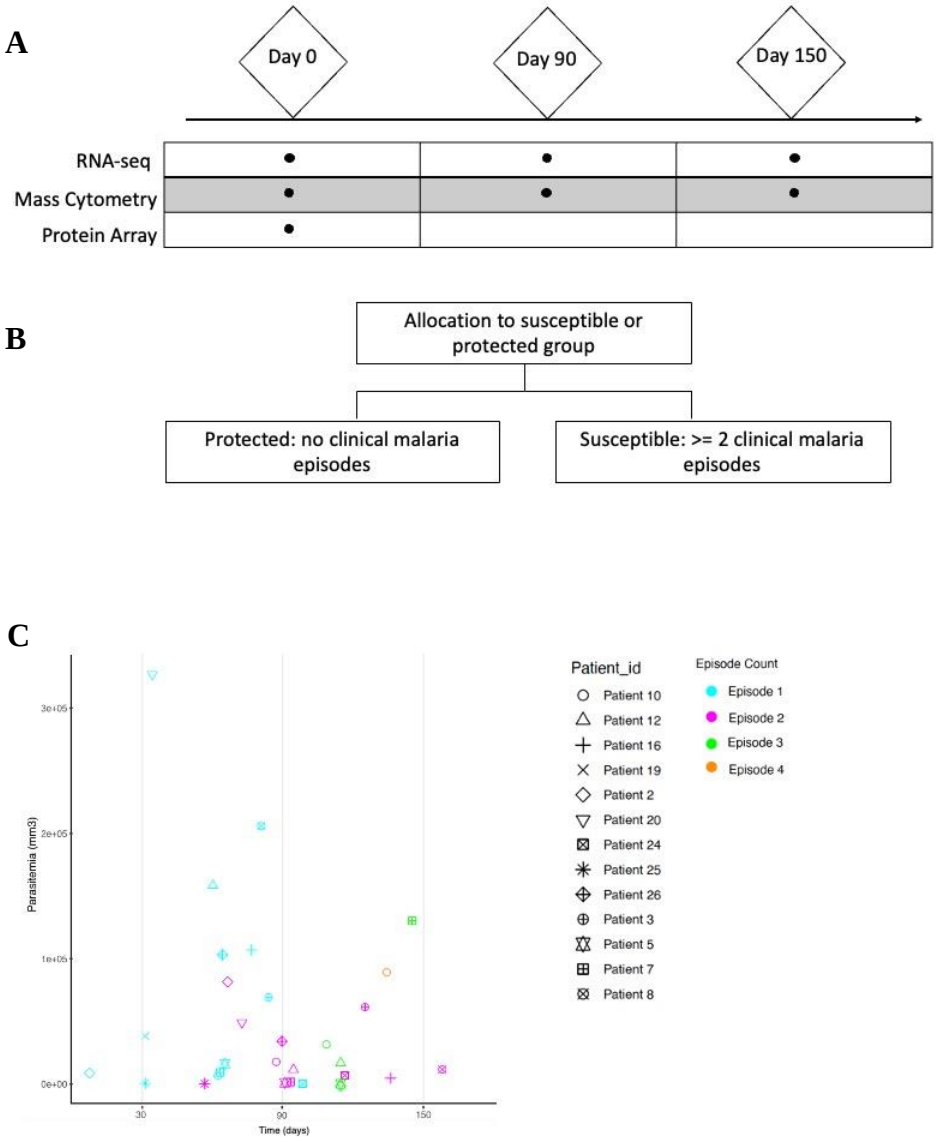

Supplementary Figure 2.1. Study design indicating sample collection, assays performed, allocation criteria and timing of clinical malaria episodes.

(**A**)PBMCs were collected from Malian children between the ages of 1-6 years at day 0, day 90, and day 150. Children were monitored for malaria symptoms and thick blood smears were used for parasite detection. (**B**) Children with greater than 2 clinical malaria episodes were classified as susceptible while children with no clinical malaria episodes were classified as protected. (**C**) Timing of clinical malaria episodes experienced by children in the "susceptible" group showing the time clinical illness was diagnosed on the x-axis and the intensity of each episode (Parasitemia/mm3 of blood) on the y-axis. Each child is represented by a unique shape. Episode counts are denoted by different colors: cyan for the first episode, magenta for the second episode, green for the third episode, and orange for the fourth episode.

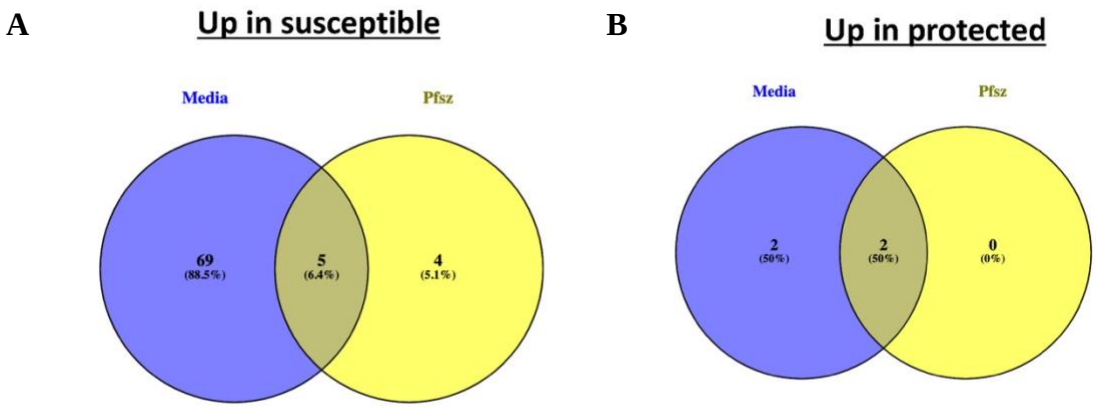

Supplementary Figure 2.2. Venn Diagram of genes upregulated in susceptible individuals

(**A**) and protected individuals (**B**) before and after antigen stimulation with *Plasmodium falciparum schizonts (Pfsz).* Venn diagram was generated with Venny 2.0 web interactive tool.

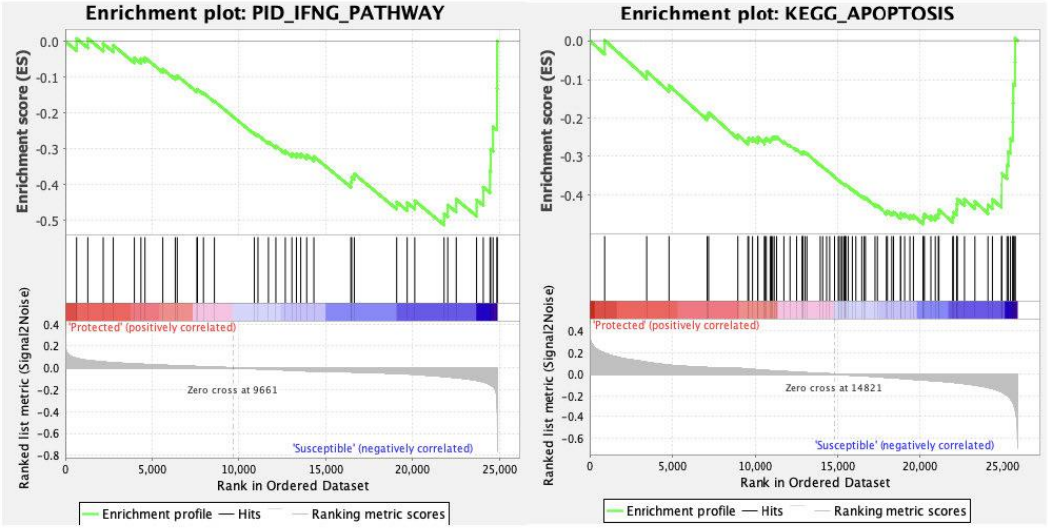

Supplementary Figure 2.3. Gene set enrichment analysis of transcripts from malaria-protected children compared to malaria-susceptible children.

GSEA results show that canonical IFN-γ and Apoptotic pathways are enriched in susceptible children.

Supplementary Figure 2.4. PfEMP1 protein microarray testing seroreactivity and serorecognition.

(**A**) Heatmap of seroreactivity to *Plasmodium falciparum* fragments. Each column represents serum from one child and each row represents a peptide fragment. Red corresponds to high reactivity, black is moderate and grey indicates no reactivity. Wilcoxon rank sum test was used to test for significance (**B**) Fluorescence intensity peaks for each protein fragment. Blue peaks correspond to susceptible and orange peaks correspond to protected. No significant differences observed between protected and susceptible individuals. (**C**) The proportion of individuals within each group with serorecognition of each protein fragment (defined as a fluorescence intensity greater than the mean plus two standard deviations for a serum panel from 10 malaria-naïve North American adults probed on the microarray). The x-axis represents the protein fragments that were recognized, while the y-axis represents the proportion of individuals from each group who recognized these fragments. Blue peaks correspond to susceptible and orange peaks correspond to protected.

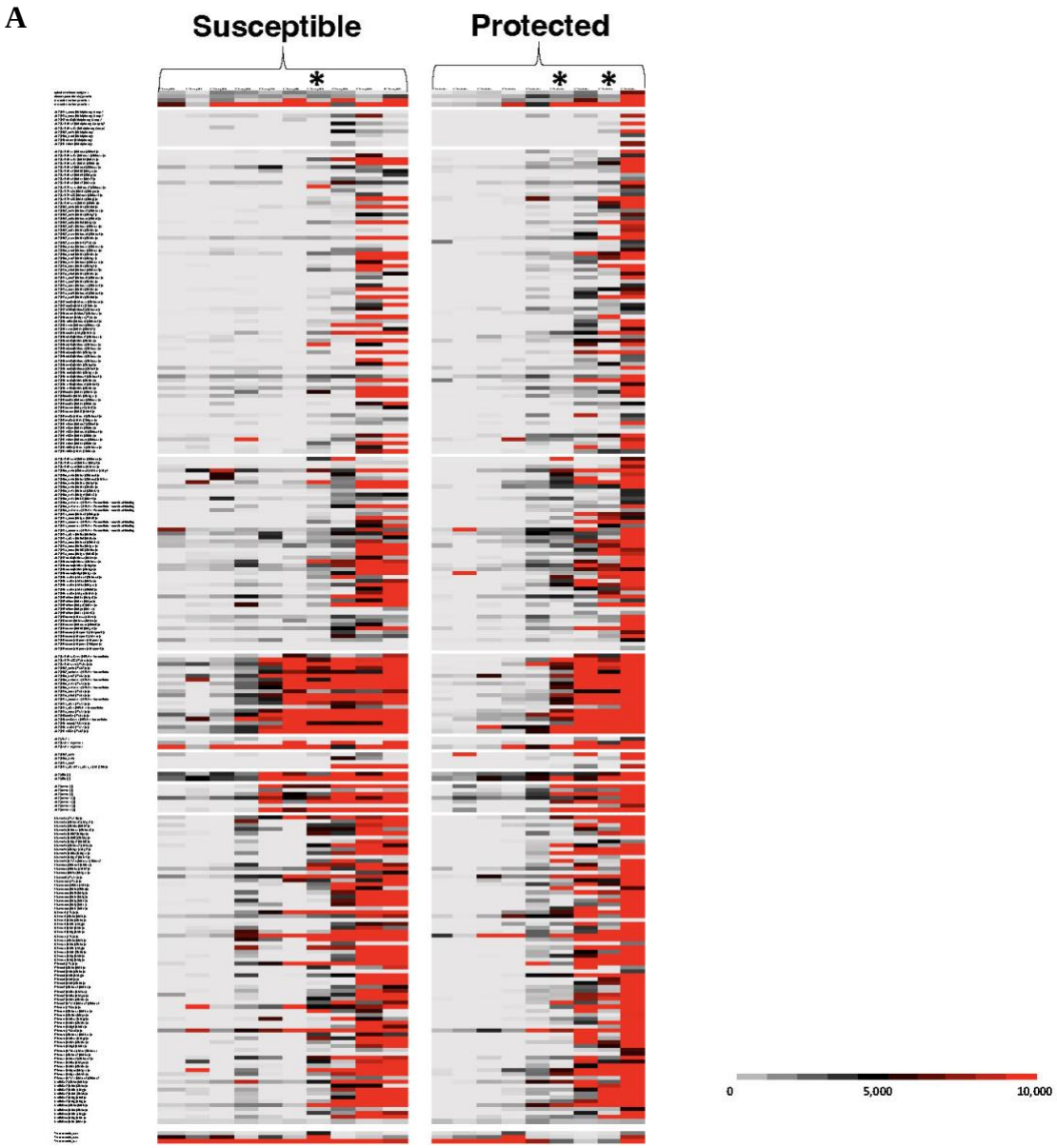

B

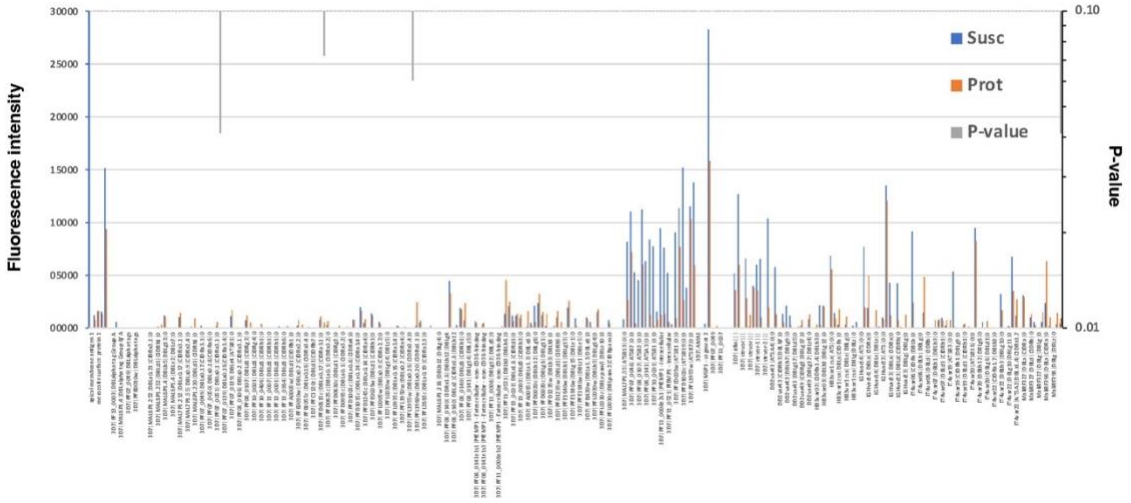
Fluorescence intensity
P-value
Susc
Prot
P-value
30000
25000
20000
15000
10000
05000
00000
0.10
0.01

C

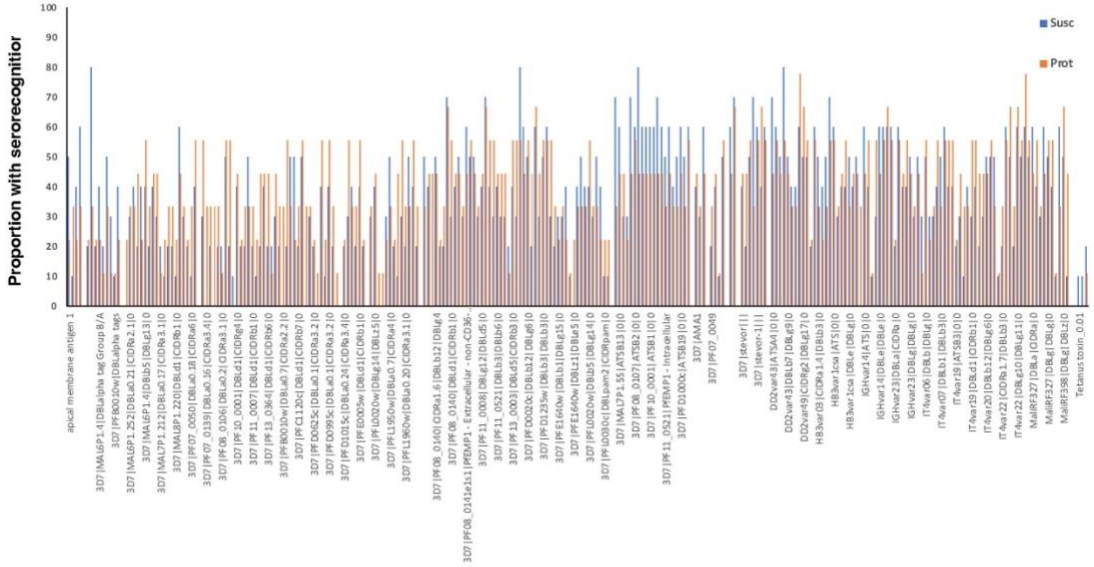
Proportion with seroreognitior
Susc
Prot
100
90
80
70
60
50
40
30
20
10
0

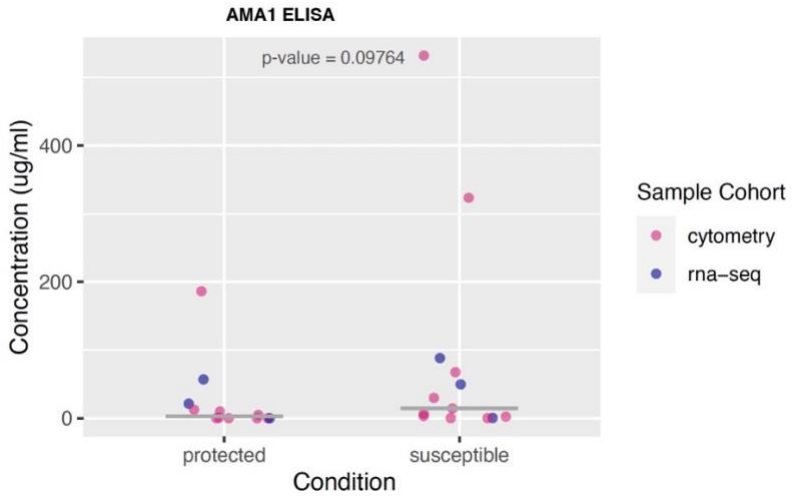

Supplementary Figure 2.5. Serum AMA1 antibody concentrations in protected and susceptible children

Jittered scatter plot comparing the concentration of Apical Membrane Antigen 1 (AMA1) antibodies present in the serum of protected versus susceptible children at baseline, prior to malaria transmission season. Mann Whitney U test used to determine significance. The antibody concentration did not differ significantly between conditions. The dashed lines represent the median concentration in each group. Samples used for RNA-seq are colored in dark blue while samples used for mass cytometry are colored in deep pink.

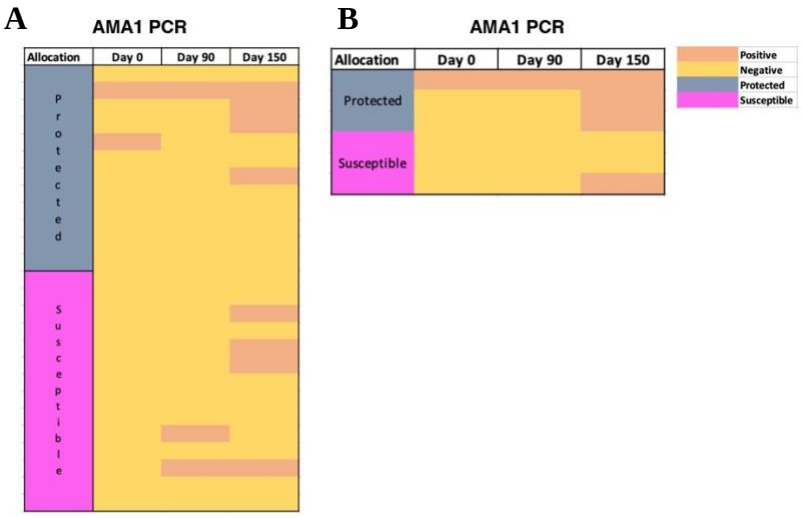

Supplementary Figure 2.6. Occurrence of asymptomatic malaria across three distinct timepoints

Heatmap showing PCR positive samples at baseline (Day 0) and across the malaria transmission season (Day 90 and Day 150) in malaria protected (grey) and malaria susceptible (hot pink) individuals. A fisher's exact test was used to determine significance between protected and susceptible children across all three timepoints. (**A**) Heatmap for all samples processed for RNA-seq and Mass Cytometry. P-value 0.22 for day 0, P-value of 0.59 for day 90 and P-value of 1 for day 150. (**B**) Heatmap for samples processed for RNA-seq only. P-value 1 for day 0, P-value of 1 for day 90 and P-value of 0.4 for day 150.

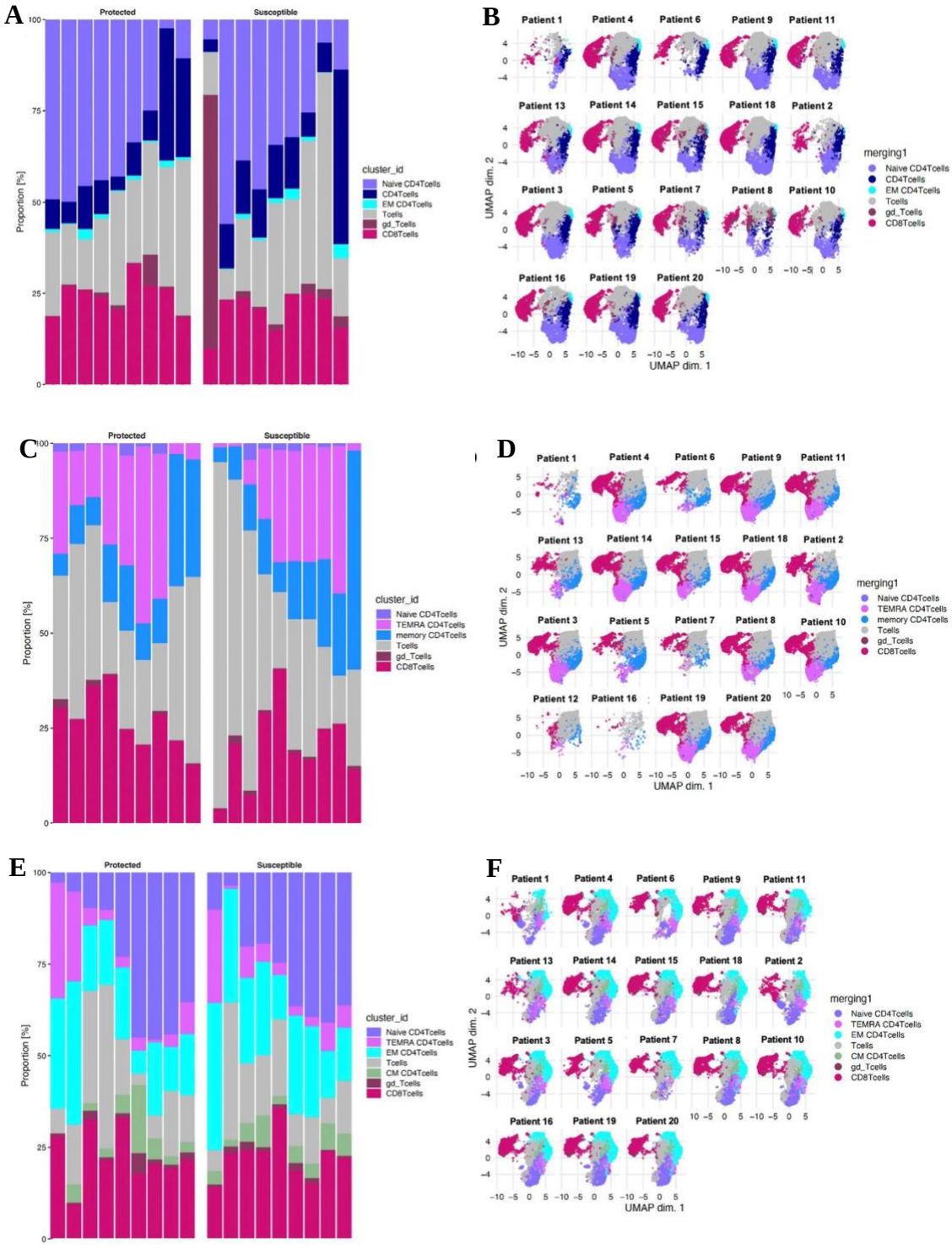

Supplementary Figure 2.7. Cell type abundance across the transmission season

(**A**-**B**) Day 0 cell type abundance. (**A**) Barplot showing distribution of each annotated cell type per sample. (**B**) UMAP cluster for each sample. (**C**-**D**) Day 90 cell type abundance. (**C**) Barplot showing distribution of each annotated cell type per sample. (**D**) UMAP cluster for each sample. (**E**-**F**) Day 150 cell type abundance. (**E**) Barplot showing distribution of each annotated cell type per sample. (**F**) UMAP cluster for each sample.

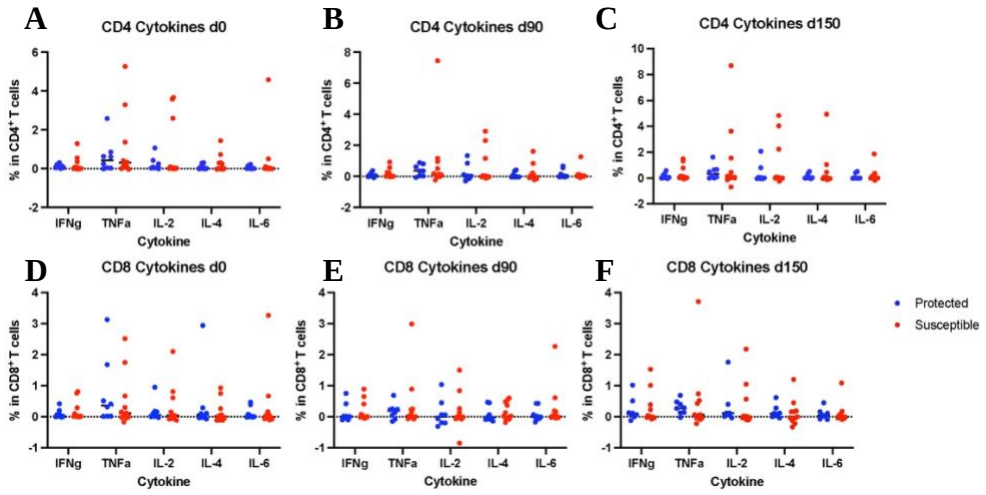

Supplementary Figure 2.8. Intracellular cytokine data for Pfsz stimulated CD4 and CD8 T cells.

(**A**) Dot plot showing CD4 cytokines at day 0. (**B**) Dot plot showing CD4 cytokines at day 90. (**C**) Dot plot showing CD4 cytokines at day 150. (**D**) Dot plot showing CD8 cytokines at day 0. (**E**) Dot plot showing CD8 cytokines at day 90. (**F**) Dot plot showing CD8 cytokines at day 150. Data for protected children is shown in blue and data in susceptible children is shown in red.

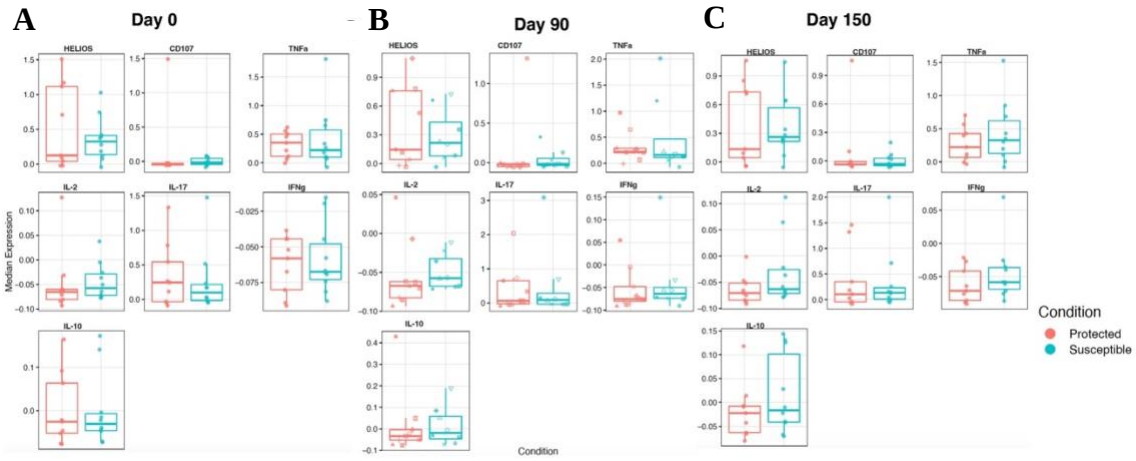

Supplementary Figure 2.9. Intracellular cytokine expression within T cells across a single malaria transmission season

(**A-C**) Box plots displaying overall median expression of intracellular markers within T cells ($CD3^+$) of Pfsz stimulated-CD25 depleted PBMCs. Expression values were subjected to Z-score scaling, transforming the values to have a mean of 0 and a standard deviation of 1 across all cells. Negative expression values indicate that the average expression of a marker is lower relative to the other markers and positive expression values indicate that the average expression of a marker is higher relative to the other markers. Expression levels for protected children are indicated in red and expression levels for susceptible children are indicated in teal. Expression values from each child are indicated by a unique shape (**A**) Median expression for molecules at day 0. (**B**) Median expression for molecules at day 90. (**C**) Median expression for molecules at day 150.

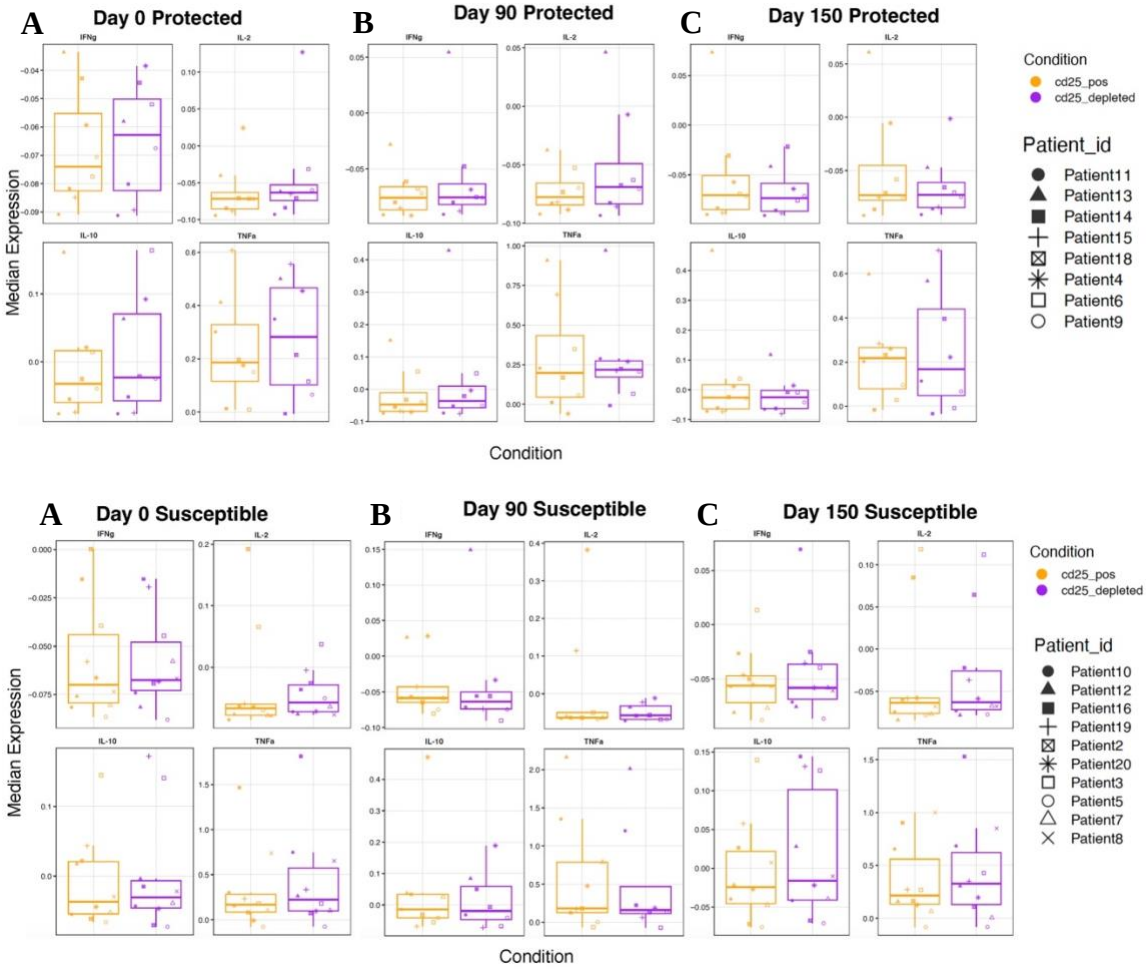

Supplementary Figure 2.10. Expression of intracellular cytokine within T cells before and after CD25 depletion

(**A-F)** Boxplot showing median expression of intracellular markers within T cells ($CD3^{+}$) of *Pfsz* stimulated PBMCs before and after CD25 depletion. Expression values were subjected to Z-score scaling, transforming the values to have a mean of 0 and a standard deviation of 1 across all cells. Negative expression values indicate that the average expression of a marker is lower relative to the other markers and positive expression values indicate that the average expression of a marker is higher relative to the other markers. Expression levels for CD25 positive cells are indicated in orange and expression levels for CD25 depleted cells are indicated in purple. Expression values from each child are indicated by a unique shape (**A**) Median expression for molecules in protected children at day 0. (**B**) Median expression for molecules in protected children at day 90. (**C**) Median expression for molecules in protected children at day 150. (**D**) Median expression for molecules in susceptible children at day 0. (**E**) Median expression for molecules in susceptible children at day 90. (**F**) Median expression for molecules in susceptible children at day 150.

Supplementary Table 3.1

Sample Name	Other ID	Season	Season	Age	Ethnicity	Egg load *	Episodes	Mal_1	Quartier	Sex
SN280	**child1**	W03	D04	6	1	0	2	52	III	1
SN422	**child10**	W03	D04	5	2	0	1	61	VII	1
SP184	**child11**	W02	D03	6	1	18	1	28	III	2
SP422	**child12**	W03	D04	5	1	3	2	20	VII	1
SN274	**child13**	W03	D04	5	1	0	2	62	V	1
SN284	**child14**	W03	D04	6	1	0	2	49	III	2
SP274	**child15**	W03	D04	5	1	77	1	31	V	1
SP284	**child16**	W03	D04	6	1	8	2	8	III	2
SN161	**child17**	W02	D03	4	1	0	1	103	VII	1
SN321	**child18**	W03	D04	8	1	0	1	100	V	2
SP161	**child19**	W02	D03	4	1	348	1	20	VII	1
SN418	**child2**	W03	D04	7	1	0	2	67	III	2
SP321	**child20**	W03	D04	8	1	30	2	1	V	2
SP418	**child3**	W03	D04	7	1	10	2	39	III	2
SP280	**child4**	W03	D04	6	19	13	1	27	III	1
SN264	**child5**	W03	D04	5	1	0	1	65	III	2
SN269	**child6**	W03	D04	5	1	0	1	42	III	1
SP264	**child7**	W03	D04	5	19	29	2	22	III	2
SP269	**child8**	W03	D04	5	19	53	2	24	III	1
SN184	**child9**	W02	D03	6	1	0	1	39	III	2

*Egg load calculated after filtering 10 mL of first catch morning urine followed by Ninhydrin staining.

Supplementary Table 3.1: Aim 2 Cohort Demographics

Table depicting sample collection details, including season collected, *S. haematobium* egg load, and the number of malaria episodes experienced by each participant.

Supplementary Table 3.2

Marker	ADT	RNA	Cluster
CD45	98.727224	94.8017149	CD4 TCM
CD16	88.2395382	86.5800866	CD16 Mono
CD14.1	92.8303303	93.5810811	CD14 Mono
CD123	99.6666667	96.6666667	pDC
CD11c	98.0603448	80.6034483	cDC2
CD20	96.519411	96.7068273	B Memory
CD19.1	98.8487282	67.6572959	B Memory
CD3	98.0439443	92.9528403	CD4 TCM
CD4.1	97.7224009	46.221865	CD4 TCM
CD8	95.9843639	83.7953092	CD8 T Naïve
TCR-Vd2	96.4088398	68.4392265	VD2 gdT
CD56	82.0448878	42.1446384	NK CD56hi

Supplementary Table 3.2: RNA and ADT Marker Expression

Table depicting percentage of annotated cells expressing corresponding cell surface marker protein (ADT) and gene (RNA).

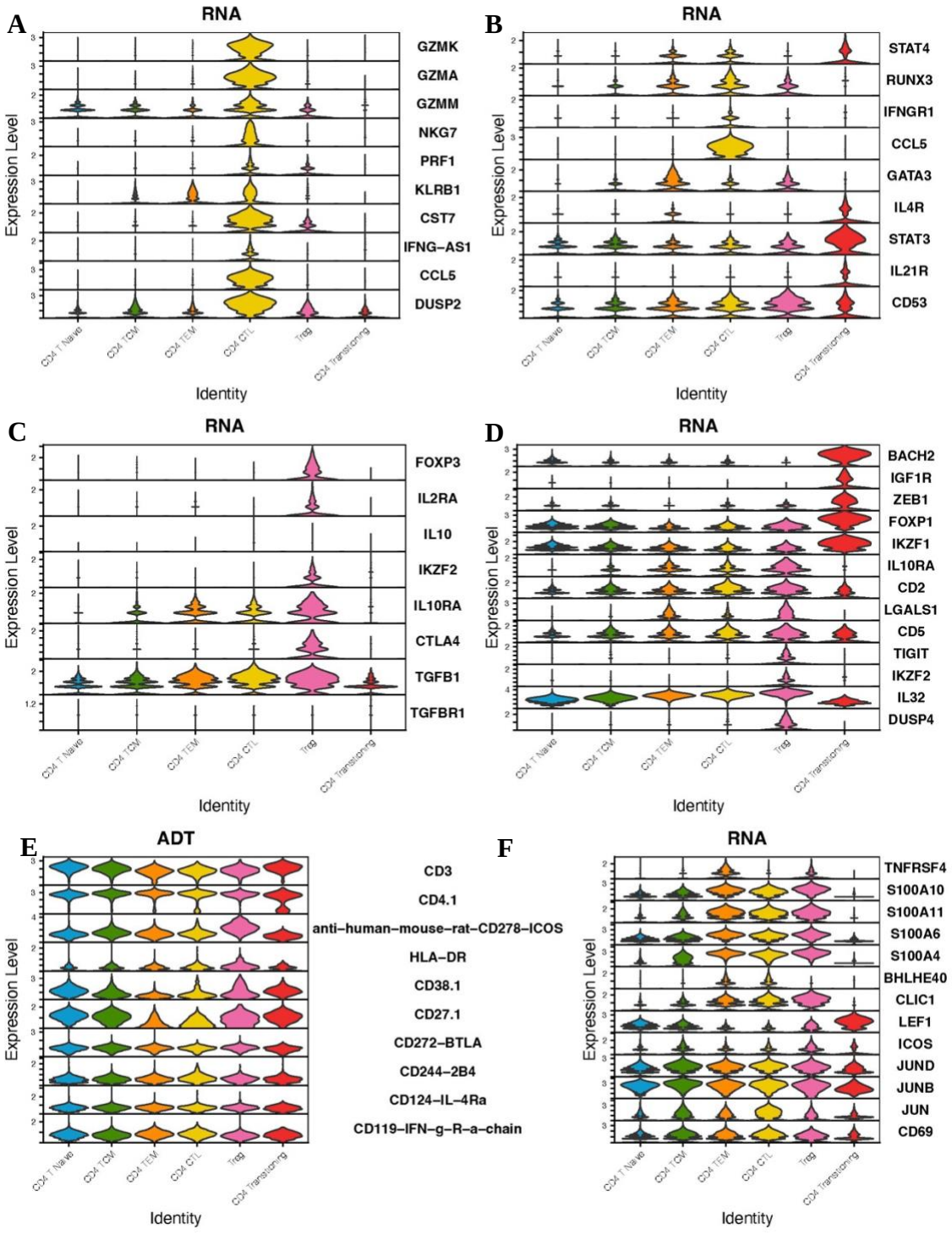

Supplementary Figure 3.1. Violin plots depicting gene and cell surface protein markers used to identify and characterize CD4 T cell subsets.

(**A,B,C,D,F**) Violin plot illustrating the gene expression profiles of key genes across annotated CD4 T cell subsets. (**E**) Violin plots depicting protein (ADT) expression of surface markers of interest within CD4 T cell subsets.

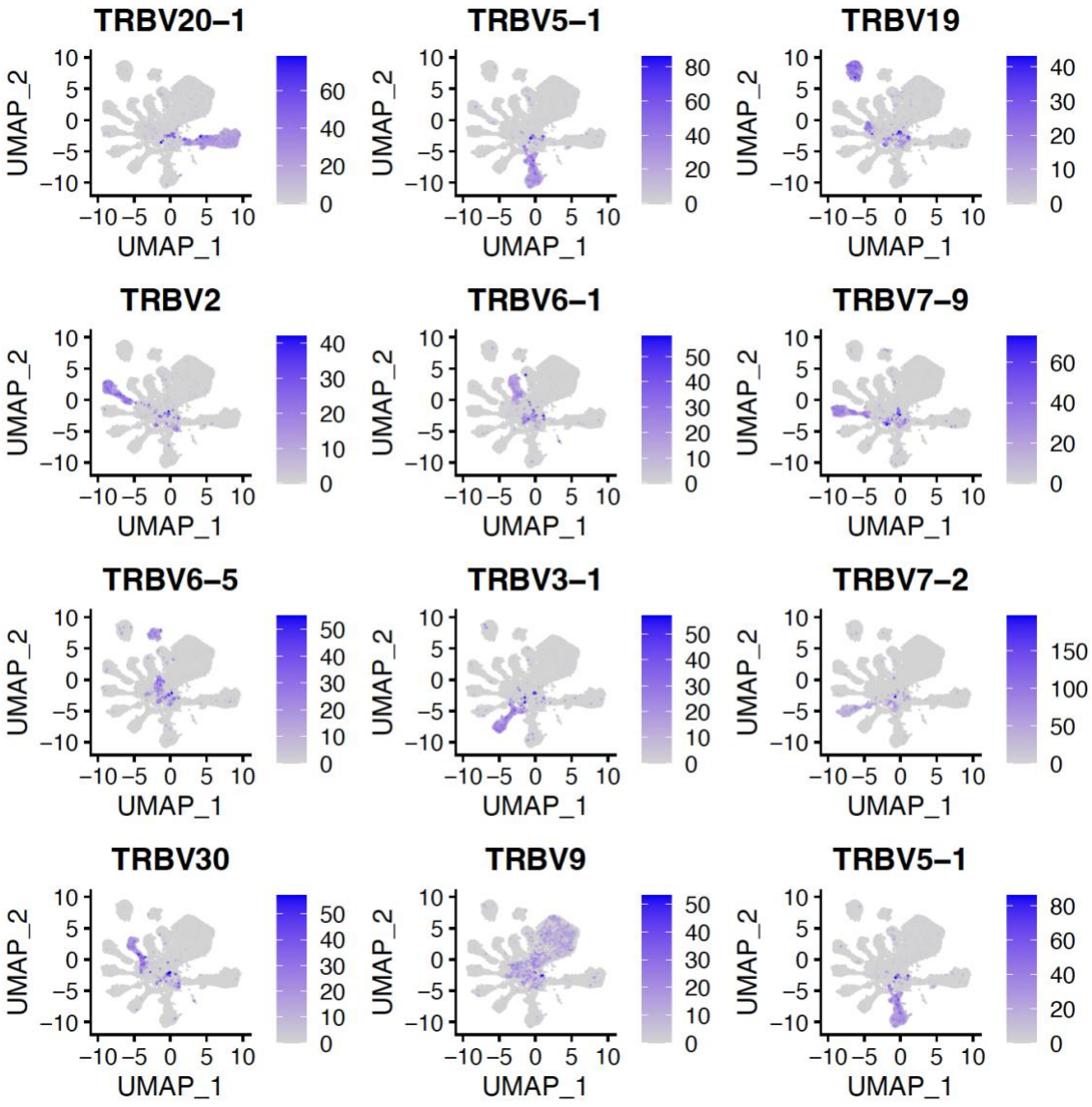

Supplementary Figure 3.2. Feature plots depicting clonal T cell receptor β variable (TRBV) gene segments enriched in each CD4 T cell node.

(**A**) Feature plots illustrating gene TRBV gene segments present in CD4 T cell subsets.

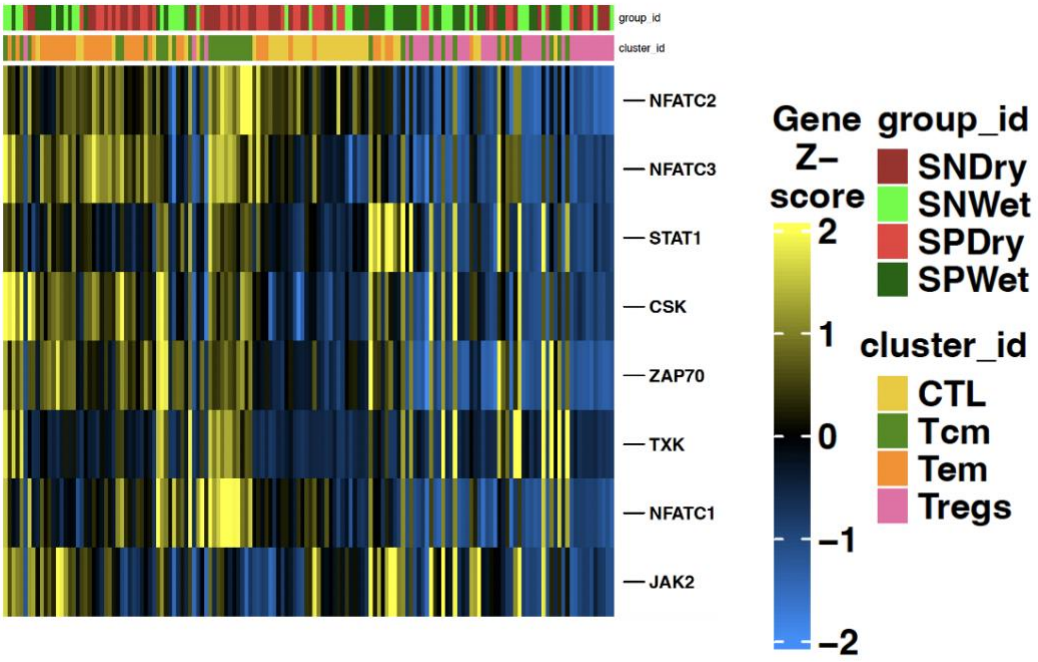

Supplementary Figure 3.3. Ubiquitously differentially expressed genes

(A) Heatmap depicting differentially expressed genes that overlap across two or more non-naïve CD4 T cell subsets. FDR < 0.05

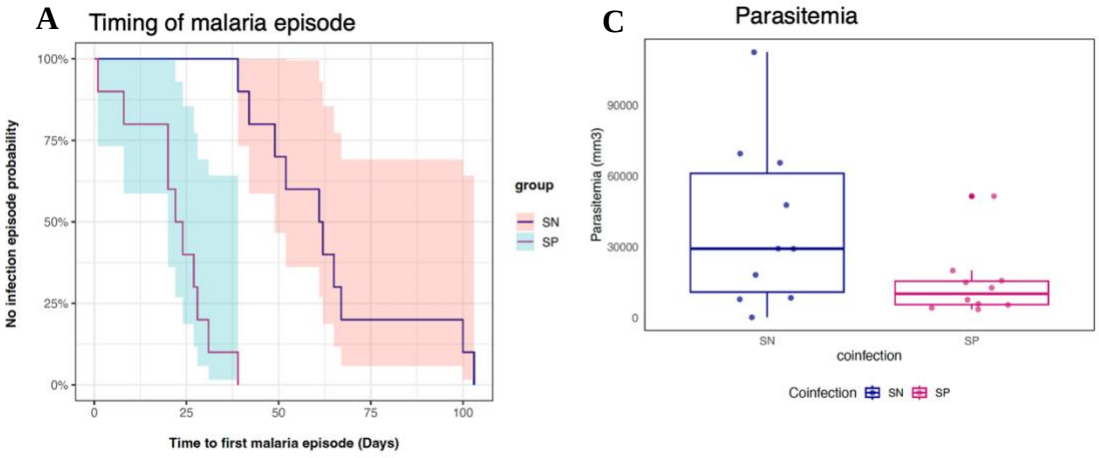

Supplementary Figure 3.4. Malaria episode timing and disease severity

(**A**) Time to event curve depicting timing of first clinical malaria episode for each group *Sh*+ (SP) and *Sh*- (SN). (SN = pink, and SP = blue). (**B**) Box plot of parasitemia of each group. Dark blue = SN and Deep pink = SP

Reference

1. World malaria report 2020: 20 years of global progress and challenges. 151 (2020).
2. Bartoloni, A. & Zammarchi, L. Clinical Aspects of Uncomplicated and Severe Malaria. *Mediterr J Hematol Infect Dis* **4**, (2012).
3. World Health Organization. *World malaria report 2021*. (World Health Organization, 2021).
4. Sinnis, P. & Fidock, D. A. The RTS,S vaccine—a chance to regain the upper hand against malaria? *Cell* **185**, 750–754 (2022).
5. Naddaf, M. Second malaria vaccine to win global approval is cheaper and easier to make. *Nature* (2023) doi:10.1038/d41586-023-03115-1.
6. Datoo, M. S. *et al.* Efficacy and immunogenicity of R21/Matrix-M vaccine against clinical malaria after 2 years' follow-up in children in Burkina Faso: a phase 1/2b randomised controlled trial. *The Lancet Infectious Diseases* **22**, 1728–1736 (2022).
7. WHO recommends R21/Matrix-M vaccine for malaria prevention in updated advice on immunization. https://www.who.int/news/item/02-10-2023-who-recommends-r21-matrix-m-vaccine-for-malaria-prevention-in-updated-advice-on-immunization.
8. Venugopal, K., Hentzschel, F., Valkiūnas, G. & Marti, M. Plasmodium asexual growth and sexual development in the haematopoietic niche of the host. *Nat Rev Microbiol* **18**, 177–189 (2020).
9. Mohandas, N. & An, X. Malaria and Human Red Blood Cells. *Med Microbiol Immunol* **201**, 593–598 (2012).
10. World malaria report 2022. https://www.who.int/publications-detail-redirect/9789240064898.

11. Lyke, K. E. *Et Al.* Association Of Schistosoma Haematobium Infection With Protection Against Acute Plasmodium Falciparum Malaria In Malian Children. *Am J Trop Med Hyg* **73**, 1124–1130 (2005).
12. Doolan, D. L., Dobaño, C. & Baird, J. K. Acquired Immunity to Malaria. *Clin Microbiol Rev* **22**, 13–36 (2009).
13. Sazawal, S. *et al.* Effects of routine prophylactic supplementation with iron and folic acid on admission to hospital and mortality in preschool children in a high malaria transmission setting: community-based, randomised, placebo-controlled trial. *The Lancet* **367**, 133–143 (2006).
14. Adam, I. Anemia, Iron Supplementation and Susceptibility to Plasmodium falciparum Malaria. *EBioMedicine* **14**, 13–14 (2016).
15. Lyke, K. E. *et al.* Association of HLA alleles with Plasmodium falciparum severity in Malian children. *Tissue Antigens* **77**, 562–571 (2011).
16. Lopera-Mesa, T. M. *et al.* Impact of red blood cell variants on childhood malaria in Mali: a prospective cohort study. *Lancet Haematol* **2**, e140–e149 (2015).
17. Smith, J. L. *et al.* Malaria risk factors in northern Namibia: The importance of occupation, age and mobility in characterizing high-risk populations. *PLoS One* **16**, e0252690 (2021).
18. Parker, B. S. *et al.* Hyperendemic malaria transmission in areas of occupation-related travel in the Peruvian Amazon. *Malaria Journal* **12**, 178 (2013).
19. Schellenberg, J. R. A. *et al.* Effect of large-scale social marketing of insecticide-treated nets on child survival in rural Tanzania. *The Lancet* **357**, 1241–1247 (2001).

20. Belachew, E. B. Immune Response and Evasion Mechanisms of Plasmodium falciparum Parasites. *J Immunol Res* **2018**, 6529681 (2018).

21. Dinko, B. & Pradel, G. Immune evasion by Plasmodium falciparum parasites: converting a host protection mechanism for the parasite′s benefit. *Advances in Infectious Diseases* **6**, 82–95 (2016).

22. Langhorne, J., Ndungu, F. M., Sponaas, A.-M. & Marsh, K. Immunity to malaria: more questions than answers. *Nature Immunology* **9**, 725–732 (2008).

23. Van geertruyden, J.-P. Interactions between malaria and human immunodeficiency virus anno 2014. *Clin Microbiol Infect* **20**, 278–285 (2014).

24. Waisberg, M. *et al.* Genetic susceptibility to systemic lupus erythematosus protects against cerebral malaria in mice. *Proceedings of the National Academy of Sciences* **108**, 1122–1127 (2011).

25. Stevenson, M. M. & Riley, E. M. Innate immunity to malaria. *Nat Rev Immunol* **4**, 169–180 (2004).

26. Tukwasibwe, S. *et al.* Variations in killer-cell immunoglobulin-like receptor and human leukocyte antigen genes and immunity to malaria. *Cell Mol Immunol* **17**, 799–806 (2020).

27. Ozarslan, N., Robinson, J. F. & Gaw, S. L. Circulating Monocytes, Tissue Macrophages, and Malaria. *J Trop Med* **2019**, 3720838 (2019).

28. Tweedell, R. E., Qi, L., Sun, Z. & Dinglasan, R. R. Kupffer Cells Survive Plasmodium berghei Sporozoite Exposure and Respond with a Rapid Cytokine Release. *Pathogens* **7**, 91 (2018).

29. Yap, X. Z., Lundie, R. J., Beeson, J. G. & O'Keeffe, M. Dendritic Cell Responses and Function in Malaria. *Front Immunol* **10**, 357 (2019).

30. Leiriao, P., Mota, M. M. & Rodriguez, A. Apoptotic Plasmodium-infected hepatocytes provide antigens to liver dendritic cells. *J Infect Dis* **191**, 1576–1581 (2005).

31. Miller, J. L., Sack, B. K., Baldwin, M., Vaughan, A. M. & Kappe, S. H. I. Interferon-Mediated Innate Immune Responses against Malaria Parasite Liver Stages. *Cell Reports* **7**, 436–447 (2014).

32. Artavanis-Tsakonas, K. & Riley, E. M. Innate Immune Response to Malaria: Rapid Induction of IFN-γ from Human NK Cells by Live Plasmodium falciparum-Infected Erythrocytes1. *The Journal of Immunology* **169**, 2956–2963 (2002).

33. King, T. & Lamb, T. Interferon-γ: The Jekyll and Hyde of Malaria. *PLoS Pathog* **11**, e1005118 (2015).

34. Favre, N., Ryffel, B., Bordmann, G. & Rudin, W. The course of Plasmodium chabaudi chabaudi infections in interferon-gamma receptor deficient mice. *Parasite Immunol* **19**, 375–383 (1997).

35. Wolf, A.-S., Sherratt, S. & Riley, E. M. NK Cells: Uncertain Allies against Malaria. *Front Immunol* **8**, 212 (2017).

36. Hart, G. T. *et al.* Adaptive NK cells in people exposed to Plasmodium falciparum correlate with protection from malaria. *Journal of Experimental Medicine* **216**, 1280–1290 (2019).

37. Kurup, S. P. & Harty, J. T. γδ T cells and immunity to human malaria in endemic regions. *Ann Transl Med* **3**, S22 (2015).

38. Kurup, S. P., Butler, N. S. & Harty, J. T. T cell-mediated immunity to malaria. *Nature Reviews Immunology* **19**, 457–471 (2019).

39. Teirlinck, A. C. *et al.* Longevity and Composition of Cellular Immune Responses Following Experimental Plasmodium falciparum Malaria Infection in Humans. *PLOS Pathogens* **7**, e1002389 (2011).

40. McMurray, J. L. *et al.* Transcriptional profiling of human Vδ1 T cells reveals a pathogen-driven adaptive differentiation program. *Cell Reports* **39**, 110858 (2022).

41. Ribot, J. C. *et al.* γδ-T cells promote IFN-γ–dependent Plasmodium pathogenesis upon liver-stage infection. *Proceedings of the National Academy of Sciences* **116**, 9979–9988 (2019).

42. Pamplona, A. & Silva-Santos, B. γδ T cells in malaria: a double-edged sword. *The FEBS Journal* **288**, 1118–1129 (2021).

43. Jagannathan, P. *et al.* Loss and dysfunction of Vδ2+ γδ T cells are associated with clinical tolerance to malaria. *Science Translational Medicine* **6**, 251ra117-251ra117 (2014).

44. Goodier, M. *et al.* γδ T cells in the peripheral blood of individuals from an area of holoendemic Plasmodium falciparum transmission. *Transactions of The Royal Society of Tropical Medicine and Hygiene* **87**, 692–696 (1993).

45. Hill, D. L. *et al.* Opsonising Antibodies to P. falciparum Merozoites Associated with Immunity to Clinical Malaria. *PLoS One* **8**, (2013).

46. Hill, D. L. *et al.* Merozoite Antigens of Plasmodium falciparum Elicit Strain-Transcending Opsonizing Immunity. *Infect Immun* **84**, 2175–2184 (2016).

47. Joos, C. *et al.* Clinical Protection from Falciparum Malaria Correlates with Neutrophil Respiratory Bursts Induced by Merozoites Opsonized with Human Serum Antibodies. *PLoS One* **5**, (2010).

48. Su, Z. & Stevenson, M. M. Central Role of Endogenous Gamma Interferon in Protective Immunity against Blood-Stage Plasmodium chabaudi AS Infection. *Infection and Immunity* **68**, 4399–4406 (2000).

49. Oakley, M. S. *et al.* T-bet modulates the antibody response and immune protection during murine malaria. *European Journal of Immunology* **44**, 2680–2691 (2014).

50. Kurup, S. P., Butler, N. S. & Harty, J. T. T cell-mediated immunity to malaria. *Nature Reviews Immunology* **19**, 457–471 (2019).

51. Walker, J. A. & McKenzie, A. N. J. TH2 cell development and function. *Nat Rev Immunol* **18**, 121–133 (2018).

52. Perez-Mazliah, D. & Langhorne, J. CD4 T-Cell Subsets in Malaria: TH1/TH2 Revisited. *Front. Immunol.* **5**, (2015).

53. Crotty, S. A brief history of T cell help to B cells. *Nat Rev Immunol* **15**, 185–189 (2015).

54. Kurup, S. P. *et al.* Regulatory T cells impede acute and long-term immunity to blood-stage malaria through CTLA-4. *Nat Med* **23**, 1220–1225 (2017).

55. Hansen, D. S. & Schofield, L. Natural Regulatory T Cells in Malaria: Host or Parasite Allies? *PLOS Pathogens* **6**, e1000771 (2010).

56. Vignali, D. A. A., Collison, L. W. & Workman, C. J. How regulatory T cells work. *Nat Rev Immunol* **8**, 523–532 (2008).

57. Farrington, L. *et al.* Both inflammatory and regulatory cytokine responses to malaria are blunted with increasing age in highly exposed children. *Malar J* **16**, 499 (2017).

58. Frimpong, A. *et al.* Asymptomatic Malaria Infection Is Maintained by a Balanced Pro- and Anti-inflammatory Response. *Frontiers in Microbiology* **11**, 2832 (2020).

59. Tran, T. M. *et al.* Transcriptomic evidence for modulation of host inflammatory responses during febrile Plasmodium falciparum malaria. *Scientific Reports* **6**, 31291 (2016).

60. Rogers, K. J., Vijay, R. & Butler, N. S. Anti-malarial humoral immunity: the long and short of it. *Microbes Infect* **23**, 104807 (2021).

61. Weisel, F. J., Zuccarino-Catania, G. V., Chikina, M. & Shlomchik, M. J. A Temporal Switch in the Germinal Center Determines Differential Output of Memory B and Plasma Cells. *Immunity* **44**, 116–130 (2016).

62. Baird, J. K. Host Age as a Determinant of Naturally Acquired Immunity to Plusmodium fcllcipcwum. 7.

63. Marsh, K. & Kinyanjui, S. Immune effector mechanisms in malaria. *Parasite Immunology* **28**, 51–60 (2006).

64. Robinson, L. J. *et al.* Cellular Tumor Necrosis Factor, Gamma Interferon, and Interleukin-6 Responses as Correlates of Immunity and Risk of Clinical Plasmodium falciparum Malaria in Children from Papua New Guinea. *Infect Immun* **77**, 3033–3043 (2009).

65. Sun, T. *et al.* A Plasmodium-encoded cytokine suppresses T-cell immunity during malaria. *Proceedings of the National Academy of Sciences* **109**, E2117–E2126 (2012).

66. Lefebvre, M. N. & Harty, J. T. You Shall Not Pass: Memory CD8 T Cells in Liver-Stage Malaria. *Trends Parasitol* **36**, 147–157 (2020).

67. Clark, R. A. Resident memory T cells in human health and disease. *Sci Transl Med* **7**, 269rv1 (2015).

68. Mabrouk, N. *et al.* CXCR6 expressing T cells: Functions and role in the control of tumors. *Front Immunol* **13**, 1022136 (2022).

69. Tse, S.-W., Cockburn, I. A., Zhang, H., Scott, A. L. & Zavala, F. Unique transcriptional profile of liver-resident memory CD8+ T cells induced by immunization with malaria sporozoites. *Genes Immun* **14**, 302–309 (2013).

70. Prime and target immunization protects against liver-stage malaria in mice | Science Translational Medicine. https://www.science.org/doi/10.1126/scitranslmed.aap9128.

71. Fernandez-Ruiz, D. *et al.* Liver-Resident Memory CD8+ T Cells Form a Front-Line Defense against Malaria Liver-Stage Infection. *Immunity* **45**, 889–902 (2016).

72. Pallett, L. J. & Maini, M. K. Liver-resident memory T cells: life in lockdown. *Semin Immunopathol* **44**, 813–825 (2022).

73. Krzych, U., Dalai, S., Zarling, S. & Pichugin, A. Memory CD8 T Cells Specific for Plasmodia Liver-Stage Antigens Maintain Protracted Protection Against Malaria. *Frontiers in Immunology* **3**, (2012).

74. Pérez-Mazliah, D., Ndungu, F. M., Aye, R. & Langhorne, J. B-cell memory in malaria: Myths and realities. *Immunol Rev* **293**, 57–69 (2020).

75. Wipasa, J. *et al.* Long-Lived Antibody and B Cell Memory Responses to the Human Malaria Parasites, Plasmodium falciparum and Plasmodium vivax. *PLoS Pathog* **6**, e1000770 (2010).

76. Opata, M. M. *et al.* Protection by and maintenance of CD4 effector memory and effector T cell subsets in persistent malaria infection. *PLoS Pathog* **14**, e1006960 (2018).

77. Opata, M. M. *et al.* Early Effector Cells Survive the Contraction Phase in Malaria Infection and Generate Both Central and Effector Memory T Cells. *The Journal of Immunology* **194**, 5346–5354 (2015).

78. Zander, R. A. *et al.* Th1-like Plasmodium-Specific Memory CD4+ T Cells Support Humoral Immunity. *Cell Reports* **21**, 1839–1852 (2017).

79. Stephens, R. & Langhorne, J. Effector Memory Th1 CD4 T Cells Are Maintained in a Mouse Model of Chronic Malaria. *PLOS Pathogens* **6**, e1001208 (2010).

80. Chan, J.-A. *et al.* Th2-like T Follicular Helper Cells Promote Functional Antibody Production during Plasmodium falciparum Infection. *Cell Rep Med* **1**, 100157 (2020).

81. Oyong, Damian. A. *et al.* Adults with Plasmodium falciparum malaria have higher magnitude and quality of circulating T-follicular helper cells compared to children. *eBioMedicine* **75**, 103784 (2022).

82. Pepper, M., Pagán, A. J., Igyártó, B. Z., Taylor, J. J. & Jenkins, M. K. Opposing Signals from the Bcl6 Transcription Factor and the Interleukin-2 Receptor Generate T Helper 1 Central and Effector Memory Cells. *Immunity* **35**, 583–595 (2011).

83. Differential regulation of antiviral T-cell immunity results in stable CD8+ but declining CD4+ T-cell memory | Nature Medicine. https://www.nature.com/articles/nm0801_913.

84. Different routes of bacterial infection induce long-lived TH1 memory cells and short-lived TH17 cells | Nature Immunology. https://www.nature.com/articles/ni.1826.

85. Lumsden, J. M. *et al.* Protective Immunity Induced with the RTS,S/AS Vaccine Is Associated with IL-2 and TNF-α Producing Effector and Central Memory CD4+ T Cells. *PLoS One* **6**, (2011).

86. Krzych, U., Zarling, S. & Pichugin, A. Memory T cells maintain protracted protection against malaria. *Immunol Lett* **161**, 189–195 (2014).

87. Palmer, D. R. & Krzych, U. Cellular and molecular requirements for the recall of IL-4-producing memory CD4+CD45RO+CD27– T cells during protection induced by attenuated Plasmodium falciparum sporozoites. *European Journal of Immunology* **32**, 652–661 (2002).

88. BROOKER, S. *et al.* EPIDEMIOLOGY OF PLASMODIUM-HELMINTH CO-INFECTION IN AFRICA: POPULATIONS AT RISK, POTENTIAL IMPACT ON ANEMIA AND PROSPECTS FOR COMBINING CONTROL. *Am J Trop Med Hyg* **77**, 88–98 (2007).

89. Anchang-Kimbi, J. K., Elad, D. M., Sotoing, G. T. & Achidi, E. A. Coinfection with Schistosoma haematobium and Plasmodium falciparum and Anaemia Severity among Pregnant Women in Munyenge, Mount Cameroon Area: A Cross-Sectional Study. *J Parasitol Res* **2017**, (2017).

90. Fonkwo, P. N. Pricing infectious disease. *EMBO Rep* **9**, S13–S17 (2008).

91. Mabbott, N. A. The Influence of Parasite Infections on Host Immunity to Co-infection With Other Pathogens. *Front. Immunol.* **9**, (2018).

92. Salazar-Castañon, V. H., Legorreta-Herrera, M. & Rodriguez-Sosa, M. Helminth Parasites Alter Protection against Plasmodium Infection. *Biomed Res Int* **2014**, (2014).

93. TELFER, S. *et al.* Parasite interactions in natural populations: insights from longitudinal data. *Parasitology* **135**, 767–781 (2008).

94. Telfer, S. *et al.* Species Interactions in a Parasite Community Drive Infection Risk in a Wildlife Population. *Science* **330**, 243–246 (2010).

95. Mahittikorn, A., Kotepui, K. U., De Jesus Milanez, G., Masangkay, F. R. & Kotepui, M. A meta-analysis on the prevalence and characteristics of severe malaria in patients with Plasmodium spp. and HIV co-infection. *Sci Rep* **11**, 16655 (2021).

96. Mount, A. M. *et al.* Impairment of humoral immunity to Plasmodium falciparum malaria in pregnancy by HIV infection. *The Lancet* **363**, 1860–1867 (2004).

97. Neglected tropical diseases. https://www.who.int/news-room/questions-and-answers/item/neglected-tropical-diseases.

98. Casulli, A. New global targets for NTDs in the WHO roadmap 2021–2030. *PLOS Neglected Tropical Diseases* **15**, e0009373 (2021).

99. Leishmaniasis. https://www.who.int/news-room/fact-sheets/detail/leishmaniasis.

100. Pinna, R. A. *et al.* Malaria-Cutaneous Leishmaniasis Co-infection: Influence on Disease Outcomes and Immune Response. *Front Microbiol* **7**, 982 (2016).

101. Specht, S. & Hoerauf, A. Does helminth elimination promote or prevent malaria? *The Lancet* **369**, 446–447 (2007).

102. Wammes, L. J. *et al.* Regulatory T cells in human geohelminth infection suppress immune responses to BCG and Plasmodium falciparum. *European Journal of Immunology* **40**, 437–442 (2010).

103. Colley, D. G., Bustinduy, A. L., Secor, W. E. & King, C. H. Human schistosomiasis. *Lancet* **383**, 2253–2264 (2014).

104. McManus, D. P. *et al.* Schistosomiasis. *Nature Reviews Disease Primers* **4**, 1–19 (2018).

105. van der Werf, M. J. *et al.* Quantification of clinical morbidity associated with schistosome infection in sub-Saharan Africa. *Acta Tropica* **86**, 125–139 (2003).

106. Lund, A. J. *et al.* Land use impacts on parasitic infection: a cross-sectional epidemiological study on the role of irrigated agriculture in schistosome infection in a dammed landscape. *Infect Dis Poverty* **10**, (2021).

107. Maddren, R. *et al.* Soil-transmitted helminths and schistosome infections in Ethiopia: a systematic review of progress in their control over the past 20 years. *Parasit Vectors* **14**, (2021).

108. McManus, D. P. *et al.* Schistosomiasis—from immunopathology to vaccines. *Semin Immunopathol* **42**, 355–371 (2020).

109. Burke, M. L. *et al.* Immunopathogenesis of human schistosomiasis. *Parasite Immunol* **31**, 163–176 (2009).

110. Botelho, M. C. *et al.* The role of estrogens and estrogen receptor signaling pathways in cancer and infertility: the case of schistosomes. *Trends in Parasitology* **31**, 246–250 (2015).

111. Molehin, A. J. Current Understanding of Immunity Against Schistosomiasis: Impact on Vaccine and Drug Development. *Res Rep Trop Med* **11**, 119–128 (2020).

112. Pearce, E. J. & MacDonald, A. S. The immunobiology of schistosomiasis. *Nat Rev Immunol* **2**, 499–511 (2002).

113. Moriyasu, T. *et al.* Schistosoma mansoni infection suppresses the growth of Plasmodium yoelii parasites in the liver and reduces gametocyte infectivity to mosquitoes. *PLOS Neglected Tropical Diseases* **12**, e0006197 (2018).

114. Degarege, A. *et al.* Plasmodium falciparum Infection Status among Children with Schistosoma in Sub-Saharan Africa: A Systematic Review and Meta-analysis. *PLoS Negl Trop Dis* **10**, e0005193 (2016).

115. Helmby, H., Kullberg, M. & Troye-Blomberg, M. Altered Immune Responses in Mice with Concomitant Schistosoma mansoni and Plasmodium chabaudi Infections. *Infect Immun* **66**, 5167–5174 (1998).

116. Laranjeiras, R. F., Brant, L. C., Lima, A. C. L., Coelho, P. M. Z. & Braga, E. M. Reduced protective effect of Plasmodium berghei immunization by concurrent Schistosoma mansoni infection. *Memórias do Instituto Oswaldo Cruz* **103**, 674–677 (2008).

117. Legesse, M., Erko, B. & Balcha, F. Increased parasitaemia and delayed parasite clearance in Schistosoma mansoni and Plasmodium berghei co-infected mice. *Acta Tropica* **91**, 161–166 (2004).

118. Silva, J. C., Egan, A., Arze, C., Spouge, J. L. & Harris, D. G. A New Method for Estimating Species Age Supports the Coexistence of Malaria Parasites and Their Mammalian Hosts. *Mol Biol Evol* **32**, 1354–1364 (2015).

119. Déchamps, S. *et al.* Rodent and nonrodent malaria parasites differ in their phospholipid metabolic pathways. *J Lipid Res* **51**, 81–96 (2010).

120. Orfano, A. S. *et al.* Species-specific escape of Plasmodium sporozoites from oocysts of avian, rodent, and human malarial parasites. *Malar J* **15**, (2016).

121. Ateba-Ngoa, U. *et al.* Cytokine and chemokine profile of the innate and adaptive immune response of schistosoma haematobium and plasmodium falciparum single and co-infected school-aged children from an endemic area of Lambaréné, Gabon. *Malaria Journal* **14**, 94 (2015).

122. Lyke, K. E. *et al.* Long-term Maintenance of CD4 T Cell Memory Responses to Malaria Antigens in Malian Children Coinfected with Schistosoma haematobium. *Front Immunol* **8**, (2018).

123. Lyke, K. E. *et al.* Antigen-Specific B Memory Cell Responses to Plasmodium falciparum Malaria Antigens and Schistosoma haematobium Antigens in Co-Infected Malian Children. *PLoS One* **7**, (2012).

124. Diallo, T. O. *et al.* Schistosomiasis co-infection in humans influences inflammatory markers in uncomplicated Plasmodium falciparum malaria. *Parasite Immunol* **26**, 365–369 (2004).

125. Lyke, K. E. *et al.* Reduced T Regulatory Cell Response during Acute Plasmodium falciparum Infection in Malian Children Co-Infected with Schistosoma haematobium. *PLoS One* **7**, (2012).

126. Tanel, A. *et al.* Cellular and molecular mechanisms of memory T-cell survival. *Expert Rev Vaccines* **8**, 299–312 (2009).

127. Wu, C. *et al.* Distinct lineages of T H 1 cells have differential capacities for memory cell generation in vivo. *Nature Immunology* **3**, 852–858 (2002).

128. Becker, T. C. *et al.* Interleukin 15 Is Required for Proliferative Renewal of Virus-specific Memory CD8 T Cells. *J Exp Med* **195**, 1541–1548 (2002).

129. Bradley, L. M., Haynes, L. & Swain, S. L. IL-7: maintaining T-cell memory and achieving homeostasis. *Trends in Immunology* **26**, 172–176 (2005).

130. Kondrack, R. M. *et al.* Interleukin 7 Regulates the Survival and Generation of Memory CD4 Cells. *J Exp Med* **198**, 1797–1806 (2003).

131. Seddon, B., Tomlinson, P. & Zamoyska, R. Interleukin 7 and T cell receptor signals regulate homeostasis of CD4 memory cells. *Nature Immunology* **4**, 680–686 (2003).

132. Allard, E.-L. *et al.* Overexpression of IL-21 promotes massive CD8+ memory T cell accumulation. *European Journal of Immunology* **37**, 3069–3077 (2007).

133. Doolan, D. L., Dobaño, C. & Baird, J. K. Acquired Immunity to Malaria. *Clin Microbiol Rev* **22**, 13–36 (2009).

134. Hodgson, S. H. *et al.* Use of gene expression studies to investigate the human immunological response to malaria infection. *Malar J* **18**, (2019).

135. Krupka, M. *et al.* Mild Plasmodium falciparum Malaria following an Episode of Severe Malaria Is Associated with Induction of the Interferon Pathway in Malawian Children. *Infect Immun* **80**, 1150–1155 (2012).

136. Illingworth, J. *et al.* Chronic Exposure to Plasmodium falciparum Is Associated with Phenotypic Evidence of B and T Cell Exhaustion. *J Immunol* **190**, 1038–1047 (2013).

137. Ockenhouse, C. F. *et al.* Common and Divergent Immune Response Signaling Pathways Discovered in Peripheral Blood Mononuclear Cell Gene Expression Patterns in Presymptomatic and Clinically Apparent Malaria. *Infect Immun* **74**, 5561–5573 (2006).

138. Tran, T. M. *et al.* A molecular signature in blood reveals a role for p53 in regulating malaria-induced inflammation. *Immunity* **51**, 750-765.e10 (2019).

139. Thera, M. A. *et al.* A Field Trial to Assess a Blood-Stage Malaria Vaccine. *N Engl J Med* **365**, 1004–1013 (2011).

140. Coulibaly, D. *et al.* Spatio-temporal analysis of malaria within a transmission season in Bandiagara, Mali. *Malar J* **12**, 82 (2013).

141. Fienberg, H., Simonds, E. F., Fantl, W. J., Nolan, G. P. & Bodenmiller, B. A platinum-based covalent viability reagent for single cell mass cytometry. *Cytometry A* **81**, 10.1002/cyto.a.22067 (2012).

142. Kim, D., Langmead, B. & Salzberg, S. L. HISAT: a fast spliced aligner with low memory requirements. *Nat Methods* **12**, 357–360 (2015).

143. Anders, S. & Huber, W. Differential expression analysis for sequence count data. *Genome Biol* **11**, R106 (2010).

144. Anders, S., Pyl, P. T. & Huber, W. HTSeq—a Python framework to work with high-throughput sequencing data. *Bioinformatics* **31**, 166–169 (2015).

145. Trapnell, C. *et al.* Differential analysis of gene regulation at transcript resolution with RNA-seq. *Nat Biotechnol* **31**, (2013).

146. Orvis, J. *et al.* gEAR: Gene Expression Analysis Resource portal for community-driven, multi-omic data exploration. *Nat Methods* **18**, 843–844 (2021).

147. Huang, D. W., Sherman, B. T. & Lempicki, R. A. Bioinformatics enrichment tools: paths toward the comprehensive functional analysis of large gene lists. *Nucleic Acids Res* **37**, 1–13 (2009).

148. Huang, D. W., Sherman, B. T. & Lempicki, R. A. Systematic and integrative analysis of large gene lists using DAVID bioinformatics resources. *Nature Protocols* **4**, 44–57 (2009).

149. Subramanian, A. *et al.* Gene set enrichment analysis: A knowledge-based approach for interpreting genome-wide expression profiles. *PNAS* **102**, 15545–15550 (2005).

150. Hahne, F. *et al.* flowCore: a Bioconductor package for high throughput flow cytometry. *BMC Bioinformatics* **10**, 106 (2009).

151. Nowicka, M. *et al.* CyTOF workflow: differential discovery in high-throughput high-dimensional cytometry datasets. *F1000Res* **6**, 748 (2019).

152. Crowell, H. L. *et al.* An R-based reproducible and user-friendly preprocessing pipeline for CyTOF data. Preprint at https://doi.org/10.12688/f1000research.26073.1 (2020).

153. Van Gassen, S. *et al.* FlowSOM: Using self-organizing maps for visualization and interpretation of cytometry data. *Cytometry Part A* **87**, 636–645 (2015).

154. Wilkerson, M. D. & Hayes, D. N. ConsensusClusterPlus: a class discovery tool with confidence assessments and item tracking. *Bioinformatics* **26**, 1572–1573 (2010).

155. Weber, L. M., Nowicka, M., Soneson, C. & Robinson, M. D. diffcyt: Differential discovery in high-dimensional cytometry via high-resolution clustering. *Commun Biol* **2**, 1–11 (2019).

156. Thera, M. A. *et al.* Safety and immunogenicity of an AMA-1 malaria vaccine in Malian adults: results of a phase 1 randomized controlled trial. *PLoS One* **3**, e1465 (2008).

157. Zhou, A. E. *et al.* Protein Microarrays as a Tool to Analyze Antibody Responses to Variant Surface Antigens Expressed on the Surface of Plasmodium falciparum-Infected Erythrocytes. *Methods Mol Biol* **2470**, 343–358 (2022).

158. Doolan, D. L. *et al.* Profiling Humoral Immune Responses to P. falciparum Infection with Protein Microarrays. *Proteomics* **8**, 4680–4694 (2008).

159. Davies, D. H. *et al.* Profiling the humoral immune response to infection by using proteome microarrays: High-throughput vaccine and diagnostic antigen discovery. *Proc Natl Acad Sci U S A* **102**, 547–552 (2005).

160. van Schie, J. J. M. *et al.* Warsaw Breakage Syndrome associated DDX11 helicase resolves G-quadruplex structures to support sister chromatid cohesion. *Nat Commun* **11**, 4287 (2020).

161. Crompton, P. D. *et al.* A prospective analysis of the Ab response to Plasmodium falciparum before and after a malaria season by protein microarray. *Proc Natl Acad Sci U S A* **107**, 6958–6963 (2010).

162. Travassos, M. A. *et al.* Seroreactivity to Plasmodium falciparum Erythrocyte Membrane Protein 1 Intracellular Domain in Malaria-Exposed Children and Adults. *J Infect Dis* **208**, 1514–1519 (2013).

163. Travassos, M. A. *et al.* Children with cerebral malaria or severe malarial anaemia lack immunity to distinct variant surface antigen subsets. *Sci Rep* **8**, 6281 (2018).

164. Bailey, J. A. *et al.* Microarray analyses reveal strain-specific antibody responses to Plasmodium falciparum apical membrane antigen 1 variants following natural infection and vaccination. *Sci Rep* **10**, (2020).

165. Griffith, J. W., Sokol, C. L. & Luster, A. D. Chemokines and Chemokine Receptors: Positioning Cells for Host Defense and Immunity. *Annual Review of Immunology* **32**, 659–702 (2014).

166. IOANNIDIS, L. J., NIE, C. Q. & HANSEN, D. S. The role of chemokines in severe malaria: more than meets the eye. *Parasitology* **141**, 602–613 (2014).

167. Dunst, J., Kamena, F. & Matuschewski, K. Cytokines and Chemokines in Cerebral Malaria Pathogenesis. *Front Cell Infect Microbiol* **7**, 324 (2017).

168. Hisaeda, H. *et al.* Escape of malaria parasites from host immunity requires CD4+CD25+ regulatory T cells. *Nat Med* **10**, 29–30 (2004).

169. Reddy, M., Eirikis, E., Davis, C., Davis, H. M. & Prabhakar, U. Comparative analysis of lymphocyte activation marker expression and cytokine secretion profile in stimulated human peripheral blood mononuclear cell cultures: an in vitro model to monitor cellular immune function. *Journal of Immunological Methods* **293**, 127–142 (2004).

170. Ioannidis, L. J. *et al.* Monocyte- and Neutrophil-Derived CXCL10 Impairs Efficient Control of Blood-Stage Malaria Infection and Promotes Severe Disease. *The Journal of Immunology* **196**, 1227–1238 (2016).

171. Liu, M. *et al.* CXCL10/IP-10 in infectious diseases pathogenesis and potential therapeutic implications. *Cytokine & Growth Factor Reviews* **22**, 121–130 (2011).

172. Wilson, N. O. *et al.* CXCL4 and CXCL10 predict risk of fatal cerebral malaria. *Disease Markers* **30**, 39 (2011).

173. Armah, H. B. *et al.* Cerebrospinal fluid and serum biomarkers of cerebral malaria mortality in Ghanaian children. *Malar J* **6**, 147 (2007).

174. Mogensen, T. H. IRF and STAT Transcription Factors - From Basic Biology to Roles in Infection, Protective Immunity, and Primary Immunodeficiencies. *Frontiers in Immunology* **9**, 3047 (2019).

175. Shi, X. *et al.* Dynamic Balance of pSTAT1 and pSTAT3 in C57BL/6 Mice Infected with Lethal Or Nonlethal Plasmodium yoelii. *Cell Mol Immunol* **5**, 341–348 (2008).

176. Kern, P., Dietrich, M., Hemmer, C. & Wellinghausen, N. Increased Levels of Soluble Fas Ligand in Serum in Plasmodium falciparum Malaria. *Infect Immun* **68**, 3061–3063 (2000).

177. Hviid, L. & Kemp, K. What Is the Cause of Lymphopenia in Malaria? *Infect Immun* **68**, 6087–6089 (2000).

178. Kakani, P., Suman, S., Gupta, L. & Kumar, S. Ambivalent Outcomes of Cell Apoptosis: A Barrier or Blessing in Malaria Progression. *Front Microbiol* **7**, (2016).

179. Pinzon-Charry, A. *et al.* Apoptosis and dysfunction of blood dendritic cells in patients with falciparum and vivax malaria. *J Exp Med* **210**, 1635–1646 (2013).

180. Toure-Balde, A. *et al.* Plasmodium falciparum induces apoptosis in human mononuclear cells. *Infect Immun* **64**, 744–750 (1996).

181. Jeong, S.-I. *et al.* XAF1 forms a positive feedback loop with IRF-1 to drive apoptotic stress response and suppress tumorigenesis. *Cell Death Dis* **9**, 806 (2018).

182. Lee, M.-G. *et al.* XAF1 directs apoptotic switch of p53 signaling through activation of HIPK2 and ZNF313. *PNAS* **111**, 15532–15537 (2014).

183. Xia, Y., Novak, R., Lewis, J., Duckett, C. S. & Phillips, A. C. Xaf1 can cooperate with TNFα in the induction of apoptosis, independently of interaction with XIAP. *Mol Cell Biochem* **286**, 67–76 (2006).

184. Tanaka, N. *et al.* Cellular commitment to oncogene-induced transformation or apoptosis is dependent on the transcription factor IRF-1. *Cell* **77**, 829–839 (1994).

185. Tippalagama, R. *et al.* HLA-DR Marks Recently Divided Antigen-Specific Effector CD4 T Cells in Active Tuberculosis Patients. *The Journal of Immunology* **207**, 523–533 (2021).

186. Ahmed, A. *et al.* Circulating HLA-DR+CD4+ effector memory T cells resistant to CCR5 and PD-L1 mediated suppression compromise regulatory T cell function in tuberculosis. *PLOS Pathogens* **14**, e1007289 (2018).

187. Lee, E. *et al.* Memory CD4 + T-Cells Expressing HLA-DR Contribute to HIV Persistence During Prolonged Antiretroviral Therapy. *Frontiers in Microbiology* **10**, (2019).

188. Tsang, J. S. *et al.* Improving Vaccine-Induced Immunity: Can Baseline Predict Outcome? *Trends in Immunology* **41**, 457–465 (2020).

189. Tsang, J. S. *et al.* Global analyses of human immune variation reveal baseline predictors of post-vaccination responses. *Cell* **157**, 499–513 (2014).

190. Gnjatic, S. *et al.* Identifying baseline immune-related biomarkers to predict clinical outcome of immunotherapy. *Journal for ImmunoTherapy of Cancer* **5**, 44 (2017).

191. Bucasas, K. L. *et al.* Early Patterns of Gene Expression Correlate With the Humoral Immune Response to Influenza Vaccination in Humans. *J Infect Dis* **203**, 921–929 (2011).

192. Schistosomiasis (Bilharzia). https://www.who.int/health-topics/schistosomiasis.

193. van Riet, E., Hartgers, F. C. & Yazdanbakhsh, M. Chronic helminth infections induce immunomodulation: Consequences and mechanisms. *Immunobiology* **212**, 475–490 (2007).

194. Long, T. T. A., Nakazawa, S., Onizuka, S., Huaman, M. C. & Kanbara, H. Influence of CD4+CD25+ T cells on Plasmodium berghei NK65 infection in BALB/c mice. *International Journal for Parasitology* **33**, 175–183 (2003).

195. Coulibaly, D. *et al.* Impact of preseason treatment on incidence of falciparum malaria and parasite density at a site for testing malaria vaccines in Bandiagara, Mali. *Am J Trop Med Hyg* **67**, 604–610 (2002).

196. Hao, Y. *et al.* Integrated analysis of multimodal single-cell data. *Cell* **184**, 3573-3587.e29 (2021).

197. Andreatta, M. & Carmona, S. J. UCell: Robust and scalable single-cell gene signature scoring. *Computational and Structural Biotechnology Journal* **19**, 3796–3798 (2021).

198. Murphy, K. M. & Reiner, S. L. The lineage decisions of helper T cells. *Nat Rev Immunol* **2**, 933–944 (2002).

199. Amezquita, R. A. *et al.* Orchestrating single-cell analysis with Bioconductor. *Nat Methods* **17**, 137–145 (2020).

200. Love, M. I., Huber, W. & Anders, S. Moderated estimation of fold change and dispersion for RNA-seq data with DESeq2. *Genome Biol* **15**, 550 (2014).

201. Hoyer, B. F. *et al.* Short-lived Plasmablasts and Long-lived Plasma Cells Contribute to Chronic Humoral Autoimmunity in NZB/W Mice. *Journal of Experimental Medicine* **199**, 1577–1584 (2004).

202. Yoshimoto, T. *et al.* IL-12 Up-Regulates IL-18 Receptor Expression on T Cells, Th1 Cells, and B Cells: Synergism with IL-18 for IFN-γ Production1. *The Journal of Immunology* **161**, 3400–3407 (1998).

203. Smeltz, R. B., Chen, J., Hu-Li, J. & Shevach, E. M. Regulation of Interleukin (Il)-18 Receptor α Chain Expression on Cd4+ T Cells during T Helper (Th)1/Th2 Differentiation. *J Exp Med* **194**, 143–154 (2001).

204. Cenerenti, M., Saillard, M., Romero, P. & Jandus, C. The Era of Cytotoxic CD4 T Cells. *Frontiers in Immunology* **13**, (2022).

205. Patil, V. S. *et al.* Precursors of human CD4+ cytotoxic T lymphocytes identified by single-cell transcriptome analysis. *Science Immunology* **3**, eaan8664 (2018).

206. Preglej, T. & Ellmeier, W. CD4+ Cytotoxic T cells – Phenotype, Function and Transcriptional Networks Controlling Their Differentiation Pathways. *Immunology Letters* **247**, 27–42 (2022).

207. Walther, M. *et al.* Distinct Roles for FOXP3+ and FOXP3− CD4+ T Cells in Regulating Cellular Immunity to Uncomplicated and Severe Plasmodium falciparum Malaria. *PLoS Pathog* **5**, e1000364 (2009).

208. McCall, M. B. B. *et al.* Early interferon-gamma response against Plasmodium falciparum correlates with interethnic differences in susceptibility to parasitemia between sympatric Fulani and Dogon in Mali. *J Infect Dis* **201**, 142–152 (2010).

209. Otterdal, K. *et al.* IL-18 and IL-18 binding protein are related to disease severity and parasitemia during falciparum malaria. *BMC Infectious Diseases* **21**, (2021).

210. Kojima, S., Nagamine, Y., Hayano, M., Looareesuwan, S. & Nakanishi, K. A potential role of interleukin 18 in severe falciparum malaria. *Acta Tropica* **89**, 279–284 (2004).

211. Ishihara, K. & Hirano, T. Molecular basis of the cell specificity of cytokine action. *Biochimica et Biophysica Acta (BBA) - Molecular Cell Research* **1592**, 281–296 (2002).

212. Liu, X. *et al.* Genome-wide analysis identifies NR4A1 as a key mediator of T cell dysfunction. *Nature* **567**, 525–529 (2019).

213. Flemming, A. What's driving T cell dysfunction? *Nat Rev Cancer* **19**, 251–251 (2019).

214. Bending, D. & Zikherman, J. Nr4a nuclear receptors: markers and modulators of antigen receptor signaling. *Current Opinion in Immunology* **81**, 102285 (2023).

215. Boi, S. K., Lan, X. & Youngblood, B. BATF targets T cell exhaustion for termination. *Nat Immunol* **22**, 936–938 (2021).

216. Seo, H. *et al.* BATF and IRF4 cooperate to counter exhaustion in tumor-infiltrating CAR T cells. *Nat Immunol* **22**, 983–995 (2021).

217. Nideffer, J. & Jagannathan, P. Type I regulatory T cells in malaria: of mice and men. *J Clin Invest* **133**, (2023).

218. Edwards, C. L. *et al.* IL-10-producing Th1 cells possess a distinct molecular signature in malaria. *J Clin Invest* **133**, (2023).

219. Kirosingh, A. S. *et al.* Malaria-specific Type 1 regulatory T cells are more abundant in first pregnancies and associated with placental malaria. *eBioMedicine* **95**, (2023).

220. Yoon, J. K. & Lau, L. F. Involvement of JunD in transcriptional activation of the orphan receptor gene nur77 by nerve growth factor and membrane depolarization in PC12 cells. *Molecular and Cellular Biology* **14**, 7731 (1994).

221. Seo, W., Jerin, C. & Nishikawa, H. Transcriptional regulatory network for the establishment of CD8+ T cell exhaustion. *Exp Mol Med* **53**, 202–209 (2021).

222. Diupotex, M., Zamora-Chimal, J., Gajón, J. A., Bonifaz, L. C. & Becker, I. CXCR5 and TIM-3 expressions define distinct exhausted T cell subsets in experimental cutaneous infection with Leishmania mexicana. *Frontiers in Immunology* **14**, (2023).

223. Marelli-Berg, F. M., Fu, H., Vianello, F., Tokoyoda, K. & Hamann, A. Memory T-cell trafficking: new directions for busy commuters. *Immunology* **130**, 158–165 (2010).

224. Harris, N. L., Watt, V., Ronchese, F. & Gros, G. L. Differential T Cell Function and Fate in Lymph Node and Nonlymphoid Tissues. *The Journal of Experimental Medicine* **195**, 317 (2002).

225. Mbambo, G. *et al.* Immunogenomic profile at baseline predicts host susceptibility to clinical malaria. *Frontiers in Immunology* **14**, (2023).

226. He, X., Xia, L., Tumas, K. C., Wu, J. & Su, X.-Z. Type I Interferons and Malaria: A Double-Edge Sword Against a Complex Parasitic Disease. *Frontiers in Cellular and Infection Microbiology* **10**, (2020).

227. Moser, K. A. *et al.* Strains used in whole organism Plasmodium falciparum vaccine trials differ in genome structure, sequence, and immunogenic potential. *Genome Medicine* **12**, 6 (2020).

228. Eldering, M. *et al.* Variation in susceptibility of African Plasmodium falciparum malaria parasites to TEP1 mediated killing in Anopheles gambiae mosquitoes. *Sci Rep* **6**, 20440 (2016).

229. Abera, D. *et al.* Genomic analysis reveals independent evolution of Plasmodium falciparum populations in Ethiopia. *Malar J* **20**, 129 (2021).

230. Takeuchi, A. & Saito, T. CD4 CTL, a Cytotoxic Subset of CD4+ T Cells, Their Differentiation and Function. *Frontiers in Immunology* **8**, (2017).

231. Lönnberg, T. *et al.* Single-cell RNA-seq and computational analysis using temporal mixture modelling resolves Th1/Tfh fate bifurcation in malaria. *Sci Immunol* **2**, (2017).

232. Soon, M. S. F. *et al.* Transcriptome dynamics of CD4+ T cells during malaria maps gradual transit from effector to memory. *Nat Immunol* **21**, 1597–1610 (2020).

233. Brooks, J. F. *et al.* Negative feedback by NUR77/Nr4a1 restrains B cell clonal dominance during early T-dependent immune responses. *Cell Reports* **36**, 109645 (2021).

234. Hiwa, R., Nielsen, H. V., Mueller, J. L., Mandla, R. & Zikherman, J. NR4A family members regulate T cell tolerance to preserve immune homeostasis and suppress autoimmunity. *JCI Insight* **6**, (2021).

235. Seo, H. *et al.* TOX and TOX2 transcription factors cooperate with NR4A transcription factors to impose CD8+ T cell exhaustion. *Proceedings of the National Academy of Sciences* **116**, 12410–12415 (2019).

236. Odagiu, L., May, J., Boulet, S., Baldwin, T. A. & Labrecque, N. Role of the Orphan Nuclear Receptor NR4A Family in T-Cell Biology. *Front Endocrinol (Lausanne)* **11**, 624122 (2021).

237. Long, C. A. & Zavala, F. Immune Responses in Malaria. *Cold Spring Harb Perspect Med* **7**, a025577 (2017).

238. McManus, D. P. *et al.* Schistosomiasis. *Nat Rev Dis Primers* **4**, 1–19 (2018).

239. Ogongo, P., Nyakundi, R. K., Chege, G. K. & Ochola, L. The Road to Elimination: Current State of Schistosomiasis Research and Progress Towards the End Game. *Front Immunol* **13**, 846108 (2022).